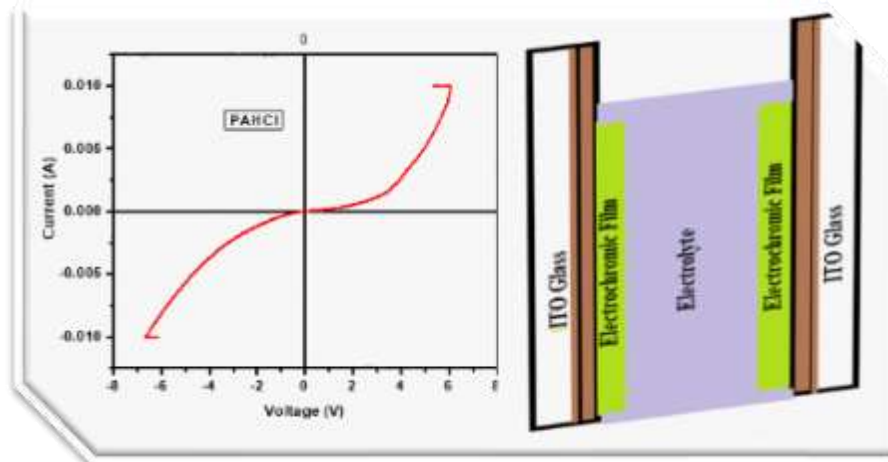


# ELECTRICAL AND OPTICAL PROPERTIES OF CONDUCTING POLYMER: POLYPYRROLE AND POLYANILINE BLENDS

BY: TEKALIGN AREGU TIKISH



**JIMMA UNIVERSITY**

**August 2020**



**JIMMA INSTITUTE OF TECHNOLOGY: SCHOOL OF  
GRADUATE STUDIES, JIMMA UNIVERSITY**

**ELECTRICAL AND OPTICAL PROPERTIES OF  
CONDUCTING POLYMER: POLYPYRROLE AND  
POLYANILINE BLENDS**

**A PHD DISSERTATION SUBMITTED TO THE SCHOOL OF GRADUATE  
STUDIES OF JIMMA UNIVERSITY IN PARTIAL FULFILMENT OF THE  
REQUIREMENTS FOR THE DEGREE OF DOCTORIAL PHILOSOPHY  
(PHD) IN MATERIALS SCIENCE AND ENGINEERING**

**BY: TEKALIGN AREGU TIKISH**

**ADVISOR: PROF. JONG YONG KIM**

**CO-ADVISOR: ASHOK KUMAR**

**JIMMA UNIVERSITY**

**FACULTY OF MATERIALS SCIENCE AND ENGINEERING**

**JIMMA INSTITUTE OF TECHNOLOGY**

**August 2020**

**EXAMINATION BOARD DISSERTATION APPROVAL FORM  
JIMMA UNIVERSITY SCHOOL OF GRADUATE STUDIES**

**Dissertation Title: Electrical and Optical Properties of Conducting Polymer of Polypyrrole and Polyaniline Blends**

**By: Mr. Tekalign Aregu Tikish**


**College of Materials Science and Engineering, Jimma University**

**Approved by the examining board**

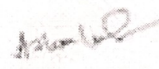
**1. Chairperson, examination board (Jury)**

**Name** Dr. Muluaem Mekonne **Signature**  **Date** Aug 3, 2020

**2. Promoter (Primary)**

**Name** Prof. Jung Yong Kim **Signature**  **Date** Aug 3, 2020  
Prof. Jung Yong Kim (PhD)  
Scientific Director  
Engineering Faculty Dean

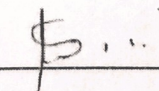
**3. Promoter (Secondary)**

**Name** Prof. Ashok Kumar **Signature**  **Date** Aug 3, 2020

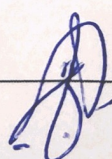
**4. External Examiner**

**Name** Prof. Shimelis Admassie **Signature**  **Date** Aug 3, 2020

**5. Internal Examiner**

**Name** Dr. Tesfaye Refera **Signature**  **Date** Aug 3, 2020

**6. Internal Examiner**

**Name** Dr. Menberu Mengesha **Signature**  **Date** Aug 3, 2020

## **Dedication**

This dissertation is gratefully dedicated to my beloved family whose unyielding love, support and encouragement have inspired me to pursue and complete this PhD.

## **Acknowledgments**

First of all, I would like to thank my supervisor, Prof. Jung Young for his sincere supports and academic advisor at the school of Chemical Engineering Jimma Institute of Technology, Ethiopia. Next, I would like to extend my gratitude to my Co-Advisor and mentor prof. Ashok Kumar for accepting me to work my Ph.D. research in his Materials Research Laboratories at the Department of physics, Tezpur University, India. And also, for his direct follow up my data and his offering training opportunities to improve my theoretical, experimental, and analysis skill.

I would like gratefully acknowledge Materials Science and Engineering faculty members for their support and encouragement. And my friends at Jimma Institute of Technology first batch Ph.D. candidates.

I would like to encompass my Special gratitude to my beloved family, my dear friends for their support encouragements and believed in me until the final day. And God bless all of you.

Final thanks to the Jimma Institute of Technology, the Ministry of Education, Materials Research Laboratories at Department of physics, Tezpur University, India, and Ethiopian Biotechnology Institute.

Tekalign Aregu Tikish

## Table of Content

<b>Acknowledgements</b> .....	<b>iv</b>
<b>List of Tables</b> .....	<b>ix</b>
<b>List of Figures</b> .....	<b>x</b>
<b>Acronyms</b> .....	<b>xii</b>
<b>Abbreviations and Symbols</b> .....	<b>ix</b>
<b>Abstract</b> .....	<b>xvi</b>
<b>Chapter One</b> .....	<b>1</b>
General Introduction .....	1
<b>1.1. Background and Rational of the Study</b> .....	1
<b>1.2. Statement of the Problems</b> .....	1
<b>1.3. Background of the Study Area</b> .....	3
<b>1.4. Objectives</b> .....	4
<b>1.5. The Scope of the current work</b> .....	4
<b>1.6. Significance of the study</b> .....	5
<b>1.7. Hypothesis Questions</b> .....	6
<b>Chapter Two</b> .....	8
Review of Literature .....	8
<b>2.1. Development of Organic Electronics and Organic Semiconductors</b> .....	8
<b>2.1.1 Background</b> .....	8
<b>2.1.2 New Electronics Age Based on Organic Semiconductors</b> .....	9
<b>2.1.3 Comparison of Organic and Inorganic Devices</b> .....	10
<b>2.1.4. Advantages and Disadvantages</b> .....	11
<b>2.1.5 Applications</b> .....	11
<b>2.2. Overview of Blends</b> .....	11
<b>2.2.1 Miscible (Single-Phase)</b> .....	12
<b>2.2.2 Partially Miscible Blends</b> .....	13
<b>2.2.3 Immiscible Blends (Phase Separated)</b> .....	13
<b>2.2.4 Miscibility</b> .....	14
<b>2.3 Different Synthesis Routes of Polymer Blends or Composite</b> .....	15
<b>2.3.1 Solution Process</b> .....	15
<b>2.3.2 Copolymerization</b> .....	16

2.3.3 Melt processing .....	18
2.3.4 In-situ Polymerization .....	18
2.3.5 Electrochemical polymerization (Layer to layer) .....	19
2.3.6 All comparison /summery .....	19
<b>2.4 Different Deposition Techniques /Film Deposition Methods.....</b>	<b>19</b>
<b>2.5 Literature Survey of Conducting Polymer Blends: Polypyrrole and Polyaniline .....</b>	<b>20</b>
<b>2.6 Advantages and Application Area of Conducting Polymer of PPy-PANI Blends.....</b>	<b>23</b>
<b>and/or Composite.....</b>	<b>23</b>
<b>2.6.1 Coating and Corrosion protection .....</b>	<b>24</b>
<b>2.6.2 Dye-Sensitized Solar Cells.....</b>	<b>24</b>
<b>2.6.3 Bio medical /Pharmaceutical Preparations, Microextraction.....</b>	<b>24</b>
<b>2.6.4 Storage .....</b>	<b>25</b>
<b>2.6.5 Sensor.....</b>	<b>26</b>
<b>2.6.6 Electrorheological (ER) Fluids and Microwave Antenna .....</b>	<b>26</b>
<b>2.6.7 Electrochromic Device .....</b>	<b>27</b>
<b>2.7 Electrical and Optical Properties of Conducting Polymer Blends.....</b>	<b>28</b>
<b>2.7.1 Polymer Blends: Electrical Property Curve and Charge Transport Models.....</b>	<b>28</b>
<b>2.7.1.1 Nonlinear J-V Characteristics in Organic Semiconductors.....</b>	<b>29</b>
<b>2.7.2 Blends of Optical Property .....</b>	<b>30</b>
<b>2.7.2.1 Absorption and Absorption Edge Study.....</b>	<b>30</b>
<b>2.7.2.2 Optical Band Gap.....</b>	<b>31</b>
<b>2.7.2.3 Calculation of Optical Gap and Urbach energy .....</b>	<b>31</b>
Chapter Three .....	40
Materials. Synthesis Method and Characterization Technique .....	40
<b>3.1 Materials .....</b>	<b>40</b>
<b>3.2 Synthesis Method .....</b>	<b>40</b>
<b>3.2.1 Synthesis of Polypyrrole (PPy).....</b>	<b>40</b>
<b>3.2.2 Synthesis of Polypyrrole (PPy) with Sodium dodecyl sulfonate (SDS) .....</b>	<b>41</b>
<b>3.2.3 Synthesis of Polyaniline (PANI) .....</b>	<b>42</b>
<b>3.2.3 Synthesis of PANI/PPy blends .....</b>	<b>43</b>
<b>3.3 Characterization Technique.....</b>	<b>44</b>

<b>3.3.1 UV-vis Spectroscopy</b> .....	44
<b>3.3.2 Fourier-Transform Infrared (FT-IR) Spectroscopy</b> .....	45
<b>3.3.3 Scanning Electron Microscope (SEM)</b> .....	46
<b>3.3.4 X-Ray Diffraction (XRD)</b> .....	47
<b>3.3.5 Current-Voltage (I-V) Characteristics</b> .....	48
<b>3.3.6 Photoluminescence (PL)</b> .....	48
<b>3.3.7 Thin Film Preparation</b> .....	49
<b>3.3.8 Electrochemical Measurement</b> .....	49
<b>Chapter Four</b> .....	50
<b>Study on the Miscibility of Polypyrrole and Polyaniline Polymer Blends</b> .....	50
<b>Abstract</b> .....	50
<b>4.1 Introduction</b> .....	50
<b>4.2 Materials and Methods</b> .....	53
<b>4.3 Results and Discussion</b> .....	54
<b>4.4 Conclusion</b> .....	59
<b>Chapter Five</b> .....	62
<b>5.1 Optical Properties of Nanostructural Polyaniline Depending on Doping or Dedoping</b> ..	62
<b>Abstract</b> .....	62
<b>5.1.1 Introduction</b> .....	62
<b>5.1.2 Experimental</b> .....	64
<b>5.1.3 Results and Discussion</b> .....	65
<b>5.1.4 Conclusions</b> .....	71
<b>5.2 Electrical and Optical Properties of Polypyrrole and Polyaniline Blends</b> .....	73
<b>Abstract</b> .....	73
<b>5.2.1 Introduction</b> .....	73
<b>5.2.2 Methods</b> .....	76
<b>5.2.5 Conclusion</b> .....	91
<b>Chapter Six</b> .....	96
<b>The PolyPyrrole-polyaniline (PPy-PANI) Blend Electrode Material for Energy Storage</b> ...	96
<b>Abstract</b> .....	96
<b>6.1 Introduction</b> .....	96
<b>6.2 Methods</b> .....	98



<b>6.3 Result and Discussion .....</b>	<b>99</b>
<b>6.4 Conclusion.....</b>	<b>109</b>
<b>Chapter Seven .....</b>	<b>113</b>
<b>General Conclusion and Recommendations (Future Perspective).....</b>	<b>113</b>
<b>7.1 General Conclusion.....</b>	<b>113</b>
<b>7.2 Recommendations (Future Perspective) .....</b>	<b>114</b>

## List of Tables

Table 2.1 Comparison of organic and inorganic devices-----	10
Table 2.2: Copolymerization of PANI/PPy using three distinct copolymers-----	17
Table 2.3: Advantage and disadvantage of different deposition techniques-----	20
Table 2.2 The band gap of conjugated polymers-----	21
Table 2.3 Conductivity, properties and limitation of common conjugated conducting polymers-----	23
Table 4.1 Glass transition of PPy, PANI and PPy:PANI = 50:50-----	59
Table 5.2.1: The FT-IR assignment of PANI, PPY and PPy/PANI=50:50Blend-----	80
Table 6.1 The band gap of conjugated polymers and their blends using Tauc model-----	86
Table 5.2.3: Conductivity of Pure PPy, PANI and Blend-----	91
Table 6.1: The blend composition-----	100

## List of Figures

Figure 2.1: The development of electronic device .....	9
Figure 2.2: Chemical structure of polyaniline (PANI) and polypyrrole (PPy). .....	21
Figure 2.3: J-V characteristics of device A at different temperatures in the range 290-100 K. .....	29
Figure 3.1: Schematic diagram of synthesis root of Polypyrrole (Ppy).....	41
Figure 3.2: Schematic diagram of synthesis root of Polyaniline (PANI) .....	43
Figure 3.3: Schematic diagram Synthesis of Ppy/PANI blends .....	44
Figure 3.4: UV/Nis spectrophotometer. ....	45
Figure 3.5: FT-IR spectrometer .....	46
Figure 3.6: JEOL Field Emission Scanning Electron Microscopy instrument .....	47
Figure 3.7: XRD instrument- Analytical X'Pert.....	48
Figure 4.1: Chemical structure of polyaniline (PANI) and polypyrrole (PPy) .....	51
Figure 4.2: FT-IR spectra of PANI, PPy, the mixture of PPy:PANI = 50:50, PPy:PANI = 70:30, PPy:PANI = 80:20, and PPy:PANI= 90:10 (wt.%). ....	55
Figure 4.3: XRD of (a) PANI, (b) PPy, and (c-f) PPy/PANI Mixture.....	57
Figure 4.4: The DSC analysis to examine the miscibility of the PPy/PANI system .....	58
Figure 5.1.1: FT-IR Spectroscopy for HCl-doped PANI (PAHCl) and dedoped PANI (PANH) by NH <sub>4</sub> OH. ....	66
Figure 5.1.2: XRD Hydrochloric acid doped PANI (PAHCL) and Dedoped By Ammonia (PANH) .....	67
Figure 5.1.3: UV- Vis spectroscopy for HCl-doped PANI (PAHCl) and dedoped PANI (PANH) by NH <sub>4</sub> OH. ....	68
Figure 5.1.4: Plot of $(\alpha hv)^2$ versus photon energy $hv$ for (a) HCl-doped PANI (PAHCl) and (b) dedoped PANI (PANH) by NH <sub>4</sub> OH. ....	69
Figure 5.2.1 FT-IR Spectra of PANI, PPY and PPy/PANI=50:50 Blend.....	77
Figure 5.2.2: SEM images of the a. PANI, b. PPy and c. PPy:PANI=50:50 blend.....	80
Figure 5.2.3: EDX Spectra of the a. PPy, b. PANI, and c. PPy:PANI=50:50 blend .....	81
Figure 5.2.4: UV-Vis spectra of the blends PPy:PANI=50:50, PPy:PANI=70:30, PPy:PANI=80:20, PPy:PANI=90:10, PPy and PANI-HCl .....	82
Figure 5.2.5: Plot of $(\alpha hv)^2$ versus photon energy $hv$ for (a) PANI and (b) PPy .....	83
Figure 5.2.6: the band gap of blends using Tauc's models (a) PPy:PANI=50:50, (b) PPy:PANI=70:30, (c) PPy:PANI=80:20 and (d) PPy:PANI=90:10.....	84
Figure 5.2.8: J-V curve PANI.....	87

Figure 5.2.9: J-V curve PPy .....	87
Figure 5.2.10: The J-V characteristics of Blends PPy:PANI= 50:50 .....	88
Figure 5.2.11: The J-V characteristics of Blend PPy:PANI=80:20 .....	89
Figure 6.1c: PPY-PANI 50:50.....	100
Figure 6.1: (d) PPy-PANI 70:30 and (e) PPy-PANI80:20 .....	101
Figure 6.1f: PPy-PANI90:10 .....	101
Figure 6.2: (a) PPy-PANI50:50_0.01 M SDS and (b) PPy-PANI50:50_0.05 M SDS .....	102
Figure 6.3: The area of working electrode .....	103
Figure 6.4: (a) PPy-PANI50:50, (b) PPy-PANI50:50+0.01 SDS and (c) PPy-PANI50:50+0.05 SDS at different current density .....	104
Figure 6.4: (d) PPy-PANI70:30 and (e) PPy-PANI80:20 at different current density .....	105
Figure 6.5: Comparison of Areal Specific capacitance of blend with Current density .....	106
Figure 6.6: (a) Nyquist Plot of PPy-PANI 50-50, (b) PPy-PANI 50-50_0.01SDS, (c) PPy-PANI 50-50_0.05SDS.and (d) The equivalent circuit of the electrode material.....	108

## Acronyms

<b>APS</b>	Ammonium persulfate
<b>BET</b>	Brunauer-Emmett-Teller
<b>BJT</b>	Bijunction Transistor
<b>CFs</b>	Cigarette filters
<b>CSA</b>	Camphor sulfonic acid
<b>DC</b>	Direct current
<b>DMSO</b>	Dimethyl sulfoxide
<b>DSSC</b>	Dye-sensitized solar cell
<b>EB</b>	Emeraldine base
<b>ECDs</b>	Electrochromic device
<b>ER</b>	Electrorheological
<b>ES</b>	Emeraldine salt
<b>FT-IR</b>	Fourier-Transform Infrared Spectroscopy
<b>HJB</b>	Heterojunction blends
<b>HOMO</b>	Highest occupied molecular orbital
<b>ISCs</b>	Inorganic semiconductors
<b>I-V</b>	Current voltage Characteristics
<b>LCST</b>	Lower critical solution temperature
<b>LED</b>	Light-emitting diode
<b>LUMO</b>	Lowest unoccupied molecular orbital
<b>OFET</b>	Organic field-effect transistors
<b>OLED</b>	Organic light-emitting diodes
<b>OPV</b>	Organic photovoltaics
<b>P3HT</b>	Poly(3-hexylthiophene)
<b>PANI</b>	Polyaniline

<b>PAP</b>	Poly(aniline-co-pyrrole)
<b>PEDOT</b>	Poly(3, 4-ethylenedioxythiophene)
<b>PL</b>	Photoluminescence
<b>PPV</b>	Poly(p-phenylene vinylene)
<b>PPy</b>	Polypyrrole
<b>PT</b>	Polythiophene
<b>RFID</b>	Radio-Frequency-Identification
<b>SCLC</b>	Space charge limited current
<b>SDBS</b>	Sodium dodecyl benzene sulfonate
<b>SDS</b>	Sodium dodecyl sulfonate
<b>SEM</b>	Scanning Electron Microscopy
<b>TCLC</b>	Trap charge limited current
<b>TEM</b>	Transmission electron microscopy
<b>TFT</b>	Thin Film Transistor
<b>TGA</b>	Thermo gravimetric analysis
<b>UCST</b>	Upper critical solution temperature
<b>UV-vis</b>	Ultraviolet-visible spectroscopy
<b>XRD</b>	X-ray diffraction

## Abbreviations and Symbols

<b>A</b>	The absorption
<b>A</b>	Area
<b>B</b>	Full width at half-maximum (FWHM)
<b>d</b>	Thickness
<b><math>E_c</math></b>	Conduction band (or LUMO)
<b><math>E_g</math></b>	Energy bandgap
<b>eV</b>	Electron volt
<b>M</b>	Molar concentration
<b>nm</b>	Nanometer
<b><math>N_T</math></b>	Total trap concentration
<b><math>N_v</math></b>	Effective density of states in the valence band
<b>°C</b>	Degree of Celsius
<b><math>\Omega \text{ cm}^{-1}</math></b>	Ohm per centimeter
<b>T</b>	Transmittance
<b><math>T_g</math></b>	Glass transition temperature
<b>V</b>	Volt / Applied voltage
<b><math>V_m</math></b>	Molar volume of each species
<b>wt. %</b>	Weight percentage
<b><math>N_t</math></b>	Traps density of states at energy $E$
<b><math>kT</math></b>	Thermal energy
<b><math>\alpha</math></b>	Absorption coefficient
<b><math>\beta</math></b>	Factor depending on the transition probability

$\chi$	Flory-Huggins interaction parameter
$\lambda$	Wavelength of X-ray radiation
$\mu$	Mobility of charge carrier
$\delta$	Hildebrand solubility parameters
$\varepsilon$	Permittivity
$\varepsilon_0$	Permittivity of free space
$\varepsilon_r$	Relative permittivity
$\Delta H_{mix}$	Enthalpy of mixing
$\Delta S_{mix}$	Entropy of mixing
$\Delta G_{mix}$	Gibbs free energy of mixing
$h\nu$	Photon energy



## Abstract

This dissertation aimed to study the electrical and optical properties of conducting polymer blends of polypyrrole (PPy) and Polyaniline (PANI). Polymer blend was a combination of two or more polymers to make a new product with unique properties. The properties of the blends depend on the miscibility of the polymer to each other. Study the effect of miscibility on the optical and electrical properties of polymer blends of common polymers PANI and PPy. Chapter 4: This report was on the miscibility and phase behavior of polypyrrole-polyaniline (PPy-PANI) as a various function of blend compositions. The PPy-PANI blends were prepared by solution processing method, using dimethyl sulfoxide (DMSO) solvent. The synthesized polymer blends were characterized based on the data analysis from FT-IR, XRD, and DSC. The PPy-PANI system was successful to form blends in the DMSO solvent. The polymer blends showed almost amorphous nature in XRD spectra because of intermolecular interaction between PPy and PANI macromolecules, which was confirmed by FT-IR data. Specifically, the DSC result for the PPy: PANI= 50:50 wt.% blend showed only one glass transition temperature ( $T_g$ ), which indicates that the two polymers are well miscible without undergoing any phase separation. Chapter 5.1: This work aims to present the optical and thermal study on doped and dedoped polyaniline (PANI) nanoparticles. Herein, PANI nanoparticles are successfully synthesized by chemical oxidative polymerization of aniline in the presence of hydrochloric acid and ammonium persulphate as oxidant. Then PANI power samples are characterized by FT-IR, XRD, TGA, and UV-Vis. The crystallinity of doped PANI is significantly decreased once it is dedoped. The average crystallite size of PANI is estimated to be ca. 24.27 nm based on Scherrer's equation. The optical absorption peaks of transition are observed at 337 nm and 320 nm for doped and dedoped PANI, respectively. Chapter 5.2: This work aimed to study the polymer-blend morphologies, electrical and optical properties of PPy/PANI materials. The polymer blends have been developed by varying the ratio of the constituent polymer. The characteristic techniques, SEM-EDX, UV-Vis, PL, and I-V were applied to study the blends. The result determines the optical band gap of different composition of the blends were in the range of 1.53-1.95 eV. The chemical composition of the PPy/PANI blends materials were determined. Finally, the electrical transport and the conductivity of the blend observed in the range of  $10^{-6}$  to  $10^{-3}$  S/cm at room temperature. The PPy/PANI blend has exhibits a semiconductor behavior. Chapter 6: This paper reported that the preparation of a thin film of pure PANI and PPy-PANI blend on Indium Tin Oxide (ITO) substrate by using the drop-casting

method. Investigated an application of the blend as an electrode material. Cyclic Voltammetry (CV) indicated that the PPy/PANI blend has an ideal capacitive behavior. Electrochemical impedance spectroscopy (EIS) and Galvanostatic charge-discharge (GCD) measurements proved that the blend electrode with composition PPy: PANI = 50:50+0.01SDS showed that the lower value of ESR, no semicircle was observed and the highest areal specific capacitance ( $134.36 \text{ F.cm}^{-2}$  at  $0.1 \text{ mA.cm}^{-2}$ ) compared to other compositions. The electrochemical studies of PPy-PANI blends showed that PPy-PANI blends were suitable materials for electrodes of the supercapacitors.

**Keywords:** Polyaniline (PANI), Polypyrrole (PPy), Blends, Electrical, Optical, Tauc model, Miscibility DSC, Energy Storage, Electrode, Cyclic Voltammetry (CV), Specific capacitance, Drop-Casting

# Chapter One

## General Introduction

This chapter contains seven subsections. The first section presents the background and rationale of the study with an emphasis on conducting polymer, its blend, and applications. The next section describes the statement of problems, the background of the study area, which elucidates the advantage, limitation, and solution in the area of conducting polymer blends. Then, the objectives of the dissertation. Toward the end, focus on the scope of this work, the significance of this study and the hypothesis question of the thesis.

### 1.1. Background and Rationale of the Study

Conducting polymers have been widely studied in the fields of flexible and low-cost electronic devices. This is because this plastic material can be processable at low temperatures as well as deposited on plastic substrates to enable the fabrication of lightweight, flexible, and ultra-thin electronic devices. Conjugated polymer semiconductors are currently used in organic field-effect transistors (OFET), organic light-emitting diodes (OLED), organic solar cells (OSC), photodiodes, and plastic lasers (Yao et al., 2016) (Shuib et al., 2015). Various important conducting polymers have been investigated continuously, which includes polypyrrole (PPy), polyaniline (PANI), polythiophene (PT), poly (3, 4-ethylene dioxythiophene) (PEDOT), trans-polyacetylene, and poly (p-phenylene vinylene) (PPV) (Le et al., 2017).

Specifically, the electrical and optical properties of conjugated polymers have attracted tremendous academic and industrial research interests over the past decades due to the interesting advantages that organic or polymeric materials offer for electronic applications and devices. Since mid-1980, the intrinsic single conducting polymers have been substituted by the conducting polymer blends in optoelectronic devices. The polymer blend is a combination of two or more polymers to make a new product with unique properties (Paul and Barlow, 1980). The polymer blend is a promising alternative because of several advantages such as simplicity in preparation, low cost, and easy control of physical properties by compositional change (Polu et al., 2014). Nevertheless, the properties of the blends depend on the miscibility of the polymer components (Robeson, 2014), which is the main interest of the researcher of this study.

Miscibility is similar to solubility in thermodynamics, namely, two or more polymers are miscible in each other if the free energy of mixing is negative (Huggins, 1942). Polymer blends have a strong tendency to be phase-separated, which process is driven by the low entropy of mixing as explained by the Flory-Huggins theory (Manias and Utracki, 2014). The phase separation depends on materials interaction parameters, i.e., exchange energy, as well as entropy depending on the composition of mixture (Benten et al., 2016). To build a high performance of an organic electronic device, an understanding of the properties of materials is required. This knowledge will lead to the design of new materials with desirable characteristics through materials engineering.

The properties of polymer blends have been studied experimentally and/or theoretically. Sometimes, the experimental method is preferable to computational. However, computational material science is significant in that it can relate to the nature of the atomic structure of organic materials to their properties. Also, computational modeling can provide a lot of useful physical insights about the whole process of the factors that affect device operation and properties that are crucial in material design including such properties as light absorption, chain conformations, electronic structures, and so forth.

## **1.2. Statement of the Problems**

Polymer blending is the simplest and most well-known technique in polymer engineering for creating new solid materials with more enhanced properties than each component polymer. Polymer mixture with other polymers or small molecules is called “polymer blend”. Polymer electronics can be manufactured at a lower cost compared to conventional silicon-based electronics. This is because organic and polymer semiconductors have van-der Waals bonding among molecules affording an inexpensive processing condition. To fabricate high-performance optoelectronic devices, the knowledge of the electrical and optical properties should be prerequisite. However, the first-generation polymer blend materials are so much limited by the difficulty of insolubility and infusibility of the materials, which can lead to poor electronic conductivity and mechanical properties. Hence, from the aforementioned factors point of view, the miscibility of polymer blends should be a determinant factor in optical and electrical properties. Polypyrrole (PPy) and Polyaniline (PANI) are promising conducting polymers due to their unique properties. These materials have been the most researched conducting polymers. Many researchers

have been reported their studies on the synthesis of PPy or PANI which showed different properties in conductivity, solubility, thermal stability, improving morphology, etc. Besides, PPy or PANI compounded with inorganic nanomaterials to widen the application area. But few researchers report on compounding PPy with PANI materials even they have excellent performance. Some researchers have been reported their studies on the copolymerization of aniline and pyrrole (PPy-PANI materials). However, the potential application of these conducting polymer is limited by low processability. Once they are formed, they are insoluble. To overcome the above drawbacks and to achieve good processability, the improvement in the miscibility of PPy-PANI compounding or blending is significant. This research work is focused on compounding PPy with PANI in solution blending method, investigate the effect of surfactant on the miscibility of polypyrrole and polyaniline (PPy-PANI) polymer blend characterize the miscibility of the compounded polymer, investigate their electrical, optical and electrochemical properties of the prepared materials. And also study the application area of the blend polymer materials. The researcher used scanning electron microscopy (SEM), transmission electron microscopy (TEM), UV-visible spectroscopy (UV-vis), photoluminescence (PL), Fourier transform infrared spectroscopy (FT-IR), x-ray diffraction (XRD), thermogravimetric analysis (TGA), and BET surface analysis.

### **1.3. Background of the Study Area**

Blending or mixing of different polymers has created new materials with useful functions that cannot be derived from each constituent polymer alone (Mayer et al., 2007). Conjugating polymers can be blended with other materials, including inert polymers and small molecules. In the organic photovoltaic field, for example, the most efficient devices are currently based on blends of conjugated polymers with fullerene derivative, e.g., (6,6)-phenyl-C61-butyric acid (PCBM) (Su, 2015). Blends have been designed to combine attractive features of each component. Resultantly, sometimes, the microstructure of a blend has new properties, which is not present in every single component. In the field of polymer electronics, where conjugated polymers are processed from solution to form the active semiconducting layer of a light-emitting diode (LED) or photovoltaic device, blending is an attractive approach to optimize the device function (McNeill and Greenham, 2009). The large-scale application of PANI-PPy composite is sometimes limited by poor

processibility leading to a malfunction of devices. Therefore, the improvement of the comprehensive properties of the PANI-PPy blend or nanocomposite is considered to be significant (Kelly et al., 2010). From the processing-structure-property-performance interrelationship point of view, the phase behavior of blend materials could be very important, because its structure had a direct relation to the function of materials when incorporated into a device. Specifically, the phase separation of blend depends on Gibbs free energy as a function of enthalpy and entropy, which factors are well considered in the Flory-Huggins theory. The issue of phase separation is particularly interested in conjugated polymer blend systems because of its rigidity,  $\pi$ - $\pi$  interaction, planar structure, limited solubility in a common solvent, etc. The knowledge of this phase behavior in conjugated polymers has been extremely useful in designing organic electronic devices such as field-effect transistors, organic light-emitting diodes (OLEDs), memory storage elements, supercapacitor, sensors, and photovoltaic cells (Usta et al., 2011).

#### 1.4. Objectives

##### General objective:

- ❖ Study the electrical and optical properties of conducting PPy/PANI blend

##### Specific objectives:

- ❖ Synthesis of PPy/PANI blend by solution methods
- ❖ Investigate the miscibility of the PPy/PANI blends
- ❖ Characterize the optical and electrical properties of the PP/PANI blend
- ❖ Characterize the electrochemical behavior of the PPy/PANI blends
- ❖ Study the application area of the PPy/PANI blends

## 1.5. The Scope of the current work

This thesis aims to study the optical and electrical properties of conductive polymer blends. The study of conducting polymers blend is based on the experimental and theoretical explanations. In this work, PANI-PPy conducting polymer blends are used as a model blend system for studying electrical and optical properties of materials. The blend of PPy-PANI is synthesized and characterized. Besides, with the help of theoretical analysis, the researcher further optimizes the properties of materials. In conducting a polymer blend system, the main problem is known to be processibility in both solution and melt processes. Hence, the miscibility of two components is studied from the processibility point of view as a blended system. Furthermore, the optical and electrical properties of the PPy-PANI blend are deeply investigated. Also, the effect of surfactant in the miscibility, solubility, and the electrical and optical properties of PPy-PANI polymer blends is well evaluated. Finally, based on the experimental data and theoretical analysis, the optical and electrical properties of the polymer blends are studied in the tested for the optoelectronic device. Because the development of solution-processable high-mobility n-type semiconducting polymers remains a major obstacle to further advances in organic electronics (Zhao and Zhan, 2011), the researcher study the n-type material in future work. Note that in this study, we have focused on the p-type polymer semiconductors such as polyaniline, polypyrrole, and blend.

## 1.6. Significance of the study

Recently, polymer blends have attracted many scientists to devote their lives to studying the polymer-polymer system to develop new functional plastics with technologically attractive properties. Polymers have been blended or mixed to enhance the performance and processability of organic polymer semiconductors for device applications. The PANI/PPy blend system is known to have a limited application because of its partial miscibility and solubility in common organic solvents. This limitation affects all optical and electrical properties of materials in a device, because of unfavorable processability. Hence, the enhancement of processability through a deep understanding of the miscibility of the PANI/PPy system is very desirable, which should be the main interest in this work. study the optoelectrical application of the blend polymer materials.

## 1.7. Hypothesis Questions

Is PPy compound with PANI in the solution process?

Which solvent is best for PPy- PANI compound?

What are the electrical properties of PPy- PANI blend?

What are the optical properties of PPy- PANI blend?

What are the electrochemical properties of PPy- PANI?

What is the effect of doping sodium dodecyl sulfate (SDS)?

Which area the PPy- PANI blend is applied?

## References

- BENTEN, H., MORI, D., OHKITA, H. & ITO, S. 2016. Recent research progress of polymer donor/polymer acceptor blend solar cells. *Journal of Materials Chemistry A*, 4, 5340-5365.
- HUGGINS, M. L. 1942. Some Properties of Solutions of Long-chain Compounds. *The Journal of Physical Chemistry*, 46, 151-158.
- KELLY, T. L., YANO, K. & WOLF, M. O. 2010. Nanoscale Control over Phase Separation in Conjugated Polymer Blends Using Mesoporous Silica Spheres. *Langmuir*, 26, 421-431.
- LE, T.-H., KIM, Y. & YOON, H. 2017. Electrical and Electrochemical Properties of Conducting Polymers. 9, 150.



- MANIAS, E. & UTRACKI, L. A. 2014. Thermodynamics of Polymer Blends. *In*: UTRACKI, L. A. & WILKIE, C. A. (eds.) *Polymer Blends Handbook*. Dordrecht: Springer Netherlands.
- MAYER, A. C., SCULLY, S. R., HARDIN, B. E., ROWELL, M. W. & MCGEHEE, M. D. 2007. Polymer-based solar cells. *Materials Today*, 10, 28-33.
- MCNEILL, C. R. & GREENHAM, N. C. 2009. Conjugated-Polymer Blends for Optoelectronics. 21, 3840-3850.
- PAUL, D. R. & BARLOW, J. W. 1980. Polymer Blends. *Journal of Macromolecular Science, Part C*, 18, 109-168.
- POLU, A., KUMAR, R. & RHEE, H.-W. J. I. V. 2014. Magnesium ion conducting solid polymer blend electrolyte based on biodegradable polymers and application in solid-state batteries. 125-132.
- ROBESON, L. 2014. Historical Perspective of Advances in the Science and Technology of Polymer Blends. 6, 1251-1265.
- SHUIB, U., MOHAMAD, K., ALIAS, A., TABET, T., GOSH, B. & SAAD, I. 2015. Modelling and Simulation Approach for Organic Thin-Film Transistors Using MATLAB Simulation. *Advanced Materials Research*, 1107, 514-519.
- SU, N. 2015. Improving Electrical Conductivity, Thermal Stability, and Solubility of Polyaniline-Polypyrrole Nanocomposite by Doping with Anionic Spherical Polyelectrolyte Brushes. *Nanoscale research letters*, 10, 997-997.
- USTA, H., FACCHETTI, A. & MARKS, T. J. 2011. n-Channel Semiconductor Materials Design for Organic Complementary Circuits. *Accounts of Chemical Research*, 44, 501-510.
- YAO, J., YU, C., LIU, Z., LUO, H., YANG, Y., ZHANG, G. & ZHANG, D. 2016. Significant Improvement of Semiconducting Performance of the Diketopyrrolopyrrole-Quaterthiophene Conjugated Polymer through Side-Chain Engineering via Hydrogen-Bonding. *Journal of the American Chemical Society*, 138, 173-185.
- ZHAO, X. & ZHAN, X. 2011. Electron transporting semiconducting polymers in organic electronics. *Chemical Society Reviews*, 40, 3728-3743.

## Chapter Two

### Review of Literature

#### 2.1. Development of Organic Electronics and Organic Semiconductors

##### 2.1.1 Background

The age of electronics has started in the 1880s. At this stage, the pioneering work was a vacuum tube or thermionic valve in the early time of electronics developments. This period is called the vacuum tube era. The next revolutionized period of electronics is called the transistor era. At this stage follows the achievement of Bardeen, Brattain, and Shockley in 1948. The transistor era has more advantages over the vacuum tube era, such as more reliable, cheaper, less power, fast and less space (Ross 1998). The materials used in electronics fabrication passed through different development ages. For example, tungsten and cesium alloy are used in the vacuum tube era (Lassner and Schubert, 1999). On the other hand, Si, Te, Ge, InSb, CdSe, CdS, and a-Si:H, (Xu, 2011) were commonly used in the transistor era. Ever since the evolution and development of the semiconductor technology have been continued and organic materials replace inorganic semiconductors. Figure 2.1 shows the overall development of electronic devices.

Note that, almost a century ago, the first electronic device has been developed by German physicist Karl Ferdinand Braun in 1897. Since then, scientists are demanding and diligently working to get new materials in the field of electronics for different advantages, i.e., large capacity, low cost, lightweight, flexible device, fast speed, small size, etc. This drive leads to paying attention to organic and polymer electronics as well as organic optoelectronics materials (Shirakawa et al., 1977). Specifically, Alan Heeger, Alan MacDiarmid, and Hideki Shirakawa have discovered semiconducting and metallic polymers in 1976. Resultantly, the Nobel Prize in chemistry was awarded to them in the year 2000 for this discovery of a conducting polymer, e.g., iodine vapor doped polyacetylene (Klauk, 2010). This emerging technology of electrically conductive polymers have radically changed outlooks on polymer materials (known as an insulator) and laid a basis for future organic polymer electronic devices. Unlike inorganic semiconductors such as Si or Ge, semiconducting polymers have the potential to be optically

transparent, rapidly and easily processable, and mechanically compliant, all of which can be potential advantages for organic electronics. Mechanical compliance in particular allows the use of semiconducting polymers in unique electronic applications, in which stretchability is a key factor (Tang et al., 1987).

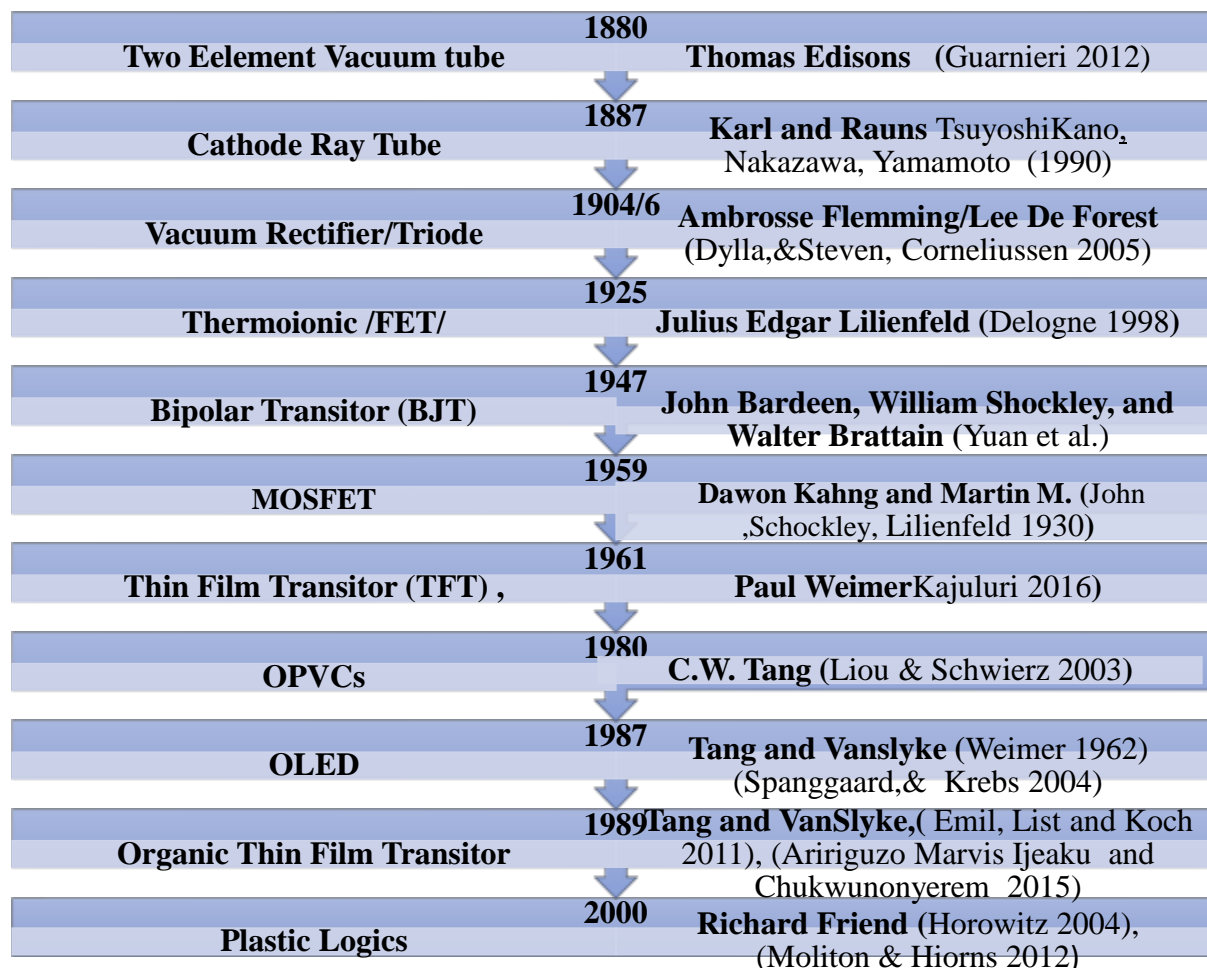


Figure 2.1: The development of the electronic device

### 2.1.2 New Electronics Age Based on Organic Semiconductors

Organic electronics is a branch of modern electronics, and it deals with organic materials, such as polymers or small molecules. The materials used in this kind of emerging technology are carbon-based, which is the same as the molecules of bio/living systems. When considering the properties of organic materials, we may not generally feel that they are electrical conductors. Oppositely, organic materials are thought to be excellent insulators in electronics applications.

However, based on  $\pi$ -electrons in  $p_z$  orbitals in the conjugated polymer backbone, a charge could be transported through the  $\pi$ -conjugated bonding or hopping through molecules. Hence, the conjugated polymer could be a semiconductor or synthetic metal. Furthermore, based on the combination of polymeric molecules, we can categorize polymer materials into two groups, e.g., intrinsic conducting polymers and polymer blend or composite polymers. Note that the discovery of the electrical conduction in organic materials can be traced back to the year 1862, in which time Henry Letheby obtained a partial conducting material by anodic oxidation of aniline in sulfuric acid. In 1962 polycyclic, 1970 polyacetylene, 1985 tris(8-hydroxyquinoline) aluminum (Alq3) and diamine, 1980s small molecules called oligomer and sexithiophene (6T) were studied as a different class of materials in organic electronics (Zaki, 2015). Currently, organic electronics is applied to a different field, such as Radio-Frequency-Identification (RFID). This new product also is expected to be able to replace official bar code, single-use electronics, low-cost sensor, and flexible display, based on each deposition on insulator (Bellan et al., 2004). Although those new products are partly successful in the market, the science in organic electronics is not full-grown for reaching its maximum potential, which allows materials scientists and engineers.

### 2.1.3 Comparison of Organic and Inorganic Devices

Table 2.1: Comparison of organic and inorganic devices

Specification	Organic Electronics	Inorganic Electronics
Field effect carrier mobility	Low pentacene: $3.2 \text{ cm}^2/\text{Vs}$ poly (2,5 phenylenevinylene): $0.22 \text{ cm}^2/\text{Vs}$	High single crystal silicon: $250\text{-}600 \text{ cm}^2/\text{Vs}$ poly silicon: $40\text{-}70 \text{ cm}^2/\text{Vs}$ a-Si: H: about $1 \text{ cm}^2/\text{Vs}$
Toughness	Tough	Brittle
Flexibility	Flexible	Fragile
Cost	$\$5/0.09 \text{ m}^2$	$\$100/0.09 \text{ m}^2$
Fabrication Cost	Low capital	$\$1\text{-}\$10 \text{ Billion}$
Device size	$3.1 \text{ m}$ Roll to roll	$<1 \text{ m}^2$
Materials	Flexible Plastic Substrate	Rigid Glass or Metal
Required condition	Ambient Processing	Ultra-Cleanroom
Process	Continuous Direct printing	Multi-step Photolithography

Ref: (Yoon et al., 2018)

#### **2.1.4. Advantages and Disadvantages**

Organic polymer semiconductors or synthetic metals are also biodegradable because they are made from carbon just like biosystems. This property opens a new door to many exciting and advanced new applications, which would be not possible if one uses inorganic materials such as copper or silicon. However, conductive polymers have high resistance in intrinsic status (i.e., without doping) and therefore they need some external doping and/or additional control of nanostructure for better electrical and optical properties. Note that, compared to inorganic semiconductors, the organic semiconductor has poor electronic property (e.g., low charge carrier mobility), because of their electronic structure with small bandwidths. Furthermore, despite a good processibility because of van der Waals bonding among molecules, this property provides only a short lifetime of materials or devices. Furthermore, they are much more dependent on environmental conditions than inorganic electronics would be because the latter has a crystal structure with covalent bonding but the former has Van der Waals bonding among molecules.

#### **2.1.5 Applications**

The organic semiconductor has three main applications, namely, organic light-emitting diodes (OLED), organic photovoltaics (OPV), and organic field-effect transistors (OFET). A further application could be supercapacitors, organic spintronics, organic sensors, and organic radio frequency identification (RFID) (Kenry et al., 2016) and smart textiles, lab on a chip, portable compact screens, and skin cancer treatment (Economou et al., 2018).

### **2.2. Overview of Blends**

Polymer blending is a very important technique for producing new polymer materials with improved properties beyond the range that can be obtained from a single polymer (Hulicova and Oya, 2003). The process of polymer blending is typically cheaper, easy and less time-consuming for the production of polymeric materials with new properties (Zhang et al., 2017), (Si et al., 2016). Essentially, the blend can be designed to combine attractive features of both components or can be designed to get the materials with required property (Yang, Wang et al. 2017). However, the properties of the blends are influenced by the composition of polymer blends, processing condition, and molecular parameters (Codou et al., 2018). In the early stage of blending

technologies, polymer blending has been developed to improve mechanical and physical properties (Findik et al., 2004) (Muller et al., 2011). Currently, to improve processibility and environmental stability,  $\pi$ -conjugated polymers have been blended with other polymers (Kumar et al., 2011). The properties of polymer blends depend strongly on the miscibility or compatibility of each polymer component. Polymer-polymer has miscibility, when specific interactions are available between the two polymers or when two polymer's chemical structure is very similar to each other, providing a negligible heat of mixing (Kuo et al., 2004). When miscibility occurs between the polymers, the contribution of the mixing entropy of polymer blends is generally negligible ( $\Delta S_{mix} \sim 0$ ) because of the high molecular weight of polymers, the miscibility of polymer blends is mainly dependent on the value of mixing enthalpy ( $\Delta H_{mix}$ ). For this purpose, to obtain a miscible blend system, it is usually necessary to guarantee that the enthalpy of mixing should be negative or negligible small. Basically, the miscibility of two components can be decided based on the Gibbs free energy of mixing,  $\Delta G_{mix}$ :

$$\Delta G_{mix} = \Delta H_{mix} - T\Delta S_{mix} \quad \text{Eq. 2.1}$$

Here,  $\Delta H_{mix}$  denotes the enthalpy of mixing and  $\Delta S_{mix}$  indicates the entropy of mixing. At this moment, it should be mentioned that the most recent polymer-blend technology has been focused on the area of biodegradable polymer systems, liquid crystalline polymer blends, and electrical conducting polymer blends (Utracki et al., 2014). There are three different types of polymer blends which are categorized by (Parameswaranpillai et al., 2014), (Kong et al., 2017). That is (a) completely miscible blends (b) partially miscible blends and (c) fully immiscible blends.

### 2.2.1 Miscible (Single-Phase)

Miscible blends are usually optically transparent and are homogeneous to the polymer segmental level. A homogeneous blend exhibits single glass transition temperatures intermediate between those the components. It is also called single-phase blends. This also undergoes phase separation that usually depends on variations in thermodynamics parameters such as temperature, pressure, and the composition of the mixture (Parameswaranpillai et al., 2014). Thermodynamically, completely miscible blends show the characteristic of  $\Delta H_{mix} < 0$ , due to

specific interactions, in which homogeneity is usually observed at least on a nanoscale, if not on the molecular level. The homogeneity of polymer materials is often considered as a key factor in the substantial improvement of some properties, such as processability, impact strength, tensile strength, and chemical resistance (Bourara et al., 2014).

### **2.2.2 Partially Miscible Blends**

An intermediate category of blends, a part of the one blend component is dissolved in the other, which are partially miscible, i.e., the miscible at the molecular level only under a certain conditions like temperature and composition blends. This type of blend, which exhibits a fine phase morphology and satisfactory properties, is referred to as compatible. There are two types of partially miscible blends depending on the borderline of miscibility/critical solution temperatures. The lower critical solution temperature (LCST) polymer blends are miscible at lower temperatures and phase-separated at a higher temperature, and the upper critical solution temperature (UCST) blends phase separate at the lower temperature and shows one phase at high temperature (Painter & Coleman, 2009), (Xavier et al., 2016). Partial solubility results in heterogeneous, two-phase structure, in which the size of the dispersed phase depends on several factors, among others on the interaction of the components and on the conditions of mixing (Dixit et al., 2009).

### **2.2.3 Immiscible Blends (Phase Separated)**

Immiscible blends are heterogeneous blends with very fine scales of segregation and have large size domains of the dispersed phase and poor adhesion between them. If the blend is formed by two polymers, two glass transition temperatures will be observed. Polymer blends are immiscible and will easily and inevitably undergo phase separation process. The phase-separated structures greatly affect the macroscopic properties, such as toughness, processability, transparency, chemical and weather resistance, thermal stability, flowability, etc. of a material and have a strong impact on the performance of the corresponding products. Specifically, for polymer blend films used in optoelectronic devices, the morphology and domain size of the microphase separation have a direct effect on their electrical and mechanical properties and hence the device performances (Slota et al., 2012), (Yuhang et al., 2014). However, the properties of the blends

depend on the miscibility of the polymer components. The thermodynamically immiscible nature of blend is originated from a large difference in their polarities, which leads to insufficient interfacial adhesion between blend components, resulting in poor mechanical properties. In general, the domain size distribution, morphology, and miscibility are influenced by the composition of polymer blends. In general, polymer blends are either exist in a homogeneous or heterogeneous state. The homogeneous blends, the average properties of the blend components are the final properties which mean the properties are divided equally and uniformly. Meanwhile, in heterogeneous blends, the properties of all blend components are present in the final material system.

#### **2.2.4 Miscibility**

Miscibility means mixing of two or more components on the molecular level, which results in a homogeneous structure with equal thermodynamic state variables. For mixing, the Gibbs free energy of mixing ( $\Delta G_{\text{mix}}$ ) must be negative for forming a homogeneous system. According to the principles of thermodynamics, when  $\Delta G_{\text{mix}}$  is negative, the thermodynamic miscibility and homogeneity can be reached. This condition can be fulfilled in the case when strong specific intermolecular interactions are located between the components of a polymer blend. Of course, sometimes, we may have a case, in which there is only moderate or poor interaction, inducing partial miscibility as a function of temperature and composition (Higgins et al., 2010), (Xing et al., 1998). Miscibility can be influenced by various factors such as morphology, crystalline phase, intermolecular interaction, and reduction of surface tension (Speight, 1996). The extent of conjugation or interaction between these units determines the polymer solution or solid-state electronics structure which in turn control polymer properties such as optical absorption, redox characterization, and molecular orbital energy level.

Miscibility is an important polymer property, which is commonly determined by considering the Flory-Huggins interaction parameter ( $\chi$ ). This parameter gives a theoretical description of the phase separation curves for polymers of different chain lengths and compositions (Budkowski, 1999). A high  $\chi$  value means a strong driving force for phase separation. Besides, composition, molecular weight, and concentration of the solution are important properties.



$$\chi_{13} = \frac{V_3}{RT} (\delta_1 - \delta_3)^2 + 0.34 \quad \text{Eq.2.2}$$

$$\chi_{12} = \frac{\sqrt{V_1 V_2}}{RT} (\delta_1 - \delta_2)^2 \quad \text{Eq. 2.3}$$

Subscripts 1, 2, and 3 respectively refer to polymer A, polymer B, and solvent. Polymer–solvent and polymer–polymer interaction parameters are calculated using Hildebrand solubility parameters ( $\delta$ ) available from literature via eq. 2.2 (solvent–solvent) and eq. 2.3 (polymer–polymer). Here,  $V_m$  ( $m = 1, 2, 3$ ) denotes the monomeric molar volume of each species. The second term on the RHS of eq. 2.2 represents an entropic correction, which is non-negligible when considering polymer–solvent interaction. It becomes negligibly small when the interaction between the two polymers is considered (Heriot and Jones, 2005).

## 2.3 Different Synthesis Routes of Polymer Blends or Composite

Conductive polymers containing two compounds can be prepared materials as copolymer, composites, bilayers, and blends. Several techniques have been known to synthesize conducting polymers as composite or blend. These are Solution blending, Copolymerization, in situ polymerization, melt process, and electrochemical polymerization. This part focused on the synthesis methods of PPy-PANI composite or blending. And the next part on deposition techniques of the blend polymer.

### 2.3.1 Solution Process

The solution process is the most common method and involves the mixing of both polymers in the common solvent. The dispersion of the components in a solvent, mixing, and evaporation are often supported by mechanical agitation, for example, ultrasonication, magnetic stirring, or shear mixing (Zahra et al., 2019). This method is advantageous from various points of view, such as cost minimization, scale-up, and roll-to-roll processing (Lee and Park, 2014). The variety of functional chain molecules can be blended with other materials for modification of device performances. The solution process is especially good for scale-up while minimizing processing

costs. Printing processes such as the roll-to-roll process can be utilized to mass-produce OFETs and prototype devices have been demonstrated already (Kang et al., 2013). Specifically, this blending approach is extremely common in organic photovoltaics (OPV) or organic field-effect transistor (OFET) when they prepare an active layer for OPV or semiconducting channel layer for OFET, respectively. Solution-cast polymer blends are prepared by dissolving a constituent polymer in a common solvent (Tikish et al., 2018), (Smith and Nie, 2009). When making a polymer-polymer blend at solution state, so-called solution blending, the interaction of solvent with polymers play an important role in tailoring the properties of polymer blends.

At this moment, the more recent developments in polymer blend technology will be briefly reviewed and discussed. These areas include liquid crystalline polymer blends and molecular composites, electrically conductive polymer blend, and biodegradable polymer systems (Fashandi and Karimi, 2015). This review may include some polymer blend technologies, focusing on polymer semiconductors or devices by solution processing. Recently, in a study (Namepetra et al., 2016), the solution-processed fullerene-free small-molecules heterojunction blends (HJB) proved that solution-processable OPV devices provide an outstanding and inexpensive platform to harvest solar energy using flexible substrates compatible with printing and coating techniques suited for high-volume production. Being lightweight, colored and semi-transparent OPV cells are of commercial interest for a wide range of applications such as power-generating windows and decorative lighting systems with reduced transportation and installation cost (Ahmad et al., 2013).

The solubility and flexibility of polymers allow devices to be processed by low-cost solution processing methods including roll-to-roll processing (Namepetra et al., 2016). Moreover, (McNeill and Greenham, 2009) studied conjugated polymer blends for optoelectronics, such as OLED and OPV, in which they noted that blending with controlled nanostructure is an essential approach to optimize the device performance considering exciton diffusion in OPV and charge recombination in OLED.

### **2.3.2 Copolymerization**

Copolymerization is another feasible method that can be used to modify the structure and properties of conductive polymers (Otero, 1999). Properties of copolymers are usually

intermediate between those of homopolymers, but significantly differ from those of the composites and the blends (Oliver et al., 2006). The copolymerization germination can be originated from the fact that the oxidation potential onsets of the monomers are close to each other. These copolymers have improved electrochemical, thermal, optical, and electronic performances, making them promising materials for applications in the field of organic electronic (Zhou and Xu, 2017). Another work (Hammad et al., 2018) have been investigated copolymerization of PANI/PPy using three distinct copolymers, conventional chemical oxidation, rapid mixing, and CO<sub>2</sub>-assisted with different morphologies and properties. The results are discussed in table 2.2 below.

Table 2.2: Copolymerization of PANI/PPy using three distinct copolymers

Copolymerization method	Structure	Size
conventional chemical oxidation	Core-Shell	25 nm shell thickness
rapid mixing	Hallow nanosphere	75 nm in diameter and 26 nm thickness
CO <sub>2</sub> -assisted	Nanoparticle	53 nm average diameter

(Hammad et al., 2018)

Furthermore, (He et al., 2018) have been reported that hierarchical polyaniline/polypyrrole (PANI/PPy) copolymer nanofiber was prepared via a two-step method with a rough surface and amorphous structure. The diameter of PANI/PPy nanofiber is within the range of 100–200 nm. and adopted as dispersing materials for electrorheological (ER) fluids. The ER efficiency  $\epsilon$  for PANI-1mLPPy and PANI-2mLPPy ER fluids at a shear rate 0.1 s<sup>-1</sup> is 36.6 and 28.5 under electric field strength E53 kV/mm, respectively. The results also indicate that the PANI/PPy composite particles have a distinctly enhanced ER effect compared with the pure PANI and PPy particles under electric stimuli. And also, (Mello and Mulato, 2018) reported that PANI and PPy copolymers prepared using the galvanostatic technique in an organic acid medium.

### 2.3.3 Melt processing

Melt blending or melt processing method has become attractive due to the advantage of being free of solvents. Insoluble polymers are processed by melt processing techniques (Zahra et al., 2019). Melt processing is preferred for industrial-scale processes, because of its speed and simplicity. This is also a preferred method for processing of polymers which are inappropriate for solution mixing or for in situ polymerization. (Mohsina, 2017) reported grafted blends of polypyrrole (PPy) and polypropylene (PP) were prepared by melt mixing in assisted sonicator twin screw extruder. The result indicates a strong interaction between PPy and PP phase while DCP has successfully acted as a crosslinking and grafting agent. Polyaniline (PANI)/polyolefin blends have been processed by melt pressed (Hosier et al., 2001).

### 2.3.4 In-situ Polymerization

In situ polymerization precursor compound (monomers) in the presence of polymeric materials. This method (Zahra et al., 2019) is important for morphology enhancement, for core and shell, and for the materials which cannot be melt processed, insoluble, and thermally unstable are often in situ polymerized directly and grafted on to the walls of the nanotubes. (Feng et al., 2013) reported PANI as the core and PPy as the shell for the composite has been prepared by in-situ polymerization. The results indicated that PPy successfully grafted on PANI and the heat resistance of nanocomposite was remarkably increased. Other work (Saini and Basu, 2012) reported that in situ polymerization was used for synthesis conducting polymers blends graphene/AuNP/PANI. In the study by (Liang et al., 2014) have been reported another efficient approach to prepare composite nanofibers by in situ chemical polymerization of pyrrole in the presence of polyaniline (PANI) nanofibril seeds for integrating the excellent properties of PANI and polypyrrole (PPy). In this approach, the PANI core and the PPy shell were prepared. The PPy shell affects the morphology, structure, and properties of composite nanofibers. A result indicated that the efficient charge transport along with the nanofiber orientation and charge transfer between the core and shell of the composite nanofibers can be improved. Furthermore, compared with neat PANI and PPy, great improvements in electrical and electrochemical properties for the composite

nanofibers can be achieved due to their unique configuration and synergistic contribution. (Su, 2015) reported that in situ layer-by-layer polymerization. The result indicated that Improved Electrical Conductivity, Thermal Stability, and solubility of Polyaniline and Polypyrrole Nanocomposite by Doping with Anionic Spherical Polyelectrolyte Brushes.

### **2.3.5 Electrochemical polymerization (Layer to layer)**

Synthesized PPy/PANI composite layer by layer. Electrochemical polymerization is a very effective technique for the deposition of Polymer coating on a various substrates. The researcher reported that the Polyaniline/ polypyrrole composite coated on Al 2024 substrate in aqueous oxalic acid solution by using cyclic voltammetry. The result indicated that the composite coatings showed distinct changes in morphology from that of the homopolymer coatings (Akundy et al., 2002).

### **2.3.6 All comparison /summery**

There is three main common methods of polymer blending, like solution mixing methods, melt processing, and in situ methods. Solution mixing is important or preferable for the polymers that are soluble in a common solvent. If the polymer is insoluble in a solvent, melt processing better for the blending of polymers. And if the polymers neither insoluble nor melt, in situ blending is a preferable method for the blending of polymers.

## **2.4 Different Deposition Techniques /Film Deposition Methods**

Coating-based methods are easily amenable to low-cost fabrication because they do not require complicated instruments. However, only soluble or solution-processable polymers can be deposited onto a substrate using coating-based methods. Polymers are either soluble or insoluble in the organic and inorganic solvent. Different routes are used to deposited soluble and insoluble polymers on the substrate. An insoluble polymer is deposited on a substrate via Vapor phase methods which are categorized either physical or chemical deposition routes, for example, CVD, sputtering, etc. and this method require well-controlled atmosphere, vacuum energy-intensive and expensive method (Eslamian et al., 2018), on the other hand, soluble polymers are easily deposited

from the liquid phase at room temperature, cost-effective way, suitable for scalability and commercialization of thin-film devices (Eslamian, 2016). Therefore, soluble polymers are deposited using Drop Casting, Spin Coating, Doctor Blading, Dip Coating, Spray Coating. Each method has its advantages and disadvantages and maybe more suitable for a particular application. Table 2.3 discussed the advantage and disadvantage of the above-mentioned deposition techniques below.

Table 2.3: Advantage and disadvantage of different deposition techniques

Deposition technique	Advantages	Disadvantages
Drop Casting (Eslamian et al., 2018)	<ul style="list-style-type: none"> <li>• Very simple</li> <li>• No waste of material</li> </ul>	<ul style="list-style-type: none"> <li>• Limitations in large area coverage</li> <li>• Thickness hard to control</li> <li>• Poor uniformity</li> </ul>
Spin Coating (Richter et al., 2017)	<ul style="list-style-type: none"> <li>• Good uniformity/reproducibility</li> <li>• Good control on thickness</li> </ul>	<ul style="list-style-type: none"> <li>• Waste of material</li> <li>• No large area</li> <li>• Film dries fast</li> </ul>
Doctor (Richter et al., 2017)	<ul style="list-style-type: none"> <li>• Large area</li> <li>• No waste of material</li> <li>• Good uniformity</li> </ul>	<ul style="list-style-type: none"> <li>• Micrometric precision of blade regulation</li> <li>• Film thickness &gt; 150÷200nm</li> </ul>
Dip Coating (Tang et al., 2017), (Nguyen-Tri et al., 2018)	<ul style="list-style-type: none"> <li>• Quite good uniformity</li> <li>• Very thin layers</li> <li>• Large area coverage</li> </ul>	<ul style="list-style-type: none"> <li>• Waste of material</li> <li>• Time-consuming</li> <li>• Double side coverage</li> </ul>
Spray Coating (Jeon et al., 2015), (Kwon et al., 2015)	<ul style="list-style-type: none"> <li>• Adjustable layer thickness</li> <li>• Large area coverage</li> <li>• Independence on substrate topology</li> </ul>	<ul style="list-style-type: none"> <li>• Homogeneity of the film</li> </ul>

## 2.5 Literature Survey of Conducting Polymer Blends: Polypyrrole and Polyaniline

Polypyrrole (PPy) is one of the most important conducting polymer materials. It has several advantages, such as easy synthesis, low cost, low toxicity, high electrical conductivity, good redox

properties, and environmental stability (Wang et al., 2017). The table below shows the band gap of conjugated polymers.

Table 2.4: The band gap of conjugated polymers

Polymers	Cal. Band gap (eV)
PANI	1.3-1.5 (Veluru et al., 2013)
PPy	1.3-2.4 (Manahil, et al., 2014) (Loguercio et al., 2015)

Polyaniline (PANI) is also one of the most extensively studied conducting polymers. That is because it has characteristics and/or applications, such as easy synthesis and doping-dedoping chemistry, low cost, high conductivity, excellent environmental stability, and wide potential applicability, erasable optical information storage, shielding of electromagnetic interference, microwave and radar electrochemical capacitors, electrochromic devices, nonlinear optical, electromechanical actuators, antistatic and anticorrosion coatings, high specific capacitance and electroactivity (Dhachanamoorthi et al., 2017).

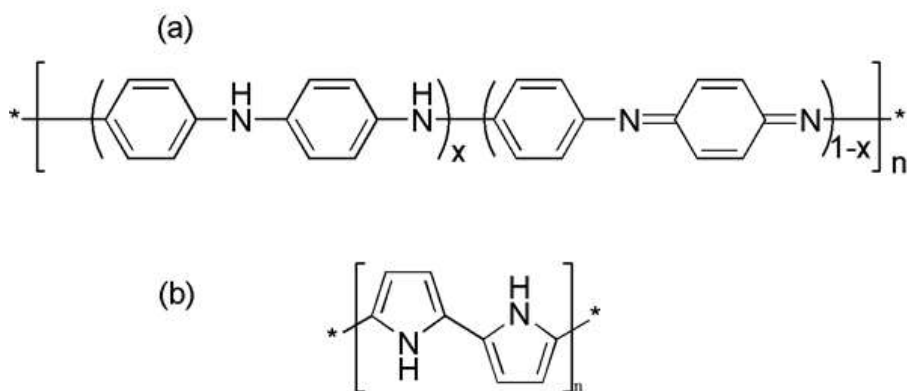


Figure 2.2: Chemical structure of polyaniline (PANI) and polypyrrole (PPy).

The large-scale application of PANI-PPy composite is sometimes limited by the difficulty of insolubility and infusibility of the material, which can lead to poor electronic conductivity and mechanical properties. The research stressed that much improvement of the properties of the PANI-PPy blend or nanocomposite should be needed (Su, 2015). Another research indicated that blending improves the properties of blend materials, which affords PANI to have various

applications when blended with a commercially available polymer with good processability and mechanical properties. This research work points out that PANI has many advantages but has low solubility in several common solvents. PANI blending with polyvinyl alcohol (PVA) improved the solubility of PANI and this novel composite can be applied for Ag nanoparticles coating (Choudhury, 2009), (Wang et al., 2013), (Ghaffari-Moghaddam and Eslahi, 2014). The following paper stated that PANI–PPy blends/composites have attracted a great deal of attention due to their multifunctional properties, including hydrophobicity, acid-base character,  $\pi$ - $\pi$  interactions, polar functional groups, ion exchange properties, hydrogen bonding, and electroactivity. Also, PANI–PPy–CFs (cigarette filters) were synthesized by chemical oxidation polymerization in a triple-phase interface system, where the composite is prepared in the presence of oxidation in the middle aqueous phase (Nascimento et al., 2016). The composite materials were used in the adsorption applications. (Hammad et al., 2018) have been investigated by chemical copolymerization of polyaniline/polypyrrole using three distinct preparation chemical polymerization methods to prepare various copolymers with different morphologies and properties.

Furthermore, more researches have been carried out for characterizing the PANI/PPy composites and/or blends. (Xing et al., 2007) prepared PANI/PPy composite from a PANI dispersion using sodium dodecylbenzene sulfate (SDBS) as both dopant and surfactant in HCl acid. And they reported that the PANI/PPy system has exhibited some specific interactions between PANI and PPy macromolecules. Also, they pointed out that their PANI/PPy composite has high conductivity based on excellent sponge-like morphologies. According to another research using copolymer such as poly (aniline-co-pyrrole) (PAP), some nanostructures were constructed for application to chemiresistive ammonia sensor, in which the copolymer PAP sensor showed improved sensing ability towards low concentration of ammonia, as compared to its homopolymer PANI or PPy sensors at room temperature. The PAP sensor was reported to be very reliable in terms of cost, recovery time, selectivity, reproducibility, detection range, and stability (Chaudhary and Kaur, 2014). The next work (Ou and Xu, 2016) indicated that highly conductive PAP copolymer was synthesized by properly controlling pre-polymerization time, which showed improved conductivity without any significant change of morphologies of a film. (Akundy et al., 2002) were applied as an electrochemical deposition technique for the synthesis of a PANI/PPy



composite on the aluminum substrates in the aqueous oxalic acid solution. They reported that some morphology changes were observed in their PANI/PPy composite. The aforementioned results are some background works for studying on the PANI/PPy blend or nanocomposite systems (Tikish et al., 2018). The conductivity of PPy films can be achieved around  $10^3 \text{ S cm}^{-1}$  depending on the type and amount of dopant.

Table 2.5 Conductivity, properties, and limitation of common conjugated conducting polymers

Polymer	Conductivity ( $\text{Scm}^{-1}$ )	Type of doping	Properties	Limitations
<b>Polypyrrole</b>	$10-7.5 * 10^3$	p	High electrical conductivity, ease of preparation and ease of surface modification	Rigid, brittle and insoluble
<b>Polyaniline</b>	30–200	n, p	Diverse structural forms, environmentally stable, low cost	Hard to process, non-biodegradable, limited solubility
<b>Polythiophene</b>	$10-10^3$	p	High electrical conductivity, ease of preparation, good optical property	Hard to process
<b>Poly (3,4-ethylene dioxothiophene)</b>	0.4–400	n, p	Transparent conductor, environmentally and electrochemically stable	Limited solubility

Ref.: (Kaur et al., 2015)

## 2.6 Advantages and Application Area of Conducting Polymer of PPy-PANI Blends and/or Composite

Conducting polymers of PPy/APNI have found uses in a range of different applications in areas such as coating and corrosion protection, Dye-Sensitized Solar Cells, Storage, sensors,

electrorheological (ER) fluids and display technologies. This part reviews some application areas and their blends advantages over the homopolymer.

### **2.6.1 Coating and Corrosion protection**

Polyaniline/polypyrrole and polyaniline-polypyrrole phosphotungstate composites were used as corrosion protection agents on the mild steel surface. Composite films give better corrosion protection than bare polyaniline and polypyrrole (Xu et al., 2015). As reported by (Ren and Zeng, 2008) showed that the bilayer PPy/PANI coating was electrodeposited on type 304 stainless steel. The bilayer coatings could reduce the corrosion of the alloy much more effectively than the single PPy coating. Another report (Pan et al., 2016) on the bilayer PPy/PANI on the copper bipolar plate has been indicated that the bilayer effectively decreases the corrosion potential of the copper substrate. Both researchers applied the materials for proton exchange membrane fuel cell (PEMFC) application.

### **2.6.2 Dye-Sensitized Solar Cells**

As reported by (Nawarathna et al., 2018) the Polyaniline and polypyrrole blends were prepared via blending the polyaniline with polypyrrole which was synthesized by chemical oxidative polymerization by using  $\text{FeCl}_3$  as the oxidant. the result showed that the polymer blend with polyaniline: polypyrrole (1:1) mass ratio has been the lower charge transfer resistance and higher solar energy to light energy conversion efficiency than cathode containing pure polymers. And the researchers recommended that the Polymer blends were better alternative than the pure polymer form of polyaniline and polypyrrole as the cathode material in the dye-sensitized solar cells. In the study, (He et al., 2014) synthesized polyaniline–single-wall nanotube (PANI–SWCNT) complexes through the reflux technique used as electrodes (CEs) for Dye-sensitized solar cell (DSSC). The DSSC employing PANI–4% SWCNT complex CE gives an impressive power conversion efficiency of 7.81%.

### 2.6.3 Biomedical /Pharmaceutical Preparations, Microextraction

In the study, (Vickackaite and Ciuvasovaite, 2007) reported electrochemical deposition of polyaniline-polypyrrole blend coating on the surface of stainless steel. A possibility to apply the coating as a new fiber for solid-phase microextraction. The blended coating should be promising for the extraction of parabens that are widely used as preservatives for pharmaceutical preparations, cosmetics, and as food additives.

### 2.6.4 Storage

In the study, (Wang et al., 2014) reported that the synergistic effects from hybrid pseudocapacitive PANI and PPy materials and the shape effects of ordered double-walled nanotube arrays (DNTAs) configurations have an important contribution to high specific capacitance (Csp), excellent long-term cycle stability, and high rate capability of PPy/PANI DNTAs. The composites of PPy and PANI have unique complementary performance compared with individual PANI and PPy. Further, (Attia and Geckeler, 2013) reported the synthesis of polyaniline-polypyrrole composite materials with network morphology was developed based on polyaniline nanofibers covered by a thin layer of polypyrrole via vapor phase polymerization. The composites have exhibited a twofold increase in hydrogen storage capacity at room temperature. The HCl-doped polyaniline nanofibers exhibit a storage capacity of 0.46 wt%, whereas the polyaniline-polypyrrole composites could store 0.91 wt% of hydrogen gas. Another work (Wang, 2016) have been prepared poly(aniline/pyrrole) (PANPY) copolymer in a mixed acid solution by electrosynthesis method. The researchers have been pointed out that the molar ratio between the aniline and pyrrole monomer has a great influence on the electrochemical performance of PANPY copolymer. The result indicated that the highest specific capacity of 227.88 F.g<sup>-1</sup> at a current density of 4 mA.cm<sup>-2</sup> have been obtained at molar concentration ratio of aniline to pyrrole to be 1:1. The poly(aniline/pyrrole) (PANPY) copolymer materials has a potential application for supercapacitor. Besides, (Zhang et al., 2011) reported that the composite of polyaniline and polypyrrole (PPYPANI) was prepared by a two-step electrochemical polymerization method. The results indicated that the polyaniline-polypyrrole composite showed better electrochemical

capacitive performance than polypyrrole (PPY) and polyaniline (PANI). The specific capacitance of the composite electrode was 523 F/g at a current of 6 mA/cm<sup>2</sup> in 0.5 M H<sub>2</sub>SO<sub>4</sub> electrolyte.

### 2.6.5 Sensor

A polyaniline/polypyrrole (PANI/PPy) polymer film was deposited on a tin oxide coated glass electrode, which was used to study the electrochemical behavior of furazolidone by cyclic voltammetry method. Two well-defined reduction peaks (c1 at -0.358V and c2 at -0.784V) and one oxidation peak were observed at 0.306 V. The results, compared with that of a glassy carbon electrode, indicate that reduction peak potential of furazolidone shifts in the negative direction and reduction peak current increases significantly at PANI/PPy modified polymer film electrode. PANI/PPy polymer electrode was given satisfactory results in the determination of furazolidone (Tiwari et al., 2007). In the study, (Mello and Mulato, 2018) reported polyaniline (PANI)/polypyrrole (PPY) blend was synthesized by the galvanostatic electrochemical method in an aqueous acid medium. The result showed that the PANI/PPY blends could be a promising chemically sensitive material for The Extended-Gate Field-Effect-Transistor (EGFET) and/or Reference Field-Effect Transistor (REFET) chemical sensor. (Thao et al., 2019) have been reported the fabrication of free-standing polypyrrole/polyaniline (PPy/PANI) composite films by interfacial polymerization at a vapor/liquid interface using FeCl<sub>3</sub> as an oxidant. The PPy/PANI composite films showed that an excellent Cr (VI) adsorption capacity of 256.41 mg g<sup>-1</sup>, much higher than that of PPy-based absorbents prepared from chemical and electrochemical polymerization routes. And the researchers suggested that this new route for the fabrication of PPy/PANI films with highly enhanced Cr (VI) adsorption capacity for practical applications.

### 2.6.6 Electrorheological (ER) Fluids and Microwave Antenna

Hierarchical polyaniline/polypyrrole (PANI/PPy) copolymer nanofiber was prepared via a two-step method and adopted as dispersing materials for electrorheological (ER) fluids (He et al., 2018). The polypyrrole/polyaniline composite thin films were prepared by a simple

electrodeposition technique on the stainless steel substrate. The materials were important for microwave antenna applications (Velhal et al., 2014). The other work reported that The ER properties of PPy and PPy/ sodium alginate (SA) nanocomposite-based ER fluids were measured using a Haake rotational rheometer under different electric field strengths. The result showed that typical ER behaviors that the shear stress increased apparently with the increasing electric fields. These materials were used as ER smart material for versatile applications (Zhang et al., 2018).

### 2.6.7 Electrochromic Device

Here, (Abaci et al., 2013) reported the construction of electrochromic device (ECDs) have been achieved using bilayer film of PPy and PANI on ITO glass. The bilayer ECDs have better optical and stability properties than monolayer ECDs. And they indicated that the bilayer were promising candidates for electrochromic applications. (Wei et al., 2013) reported that the PANI/GO nanocomposite films have been prepared by electrodeposition of PANI onto the GO coated ITO glass. The nanocomposite films display a multi-color electrochromic at different potentials. A coloration efficiency as high as  $59.3 \text{ cm}^2 \text{ C}^{-1}$  can be obtained. The PANI/GO nanocomposite films were shown to have promising potentials for the electrochromic and energy storage devices applications. Also, (Ninh et al., 2016) synthesized PANI/ITO/Glass thin films by electropolymerized in the presence of 0.5 M concentration of  $\text{H}_2\text{SO}_4$ . The PANI films were formed in polycrystalline micro belts separated from each other by micropores. The electrochromic performance of the PANI-ECD device was carried out in 0.1 M  $\text{LiClO}_4$  + propylene carbonate electrolyte, and a good reversible coloration and bleaching process was obtained. The response time and the coloration efficiency of the coloration of PANI/ITO films were found to be 15 s and  $8.85 \text{ cm}^2 \times \text{C}^{-1}$ , respectively. The results of the ECD performance for 100 cycles showed that electropolymerized PANI thin films possess long durability. Thus, polyaniline thin films can be served as a good candidate for ECD applications, taking advantage of their excellent properties in terms of chemical stability. In the study, (Zhang et al., 2017) have synthesized nanocellulose (NC)/PANI nanocomposites by in situ polymerization. The NC/PANI nanocomposite films showed significant color changes (yellow, green, and blue) at different electrical potentials. As compared with pure PANI film, the NC/PANI nanocomposite films exhibited higher optical

contrast values, higher coloration efficiencies, lower response times, and better electrochromic stabilities. The film with a composition of PN40 demonstrated the highest transmittance difference ( $\Delta T$  62.9%) and the fastest response speed for coloring and bleaching (1.0 and 1.5 s) and was preferred as an electrochromic material.

## **2.7 Electrical and Optical Properties of Conducting Polymer Blends**

This section considers the electrical and optical properties of polymer blend materials. In 1985 many types of research have been dedicated to studying the polymer blends, to get unique property and to develop new polymers. Consequently, understanding the property of newly developed polymer composite or blends materials is significant to design electronic devices. One of the common characteristics of polymer blend materials is optical and electrical properties. Therefore, in this part reviews describe a variety of models or theoretical approaches to study electrical and optical property.

### **2.7.1 Polymer Blends: Electrical Property Curve and Charge Transport Models**

One of the common characteristics of polymer blend materials is electrical property. Electrical properties constitute one of the most convenient and sensitive methods for studying the polymer structures (Kimura and Kajiwara, 1998),(Deshmukh et al., 2007). Electrical property in disorder materials particularly amorphous semiconductors covering a wide range of composition with interesting electrical properties. Organic semiconductors are also categorized ordered crystals and disordered amorphous materials. Charge transport is a fundamental phenomenon that governs the functionality of the organic devices, which of course much depends on the structure of semiconductors, e.g., ordered or disordered. To design a device with improved performances of a device, the researcher needs to understand the fundamental process-structure-property relationship of materials. In general, there is three mechanisms of charge transport such as diffusion, drift (also called migration), and convection (Wang et al., 2009). Several models have been developed to describe each type of charge transport mechanism. Organic semiconductors, however, are usually disordered, and therefore the electrical transport has to be described differently from that of the conventional inorganic semiconductors. To gain deeper insight into the carrier transport processes, the researchers examine the current density vs voltage (J–V) characteristics of organic electronic

devices (Tsai et al., 2018). In the design of organic semiconductor materials and devices, understanding this J-V behavior is significantly important. Besides, the J-V curve is important to understand the charge transport mechanism including mobility and conductivity. Electric transport in the disordered semiconductors is explained in terms of different transport regimes, such as space charge limited current (SCLC) or trap charge limited current (TCLC) regimes.

### 2.7.1.1 Nonlinear J-V Characteristics in Organic Semiconductors

The log  $J$ -I of  $V$  characteristics of ITO/PEDOT: PSS/PFO/Au have been studied at different temperatures in the range of 100-290 K. These curves in figure 2.3 can be divided into three distinct regions (I), (II), and (III). Region (I) is ohmic, where the current density is proportional to the voltage, region (II) is the SCLC limited by discrete traps where the current density is directly proportional to the square of the voltage and region (III) is the trapped charge limited conduction where current increases exponentially and the onset of the trap-filled voltage  $V_{TFL}$  gives the density of traps  $N_t$ . Ideally, there must be another region (IV) which is the trap-filled SCLC which is free from the influence of traps. But this region was not observed due to the failure of the device at higher voltages (Bajpai et al., 2010). The values of fitting parameters for both devices fitted with traps distributed SCLC models are tabulated in the literature (Yossifon et al., 2009)

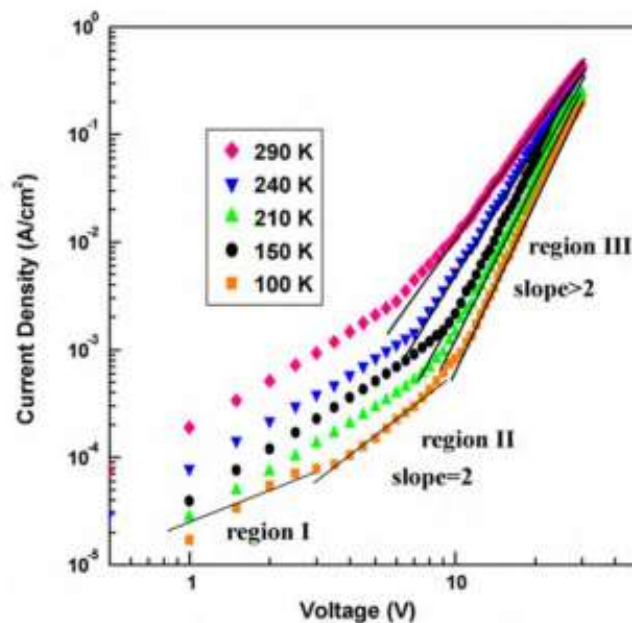


Figure 2.3: J-V characteristics of device A at different temperatures in the range 290-100 K.

## 2.7.2 Blends of Optical Property

Polymer blending is one of the most substantial methods for the designing of new polymeric materials and thus it is a valuable method for developing materials with a variety of properties. The final product from the blending process can be modified according to the requirements of each application, which cannot be proficient alone by one polymer (Kumar et al., 2014). Understanding the optical property of materials plays a critical role in the design of materials. Thus, the researcher needs to understand these properties for prepared polymer blend materials. Therefore, this section, describes absorption, absorption edge, and band gap in optical materials.

### 2.7.2.1 Absorption and Absorption Edge Study

Optical absorption is widely used to characterize the electronic properties of materials, which reveals the evidence concerning electronic transitions such as band gap, valence band tails, and excited-state lifetime (Sánchez-Vergara et al., 2012). The amount of light absorbed by a material is measured by the absorption coefficient ( $\alpha$ ), which is defined by the fraction of incident radiation absorbed per thickness of the absorber. Absorption and scattering occur at the molecular and atomic levels. The absorption coefficient is calculated using the following equations 2.4 and 2.5.

$$\alpha(\lambda) = (2.303) \left[ \frac{A}{d} \right], \quad \text{Eq. 2.4}$$

$$A = \log\left(\frac{1}{T}\right), \quad \text{Eq. 2.5}$$

where  $d$  is the thickness of the sample and  $A$  is the absorption data (Aziz, 2017). Also, it is calculated from the transmittance data using a relation equation 2.6:

$$\alpha(\lambda) = (2.303) \left[ \frac{\log\left(\frac{1}{T}\right)}{d} \right], \quad \text{Eq. 2.6}$$

where  $T$  is the transmittance, and  $d$  is the thickness of the sample. The absorption coefficient is determined from the UV-VIS spectra.



### 2.7.2.2 Optical Band Gap

The band gap energy denotes the energy separation between the highest occupied molecular orbital (HOMO) and the lowest unoccupied molecular orbital (LUMO), the analogs to the valence and conduction bands of the inorganic semiconductors (ISCs), respectively. The molecular alignment and packing influence the HOMO and LUMO energy levels. The control of HOMO to LUMO energy gap of  $\pi$ -conjugated systems (i.e., that of the band gap of the corresponding materials) is a critical task for the semiconductor and nanomaterial industries (Smith and Nie, 2010). The magnitude of the band gap and the positions of the HOMO and LUMO energy levels are vital parameters for determining the electrical and optical characteristics of the given conjugated polymer (Kanwal et al., 2015). The band gap energy in an undoped organic semiconductor is typically between 2 and 4 eV and the Fermi energy level in an intrinsic semiconductor is positioned in the middle of the band gap. Other paper illustrates that the band-gap of semiconductors is usually in the range of 1–5 eV (Jiang et al., 2017). Semiconducting materials have a similar structure as compared to insulators at very low temperatures. The HOMO energy level (in the molecular picture), i.e. the top of the filled valence band (in the solid-state picture), is distinctly separated from the LUMO energy level, i.e. the low-energy states of the conduction band, by a band gap with no allowed energy state. Electrons can be thermally excited to the LUMO energy level when the temperature increases, even though this thermal effect is considered negligible in most organic semiconductors due to their relatively high band gaps compared to inorganic semiconductors. Some models have been developed to provide an approximation of the optical band gap. The Tauc, Forouhi-Bloomer, and Cody models, are most applicable for the aforementioned purpose. Herein, we will describe how to calculate the optical band gap using the Tauc model (Rodríguez-Gómez et al., 2014).

### 2.7.2.3 Calculation of Optical Gap and Urbach energy

The determination of optical bandgap has been carried out by the extrapolation in Tauc's plot. The estimation of materials energy gap is essential in the field of semiconductors, nanomaterials, and solar industries. The optical absorption spectrum is usually utilized to determine the band gap

and type of electronic transitions, governing the optoelectronics behavior of materials. The optical energy gap of the composite films is calculated by using Tauc's equation 2.7 (Shaw, 2016).

$$\alpha = \frac{\beta(h\nu - E_g)^n}{h\nu}, \quad \text{Eq. 2.7}$$

where ( $\alpha$ ) is the absorption coefficient,  $h\nu$  is the photon energy, ( $E_g$ ) is the optical energy gap,  $\beta$  a constant known as the disorder parameter, which is nearly independent on the photon energy and ( $n$ ) is a parameter indicating the type of electronics transition that is related to the distribution of the density of states. The value of ( $n$ ) is equal to 1/2 and 3/2 for allowed and forbidden direct transitions, respectively, while it takes 2 and 3 in the case of allowed and forbidden indirect transitions, respectively (Abdulwahid et al., 2016). The value of  $m$  is 1/2, 3/2, 2, and 1/3 for direct allowed transition, direct forbidden transition, indirect allowed transition, and indirect forbidden transition, respectively. By plotting a graph of  $(\alpha h\nu)^2$  versus  $h\nu$  and then extrapolating the curve to the  $(\alpha h\nu)^2 = 0$  axis, we can obtain the  $E_g$  value (Shaw, 2016). The Urbach energy gives information about the structural order of a material and can be calculated as Eq. 2.8.

$$\alpha(h\nu) = \alpha_o e^{\left(\frac{h\nu}{E_u}\right)}, \quad \text{Eq. 2.8}$$

where  $\alpha_o$  is a constant,  $h\nu$  the energy of the incoming photon and  $E_u$  the Urbach energy. Such values are generally interpreted as a quality indicator in inorganic amorphous semiconductors (Ikhmayies and Ahmad-Bitar, 2013).

## References:

ABDULWAHID, R. T., ABDULLAH, O. G., AZIZ, S. B., HUSSEIN, S. A., MUHAMMAD, F. F. & YAHYA, M. Y. 2016. The study of structural and optical properties of PVA: PbO<sub>2</sub> based solid polymer nanocomposites. *Journal of Materials Science: Materials in Electronics*, 27, 12112-12118.

- AKUNDY, G. S., RAJAGOPALAN, R. & IROH, J. O. 2002. Electrochemical deposition of polyaniline–polypyrrole composite coatings on aluminum. 83, 1970-1977.
- AZIZ, S. B. 2017. Morphological and Optical Characteristics of Chitosan((1-x)):Cu(o)(x) ( $4 \leq x \leq 12$ ) Based Polymer Nano-Composites: Optical Dielectric Loss as an Alternative Method for Tauc's Model. *Nanomaterials* (Basel, Switzerland), 7, 444.
- BAJPAI, M., SRIVASTAVA, R., KAMALASANAN, M. N., TIWARI, R. S. & CHAND, S. 2010. Charge transport and microstructure in PFO:MEH-PPV polymer blend thin films. *Synthetic Metals*, 160, 1740-1744.
- BELLAN, C., LEE, J. & RHEE, S. W. 2004. Organic Thin Film Transistors: Materials, Processes and Devices. *Korean Journal of Chemical Engineering*, 21, 267-285.
- BOURARA, H., HADJOUT, S., BENABDELGHANI, Z. & ETXEBERRIA, A. 2014. Miscibility and Hydrogen Bonding in Blends of Poly(4-vinylphenol)/Poly(vinyl methyl ketone). 6, 2752-2763.
- BUDKOWSKI, A. 1999. Interfacial Phenomena in Thin Polymer Films: Phase Coexistence and Segregation. *Interfaces Crystallization Viscoelasticity*. Berlin, Heidelberg: Springer Berlin Heidelberg.
- C M, N., CHIKKER, R., BARAKOV, B. & CAN, O. 2016. Organic Light Emitting Diodes (OLED).
- CHAUDHARY, V. & KAUR, A. 2014. Enhanced and selective ammonia sensing behaviour of poly(aniline co-pyrrole) nanospheres chemically oxidative polymerized at low temperature. *Journal of Industrial and Engineering Chemistry*, 26, 143-148.
- CHOUDHURY, A. 2009. Polyaniline/silver nanocomposites: Dielectric properties and ethanol vapour sensitivity. *Sensors and Actuators B: Chemical*, 138, 318-325.
- CODOU, A., ANSTEY, A., MISRA, M. & MOHANTY, A. K. 2018. Novel compatibilized nylon-based ternary blends with polypropylene and poly(lactic acid): morphology evolution and rheological behaviour. *RSC Advances*, 8, 15709-15724.
- DELOGNE, P. 1998. Lee De Forest, The Inventor Of Electronics: A Tribute To Be Paid. *Proceedings of the IEEE*, 86, 1878-1880.
- DESHMUKH, S. H., BURGHATE, D. K., AKHARE, V. P., DEOGAONKAR, V. S., DESHMUKH, P. T. & DESHMUKH, M. S. 2007. Electrical conductivity of polyaniline doped PVC-PMMA polymer blends. *Bulletin of Materials Science*, 30, 51-56.

- DHACHANAMOORTHY, N., CHANDRA, L., SURESH, P. & PERUMAL, K. 2017. Facile Preparation and Characterization of Polyaniline-iron Oxide Ternary Polymer Nanocomposites by Using " Mechanical Mixing " Approach.
- DIXIT, M., MATHUR, D. V., GUPTA, S., BABOO, M., SHARMA, K. & SAXENA, N. 2009. Investigation of miscibility and mechanical properties of PMMA/PVC blends. *Optoelectronics and Advanced Materials, Rapid Communications*, 3, 1099-1105.
- DIXIT, M., MATHUR, D. V., GUPTA, S., BABOO, M., SHARMA, K. & SAXENA, N. 2009. Investigation of miscibility and mechanical properties of PMMA/PVC blends. *Optoelectronics and Advanced Materials, Rapid Communications*, 3, 1099-1105.
- DYLLA, H. F. & CORNELIUSSEN, S. T. 2005. John Ambrose Fleming and the beginning of electronics. *Journal of Vacuum Science Technology*, 23, 1244-1251.
- ECONOMOU, A., KOKKINOS, C. & PRODRONIDIS, M. 2018. Flexible plastic, paper and textile lab-on-a chip platforms for electrochemical biosensing. *Lab on a Chip*, 18, 1812-1830.
- FINDIK, F., YILMAZ, R. & KÖKSAL, T. 2004. Investigation of mechanical and physical properties of several industrial rubbers. *Materials & Design*, 25, 269-276.
- GHAFFARI-MOGHADDAM, M. & ESLAHI, H. 2014. Synthesis, characterization and antibacterial properties of a novel nanocomposite based on polyaniline/polyvinyl alcohol/Ag. *Arabian Journal of Chemistry*, 7, 846-855.
- HAMMAD, A., NOBY, H., ELKADY, M. & EL-SHAZLY, A. 2018. In-situ Polymerization of Polyaniline/Polypyrrole Copolymer using Different Techniques. *IOP Conference Series: Materials Science and Engineering*, 290, 012001.
- HASE, T., KANO, T., NAKAZAWA, E. & YAMAMOTO, H. 1990. Phosphor Materials for Cathode-Ray Tubes. In: HAWKES, P. W. (ed.) *Advances in Electronics and Electron Physics*. Academic Press.
- HERIOT, S. & JONES, R. 2005. An Interfacial Instability in a Transient Wetting Layer Leads to Lateral Phase Separation in Thin Spin-Cast Polymer-Blend Films. *Nature materials*, 4, 782-6.
- HIGGINS, J. S., LIPSON, J. E. G. & WHITE, R. P. 2010. A simple approach to polymer mixture miscibility. *368*, 1009-1025.

- HULICOVA, D. & OYA, A. 2003. The polymer blend technique as a method for designing fine carbon materials. *Carbon*, 41, 1443-1450.
- IKHMAYIES, S. J. & AHMAD-BITAR, R. N. 2013. A study of the optical bandgap energy and Urbach tail of spray-deposited CdS:In thin films. *Journal of Materials Research and Technology*, 2, 221-227.
- JIANG, C., MONIZ, S. J. A., WANG, A., ZHANG, T. & TANG, J. 2017. Photoelectrochemical devices for solar water splitting – materials and challenges. *Chemical Society Reviews*, 46, 4645-4660.
- KAJULURI, V. K. 2016. *Microelectronics Processing - Transistor Fabrication*.
- KANWAL, F., BATOOL, A., ADNAN, M. & NASEEM, S. 2015. The effect of molecular structure, band gap energy and morphology on the dc electrical conductivity of polyaniline/aluminium oxide composites. *Materials Research Innovations*, 19, S8-354-S8-358.
- KAUR, G., ADHIKARI, R., CASS, P., BOWN, M. & GUNATILLAKE, P. 2015. Electrically conductive polymers and composites for biomedical applications. *RSC Advances*, 5, 37553-37567.
- KENRY, YEO, J. C. & LIM, C. T. 2016. Emerging Flexible and Wearable Physical Sensing Platforms for Healthcare and Biomedical Applications. *Microsystems & Nanoengineering*, 2, 16043.
- KIMURA, T. & KAJIWARA, M. 1998. Electrical properties of poly(n-butylamino) (di-allylamino) phosphazene. *Journal of Materials Science*, 33, 2955-2959.
- KONG, Y., MA, Y., LEI, L., WANG, X. & WANG, H. 2017. Crystallization of Poly( $\epsilon$ -caprolactone) in Poly(vinylidene fluoride)/Poly( $\epsilon$ -caprolactone) Blend. 9, 42.
- KUMAR, A., ALI, V., KUMAR, S. & HUSAIN, M. 2011. Studies on Conductivity and Optical Properties of Poly(o-toluidine)ferrous Sulfate Composites. *International Journal of Polymer Analysis and Characterization - INT J POLYM ANAL CHARACT*, 16, 298-306.
- KUMAR, K. K., RAVI, M., PAVANI, Y., BHAVANI, S., SHARMA, A. K. & NARASIMHA RAO, V. V. R. 2014. Investigations on PEO/PVP/NaBr complexed polymer blend electrolytes for electrochemical cell applications. *Journal of Membrane Science*, 454, 200-211.

- KUO, S.-W., SHIH, C.-C., SHIEH, J.-S. & CHANG, F.-C. 2004. Specific interactions in miscible polymer blends of poly(2-hydroxypropyl methacrylate) with polyvinylpyrrolidone. 53, 218-224.
- LIU, J. J. & SCHWIERZ, F. 2003. RF MOSFET: recent advances, current status and future trends. *Solid-State Electronics*, 47, 1881-1895.
- LIU, J. J., ORTIZ-CONDE, A. & GARCIA-SANCHEZ, F. 1998. MOSFET physics and modeling. *Analysis and Design of Mosfets: Modeling, Simulation and Parameter Extraction*. Boston, MA: Springer US.
- LIST, E. J. W. & KOCH, N. 2011. Focus Issue: Organic light-emitting diodes—status quo and current developments. *Optics Express*, 19, A1237-A1240.
- LOGUERCIO, L. F., ALVES, C. C., THESING, A. & FERREIRA, J. 2015. Enhanced electrochromic properties of a polypyrrole–indigo carmine–gold nanoparticles nanocomposite. *Physical Chemistry Chemical Physics*, 17, 1234-1240.
- MANAHIL, E. M., ZAINAL, A.T., HASSAN, H. W., ABDU, A. A., JOSEPHINE, L. Y., IBRAHIM, B. M., NODAR, O. KH., 2014. Preparation and Characterization of Polypyrrole Conjugated Polymer in the Presence of Ionic Surfactant. *Journal of Optoelectronics and Biomedical Materials*, Vol. 6 ( 4), pp. 111 - 117.
- MOLITON, A. & HIRNS, R. C. 2012. The origin and development of (plastic) organic electronics. 61, 337-341.
- MULLER, D., GARCIA, M., SALMORIA, G., PIRES, A., PANIAGO, R. & BARRA, G. 2011. SEBS/PPy.DBSA Blends: Preparation and Evaluation of Electromechanical and Dynamic Mechanical Properties. *Journal of Applied Polymer Science*, 120, 351-359.
- NASCIMENTO, T. A., AVELAR DUTRA, F. V., PIRES, B. C., TEIXEIRA TARLEY, C. R., MANO, V. & BORGES, K. B. 2016. Preparation and characterization of a composite based on polyaniline, polypyrrole and cigarette filters: adsorption studies and kinetics of phenylbutazone in aqueous media. *RSC Advances*, 6, 64450-64459.
- OU, X. & XU, X. 2016. A simple method to fabricate poly(aniline-co-pyrrole) with highly improved electrical conductivity via pre-polymerization. *RSC Advances*, 6, 13780-13785.
- PAINTER, PAUL C., COLEMAN, MICHAEL M. (2009). *Essentials of Polymer Science and Engineering* , : Lancaster, PA : DEStech Publications, Inc..

- PARAMESWARANPILLAI, J., THOMAS, S. & GROHENS, Y. 2014. Polymer Blends: State of the Art, New Challenges, and Opportunities.
- Polymer Blends: State of the Art, New Challenges, and Opportunities. Characterization of Polymer Blends.
- RODRÍGUEZ-GÓMEZ, A., SÁNCHEZ-HERNÁNDEZ, C., FLEITMAN-LEVIN, I., ARENAS-ALATORRE, J., CARLOS, J., HUITRÓN, A. & VERGARA, M. 2014. Optical Absorption and Visible Photoluminescence from Thin Films of Silicon Phthalocyanine Derivatives. *Materials*, 7, 6585-6603.
- SÁNCHEZ-VERGARA, M. E., ALONSO-HUITRON, J. C., RODRIGUEZ-GÓMEZ, A. & REIDER-BURSTIN, J. N. 2012. Determination of the optical GAP in thin films of amorphous dilithium phthalocyanine using the Tauc and Cody models. *Molecules (Basel, Switzerland)*, 17, 10000-10013.
- SHAW, T. C., 2016. Preparation of Derivatized Polyaniline for Biosensing Applications. Electronic theses & dissertations collection for the Atlanta University & Clark Atlanta University, Issue 54.
- SI, P., LUO, F. & LUO, F. 2016. Miscibility, Morphology and Crystallization Behavior of Poly(Butylene Succinate-co-Butylene Adipate)/Poly(Vinyl Phenol)/Poly(L-Lactic Acid) Blends. *Polymers*, 8, 421.
- SLOTA, J. E., ELMALEM, E., TU, G., WATTS, B., FANG, J., OBERHUMER, P. M., FRIEND, R. H. & HUCK, W. T. S. 2012. Oligomeric Compatibilizers for Control of phase Separation in Conjugated Polymer Blend Films. *Macromolecules*, 45, 1468-1475.
- SMITH, A. M. & NIE, S. 2010. Semiconductor nanocrystals: structure, properties, and band gap engineering. *Accounts of chemical research*, 43, 190-200.
- SPANGGAARD, H. & KREBS, F. 2004. Krebs, F.C.: A brief history of the development of organic and polymeric photovoltaics. *Sol. Energy Mater. Sol. Cells* 83, 125-146. *Solar Energy Materials and Solar Cells*, 83, 125-146.
- SPEIGHT, J. 1996. A review of: "Physical Properties of Polymers Handbook" Mark, J.E. (Editor) American Institute of Physics Press, Woodbury, New York, 1996 ISBN No: 1-56396-295-0 \$120.00. *Fuel Science and Technology International*, 14, 1461-1461.

- SU, N. 2015. Improving Electrical Conductivity, Thermal Stability, and Solubility of Polyaniline-Polypyrrole Nanocomposite by Doping with Anionic Spherical Polyelectrolyte Brushes. *Nanoscale Research Letters*, 10, 301.
- TIKISH, T. A., KUMAR, A. & KIM, J. Y. 2018. Study on the Miscibility of Polypyrrole and Polyaniline Polymer Blends %J *Advances in Materials Science and Engineering*. 2018, 5.
- TSAI, H., ASADPOUR, R., BLANCON, J.-C., STOUMPOS, C. C., EVEN, J., AJAYAN, P. M., KANATZIDIS, M. G., ALAM, M. A., MOHITE, A. D. & NIE, W. 2018. Design principles for electronic charge transport in solution-processed vertically stacked 2D perovskite quantum wells. *Nature Communications*, 9, 2130.
- UTRACKI, L. A., MUKHOPADHYAY, P. & GUPTA, R. K. 2014. Polymer Blends: Introduction. In: UTRACKI, L. A. & WILKIE, C. A. (eds.) *Polymer Blends Handbook*. Dordrecht: Springer Netherlands.
- VELURU, J. B., VEMPATI, S. & RAMAKRISHNA, S. 2013. Conducting Polyaniline-Electrical Charge Transportation. *Materials Sciences and Applications*, 04, 1-10.
- WANG, J., LI, X., DU, X., WANG, J., MA, H. & JING, X. J. C. P. 2017. Polypyrrole composites with carbon materials for supercapacitors. 71, 293-316.
- WANG, X., SHAPIRO, B. & SMELA, E. 2009. Development of a Model for Charge Transport in Conjugated Polymers. *The Journal of Physical Chemistry C*, 113, 382-401.
- WANG, X.-Q., XIN, B.-J. & XU, J. 2013. Preparation of Conductive PANI/PVA Composites via an Emulsion Route %J *International Journal of Polymer Science*. 2013, 6.
- WEIMER, P. K. 1962. The TFT A New Thin-Film Transistor. *Proceedings of the IRE*, 50, 1462-1469.
- XAVIER, P., RAO, P. & BOSE, S. 2016. Nanoparticle induced miscibility in LCST polymer blends: critically assessing the enthalpic and entropic effects. *Physical Chemistry Chemical Physics*, 18, 47-64.
- XING, P., AI, X., DONG, L. & FENG, Z. 1998. Miscibility and Crystallization of Poly( $\beta$ -hydroxybutyrate)/Poly(vinyl acetate-co-vinyl alcohol) Blends. *Macromolecules*, 31, 6898-6907.
- XING, S., ZHAO, C., ZHOU, T., JING, S. & WANG, Z. 2007. Preparation and characterization of polyaniline-polypyrrole composite from polyaniline dispersions. 104, 3523-3529.
- YOON, D. G., KANG, M., KIM, J. B. & KANG, K.-T. 2018. Nozzle Printed-PEDOT:PSS for Organic Light Emitting Diodes with Various Dilution Rates of Ethanol. 8, 203.



- YOSSIFON, G., MUSHENHEIM, P. & CHANG, Y.-C. 2009. Nonlinear current-voltage characteristics of nanochannels. *Physical review. E, Statistical, nonlinear, and soft matter physics*, 79, 046305.
- YOUSEFI, A. & EISAZADEH, H. 2012. Preparation and Characterization of Polypyrrole Nanocomposites using Various Surfactants in Aqueous and Aqueous/Non-Aqueous Media. *Research Journal of Applied Sciences, Engineering and Technology*, 4.
- YUAN, J. S. & LIOU, J. J. 1998. *Bipolar Junction Transistors. Semiconductor Device Physics and Simulation*. Boston, MA: Springer US.
- YUHANG, L., ZHAO, J., LI, Z., MA, W., HUAWEI, H., JIANG, K., LIN, H., ADE, H. & YAN, H. 2014. Aggregation and morphology control enables multiple cases of high-efficiency polymer solar cells. *Nat Commun* 5:5293. *Nature communications*, 5, 5293.
- ZAKI, T. 2015. *Organic Thin-Film Transistors. Short-Channel Organic Thin-Film Transistors: Fabrication, Characterization, Modeling and Circuit Demonstration*. Cham: Springer International Publishing.
- ZHANG, Q., ZHANG, B.-Y., GUO, Z.-X. & YU, J. 2017. Tunable Electrical Conductivity of Carbon-Black-Filled Ternary Polymer Blends by Constructing a Hierarchical Structure. 9, 404.
- ZHANG, T., ZHANG, W., WANG, B. & LIU, J. 2018. One-step synthesis of core/shell-like structured polypyrrole/sodium alginate nanocomposites and their electro-responsive performances. 29, 232-241.

## Chapter Three

### Materials. Synthesis Method and Characterization Technique

#### Experimental Details

This chapter deals with (1) the materials and methods for the synthesis of polyaniline (PANI) and Polypyrrole (PPy) and PANI/PPy blends, (2) schematic diagrams of sample preparation process, and (3) techniques used for the characterization of polymerization and blend materials such as UV-vis spectroscopy, Fourier transforms infrared spectroscopy (FT-IR), Scanning Electron Microscope (SEM), X-Ray diffraction (XRD), I-V Characteristics (IV), Photoluminescence (PL).

#### 3.1 Materials

Aniline (98%) and pyrrole (>98%,) monomers were purchased from Zenith India and Aldrich respectively. Hydrochloric acid (HCl, Zenith India) and ammonium persulfate (APS, Merck, 98%) were used as an oxidant to initiate polymerization of PANI. Ferric chloride ( $\text{FeCl}_3$ , Merck, 99.0%) was used to initiate polymerization of PPy. Double distilled water was used as a solvent in polymerization for the synthesis of PANI and PPy. Sodium dodecyl sulfate (SDS, Merck, 99.5%) was used as a doping agent as a surfactant. Methanol (Merck, 99.9%) was used to terminate the polymerization process, and acetone (Merck, 99.8%) was used to wash the obtained samples. Dimethyl sulfoxide (DMSO, Merck, 99.9%) was used as a solvent for the polymer blends, PANI/PPy.

#### 3.2 Synthesis Method

##### 3.2.1 Synthesis of Polypyrrole (PPy)

Polypyrrole was synthesized by chemical oxidative polymerization of pyrrole. First, 1 M of pyrrole solution was prepared by 0.698 ml of pyrrole was added into 10 ml of double-distilled water. Then 1.622 g of  $\text{FeCl}_3$  was dissolved in 50 ml of double-distilled water. After that, the  $\text{FeCl}_3$  solution was added slowly with a dropwise manner to pyrrole solution under constant stirring for 30 minutes at 5 °C. Then allow the polymerization for 6h under stirring. Then the reactor flask was

kept unagitated for 24 h for PPy powder to settle down. The resulting precipitate was collected by filtration. Then the product was washed by double distilled water many times and dried by the oven for 12 h at 50 °C.

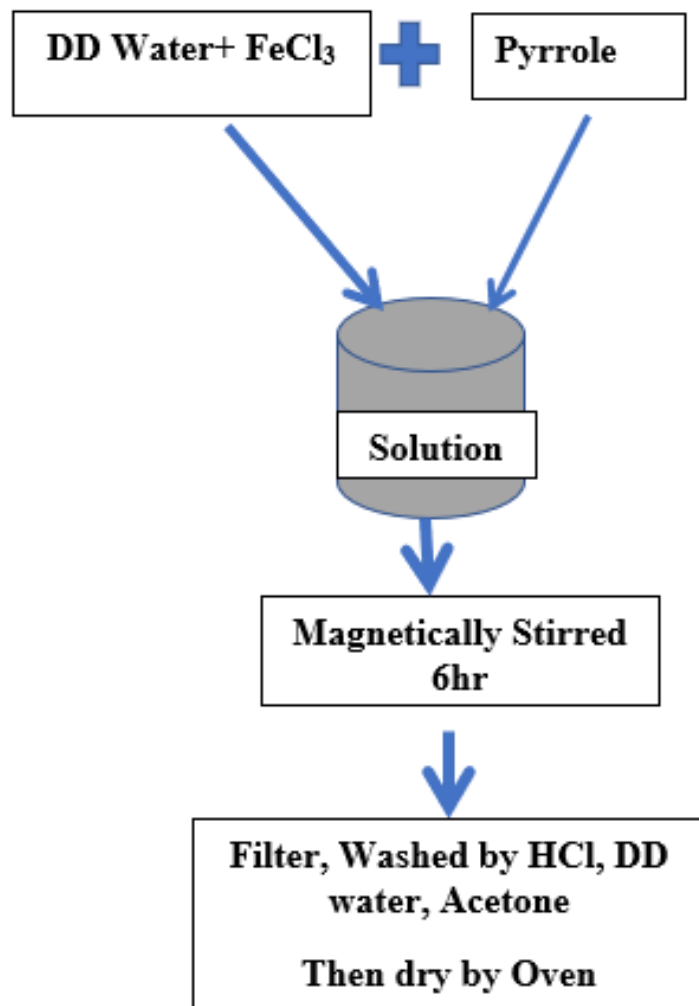


Figure 3.1: Schematic diagram of synthesis route of Polypyrrole (PPy)

### 3.2.2 Synthesis of Polypyrrole (PPy) with sodium dodecyl sulfate (SDS)

Polypyrrole was synthesized by chemical oxidative polymerization of pyrrole with the help of surfactant SDS. First, 1 M of pyrrole solution was prepared by 0.698 ml of pyrrole was added into 10 ml of double-distilled water. Then 1.622 g of FeCl<sub>3</sub> and 0.5 mg of SDS was dissolved in 50 ml of double-distilled water. After that, the FeCl<sub>3</sub> solution was added slowly with a dropwise

manner to pyrrole solution under constant stirring for 30 minutes at 5 °C. Then allow the polymerization for 6h under stirring. Then the reactor flask was kept unagitated for 24 h for PPy powder to settle down. The resulting precipitate was collected by filtration. Then the product was washed by double distilled water many times and dried by the oven for 12 h at 50 °C. Repeated the above procedure for 2.5 mg and 5 mg of SDS for PPy synthesis.

### **3.2.3 Synthesis of Polyaniline (PANI)**

Polyaniline (PANI) was synthesized by chemical oxidative polymerization of aniline. First, 1 M of aniline solution was prepared by 0.911 ml of aniline was dissolved in 1 M of hydrochloride solution. Then 0.15 M ammonium persulfate (APS) was prepared by 1.7114 g of APS dissolved in 50 ml of double-distilled water. After that, the APS solution was added in a dropwise manner to hydrochloride solution (1 M) to initiate the polymerization of the aniline. The mixture was stirred with a magnetic stirrer for 9h under 5 °C temperature. Then, methanol was added to stop polymerization and leave unagitated until precipitated. The resulting precipitate was collected by filtration. After that, the product was washed by 0.2 M of hydrochloride, double distilled water, and acetone, sequentially. Washing with hydrochloride removes any residuals and monomers, oxidants, and decomposed products. This process also gives uniform protonation to PANI. Then additional washing by acetone removes low molecular weight organic intermediates and oligomers. The product was obtained as the fine powder, which was dried under vacuum at 50 °C for 24 h.

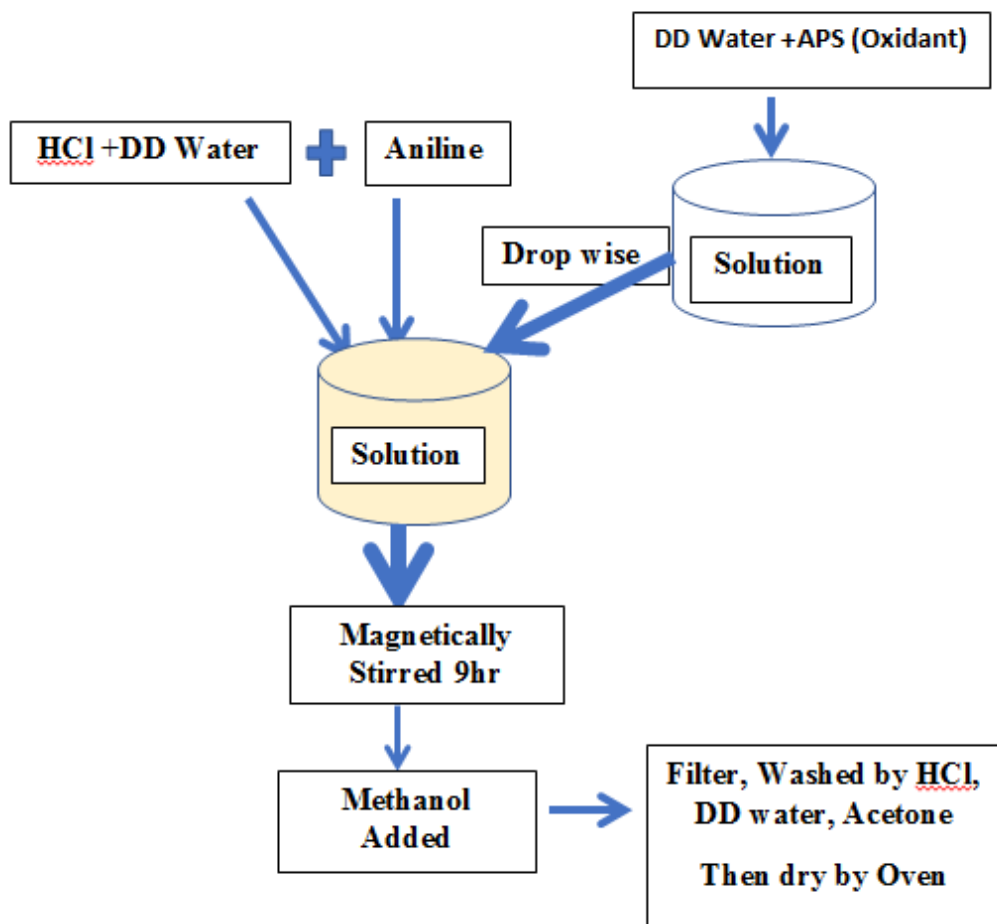


Figure 3.2: Schematic diagram of synthesis route of Polyaniline (PANI)

### 3.2.3 Synthesis of PANI/PPy blends

The polymer blend samples were prepared by solution processing method. The polymer PPy blended with PANI in various compositions of PPy-PANI 50:50, PPy-PANI 70:30, PPy-PANI 80:20, and PPy-PANI 90:10 in wt. % were prepared by using a solvent, DMSO. First, each solution of PPy and PANI was prepared individually in 10ml of solvent and then ultrasonicated for 10 min. Then after mixing the two solutions, and it was ultrasonicated again for an additional 1hr. Then, lastly, the solvent was evaporated on oven 50 °C for 12 h.

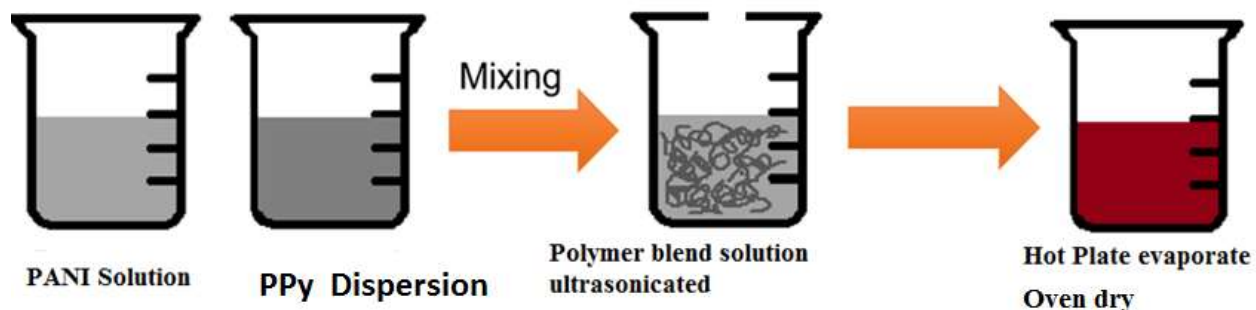


Figure 3.3: Schematic diagram Synthesis of Ppy/PANI blends

### 3.3 Characterization Technique

#### 3.3.1 UV-vis Spectroscopy

UV-vis spectroscopy is a measurement of the absorption of light when it passes through a sample solution or substrate. On the other hand, it can be a measurement of reflectance, where the beam of light is reflected at the sample's surface. It is usually used to study the absorption, transmission, and reflectivity of various materials, which provides information about the optical and electronic properties of materials. The spectral region of the UV-Vis is in the range of UV to near-infrared through the visible frequencies. A spectrophotometer in the below figure was used to extract the UV-vis spectrum of the polyaniline, polypyrrole, and blends.



Figure 3.4: UV/Vis spectrophotometer.

### 3.3.2 Fourier-Transform Infrared (FT-IR) Spectroscopy

FT-IR spectroscopy is a technique used to deliver specific evidence about vibrational and rotation chemical bond and molecular structure, making it useful for the identification of organic molecules, functional groups, and molecular structure of organic compounds. The infrared spectrum characterizes the fingerprint of a sample with the absorption of peaks corresponding to the frequencies between the bond of atoms consisting of materials. Each material is a combination of different atoms. Therefore, no two compounds can produce the same infrared spectra. It can also be used as a quantitative technique to identify unknown materials and the number of components in a mixture. The spectrum results in certain absorption peaks, which are frequencies from vibrations of the bonds of the atoms. The size of the peaks provides us the amount of each material present. FT-IR spectrometer in figure 3.5 was used in both transmission and reflection modes to understand the polyaniline, polypyrrole, and their blends in a different compositions.



Figure 3.5: FT-IR spectrometer

### 3.3.3 Scanning Electron Microscope (SEM)

Field-Emission SEM (JEOL) is an instrument used to study the microscopic structure of the samples. It is one of the most widely used electron microscopes. The microstructural image of a sample can be obtained by scanning the surface of the sample using a focused electron beam. The powder sample can be used for characterization.





Figure 3.6: JEOL Field Emission Scanning Electron Microscopy instrument

### 3.3.4 X-Ray Diffraction (XRD)

XRD is a method performed to determine the material's crystal structure for PANI, PPy, and PANI/PPy blends. The phase behavior of each blended sample was studied using this XRD as a function of composition, indicating the information of the miscibility of each blend. The instrument used was an x-ray diffractometer with electromagnetic radiation with a wavelength of  $\lambda = 0.154 \text{ nm}$ . XRD works by measuring the diffraction intensity by varying the incident angle of the beam as shown in figure 3.7.



Figure 3.7: XRD instrument- Analytical X'Pert

### 3.3.5 Current-Voltage (I-V) Characteristics

The I-V curves were measured using the compressed pellets of PANI, PPy, and PANI/PPy blend powders. The pellet was 0.2/0.1 micrometer thick with a diameter of 10 mm. The electrical properties of PANI were extracted by studying the linear potential method using the Voltmaster software. As such, the current density vs. voltage (J-V) plot was obtained. In this study, the two-terminal setup for the J-V curve was used using a two-point electrode with a lateral connection and an across the connection.

### 3.3.6 Photoluminescence (PL)

Photoluminescence (PL) is an interesting tool in this study, where the basic excitation of organic blend materials was characterized. The PL behavior, usually, describes the photoexcitation or light generation of the polymer blends.

### **3.3.7 Thin Film Preparation**

The PPy, PANI and its blend film were fabricated on Indium Tin Oxide (ITO) substrate by using the drop-casting method. Before drop-casting, the ITO substrates were consecutively cleaned in DI water and detergent, acetone followed by sonification (Branson 2500) for 15min, then sonicate the ITO glass with Isopropanol alcohol (IPA) for 15 Min and dry by air.

### **3.3.8 Electrochemical Measurement**

The three electrodes Electrochemical was used for the electrochemical measurements. Then drop -the casted film was characterized by different scan rate in 0.5 M H<sub>2</sub> SO<sub>4</sub>.

## Chapter Four

### Study on the Miscibility of Polypyrrole and Polyaniline Polymer Blends

#### Abstract

This report on the miscibility and phase behavior of polypyrrole-polyaniline (PPy-PANI) as a function of the blend composition. The PPy-PANI blends were prepared by solution processing method, using dimethyl sulfoxide (DMSO) solvent. Characterization of the polymer blends was carried out based on the data analysis from Fourier-Transform Infrared Spectroscopy (FT-IR), X-ray diffraction (XRD), and differential scanning calorimetry (DSC). The PPy-PANI system was successful to form blends in the DMSO solvent. The polymer blends showed almost amorphous nature in XRD spectra because of intermolecular interaction between PPy and PANI macromolecules, which was confirmed by FT-IR data. Specifically, the DSC result for the PPy: PANI= 50:50 wt.% blend showed only one glass transition temperature ( $T_g$ ), which indicates that the two polymers are well miscible without undergoing any phase separation.

#### 4.1 Introduction

Recently, polymer blends have attracted many scientists to devote their lives to study the polymer-polymer system to develop new functional plastics with technologically attractive properties (Seong et al., 2016). Hence, the polymer blend has been one of the hot research areas for materials scientists and engineers, because of its versatile applications (Facchetti, 2011). Specifically, the conjugated polymer blend system is not an exception for this trend of attraction. So far, conjugated polymers showing metallic or semiconducting properties have been commonly synthesized through electrochemical and chemical oxidative polymerization (Le et al., 2017). Between these two methods, the former electrochemical methods produce a film with brittle and not processable property (Li et al., 2013). However, the latter method, i.e., chemical oxidative polymerization provides a better opportunity for producing significantly a solution-processable polymer, compared to the electrochemical methods. Thus, many efforts have been made to further improve the processability by preparing soluble conducting polymer through the chemical

oxidative method, e.g., grafting alky side chains to polymeric backbone, etc. (Behniafar and Malekshahinezhad, 2014). The other approach to improve the processability of conducting polymer is to blend it with another material such as saturated hydrocarbon or  $\pi$ -conjugated semiconducting polymer (Wang et al., 2014). Since the mid-1980s, the blending of polyaniline (PANI) with other soluble insulating polymers has received great attention for its potential application to a wide variety of optical and electronic devices (Hasegawa et al., 1998). For example, the blending of PANI with polypyrrole (PPy) has enhanced the performance of materials, based on improved mechanical, thermal, electrical, and other processing properties (Tahalyani et al., 2016). The recent approaches for preparing polymer semiconductors are through solution processing methods. This method is advantageous from various points of view, such as cost minimization, scale-up, and roll-to-roll processing (Kang et al., 2013). The variety of functional chain molecules can be blended with other materials for fine-tuning a device performance. Specifically, this blending approach is extremely common in organic photovoltaics (OPV) or organic field-effect transistor (FETs) when they prepare an active layer or semiconducting channel layer, respectively (Li et al., 2012). In line with this blended approach, the conjugated polymer such as PPy or PANI also has been compounded with various nanomaterials, nanoparticles, and other organic materials for improving materials' properties for advanced applications. Figure 4.1 shows their chemical structures.

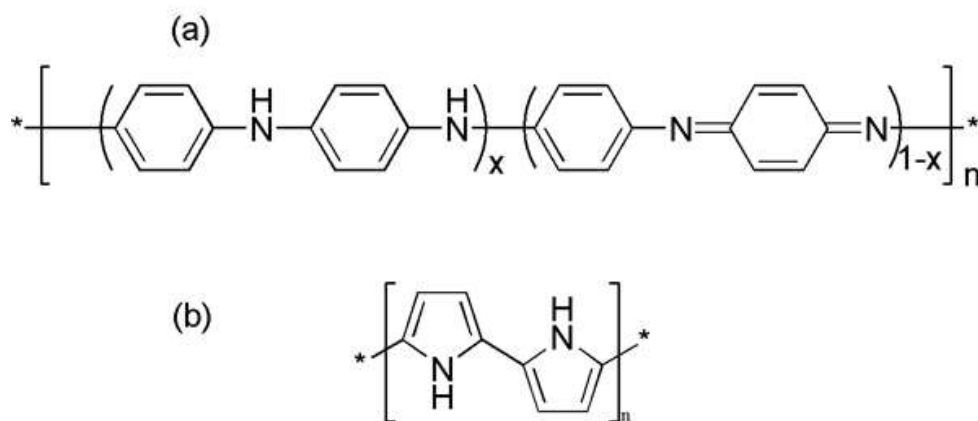


Figure 4.1: Chemical structure of polyaniline (PANI) and polypyrrole (PPy)

To date, some amounts of researches have been carried out for characterizing the PANI/PPy composites and/or blends. (Xing et al., 2007) prepared PANI/PPy composite from a PANI dispersion using sodium dodecylbenzene sulfate (SDBS) as both dopant and surfactant in HCl acid. And they reported that the PANI/PPy system has exhibited some specific interactions between PANI and PPy macromolecules. Also, they pointed out that their PANI/PPy composite has high conductivity based on excellent sponge-like morphologies. According to another research using copolymer such as poly(aniline-co-pyrrole) (PAP), some nanostructures were constructed for application to chemiresistive ammonia sensor, in which the copolymer PAP sensor showed improved sensing ability towards low concentration of ammonia, as compared to its homo-polymer PANI or PPy sensors at room temperature. The PAP sensor was reported to be very reliable in terms of cost, recovery time, selectivity, reproducibility, detection range, and stability (Chaudhary and Kaur, 2015). A next work indicated that highly conductive PAP copolymer was synthesized by properly controlling pre-polymerization time, which showed improved conductivity without any significant change of morphologies of a film (Ou and Xu, 2016). In the study, (Akundy et al., 2002) used the electrochemical deposition technique for the synthesis of a PANI/PPy composite on the aluminum substrates in the aqueous oxalic acid solution. They reported that some morphology changes were observed in their PANI/PPy composite. The aforementioned results are some background works for studying on the PANI/PPy blend or nanocomposite systems.

In general, there are three common categories of synthesis of PANI/PPy blends or composites, which are (a) electrochemical deposition, (b) copolymerization, and (c) solution processing (Pud et al., 2003). Their applications are drug delivery, encapsulating, supercapacitor, sensor, and other optoelectronic/electronic devices such as solar cells, light-emitting diode, FET, etc. (Facchetti, 2011). However, the PANI/PPy system has only a limited application because of its partial miscibility or solubility in the common organic solvents. This limitation affects all optical and electrical properties because of unfavorable processability. Hence, the enhancement of processability through enhanced miscibility of the PANI/PPy system is very desirable (Su, 2015).

In thermodynamics, miscibility or solubility means mixing of two or more components on the molecular level, which results in a homogeneous structure with equal thermodynamic state variables. For mixing, the Gibbs free energy of mixing ( $\Delta G_{mix}$ ) must be negative for forming a

homogeneous system. According to the principles of thermodynamics, when  $\Delta G_{\text{mix}}$  is negative, the thermodynamic miscibility and homogeneity can be reached. This condition can be fulfilled in the case when strong specific intermolecular interactions are located between the components of a polymer blend. Of course, sometimes, we may have a case, in which there is only moderate or poor interaction, inducing partial miscibility as a function of temperature and composition (Guenther et al., 2012). At this moment, note that one way to examine the miscibility and preliminary affinity between two polymers is to study the change in the glass transition temperature ( $T_g$ ) of polymers after mixing. If the mixture exhibits a single  $T_g$ , this evidence means that the two homopolymers are usually miscible. However, oppositely, if the mixture displays more than one  $T_g$ , the system is believed to be partially miscible or immiscible (Fekete et al., 2000). Based on these knowledge, in this study, we report the miscibility and phase behavior of the PANI/PPy system as a function of blending composition, for which FT-IR, XRD, and DSC were utilized.

## 4.2 Materials and Methods

Polyaniline was synthesized by chemical oxidative polymerization of aniline in the presence of hydrochloric acid and ammonium persulphate. A 1M of aniline was dissolved in the hydrochloride solution. Then 0.15M ammonium persulfate (APS) was dissolved in 50ml of double-distilled water. After that, we added a dropwise manner the APS solution to hydrochloride solution to initiate the polymerization of aniline. The mixture was stirred with a magnetic stirrer for 9h under 5°C temperature. Then we added methanol to stop further polymerization and let it unagitated until being precipitated. The resulting precipitate was collected by filtration. Then the product was washed successively by 0.2M of hydrochloride, double distilled water, and acetone, sequentially. Through washing the samples with hydrochloride, we can remove any undesirable residual monomer, oxidant, and other decomposed products. And also, we provide uniform protonation to PANI and wash the sample again by acetone for removing low molecular weight organic intermediates and oligomers. Then, finally, our product was obtained as a fine powder, which was dried under vacuum at 50°C for 24h.

Polypyrrole was synthesized by chemical oxidative polymerization of pyrrole. The 1M of pyrrole was dissolved in double-distilled water (10ml). Then 1.622 g of  $\text{Fe}_2\text{Cl}_3$  was dissolved into 50ml of double-distilled water. After that, the reacting monomers were mixed slowly with a

dropwise manner under constant stirring for 30 minutes at 5°C. After that, the polymerization was allowed for 6h under stirring. Then we kept it unagitated for 24h until PPy powders were settled down. The resulting precipitate was collected by filtration. And the products were washed by double distilled water many times and then dried in the oven for 12h at 50°C.

The PANI/PPy samples were prepared by the solution processing method. The PPy polymer was blended with PANI in various compositions, such as PPy: PANI = 50:50, 70:30, 80:20, and 90:10 in wt.%, for which the solvent DMSO was used. As a first step, the PPy and PANI solutions were prepared, respectively, in which ca. 20 mg of the polymer was dissolved in 10ml of DMSO and the mixture was ultrasonicated for 10 min. Then, the two individual solutions were mixed according to the desirable weight ratio and again ultrasonicated for an additional 1h. Finally, the solvent used was evaporated on the oven at 50°C for 12 h for obtaining our PANI/PPy samples.

## 4.3 Results and Discussion

### 4.3.1 The FT-IR Characteristics

In Figure 4.2a, the FT-IR spectra of PANI samples, the peak observed at  $3433.75\text{ cm}^{-1}$  is due to N-H stretching. The absorption bands at  $2923.21$  and  $2825.55\text{ cm}^{-1}$  are due to asymmetric C-H stretching and symmetric C-H stretching vibrations, respectively. The absorption peaks observed at  $1637.68\text{ cm}^{-1}$  were attributed to C=C stretching in aromatic nuclei. The band obtained at  $1600\text{-}1500\text{ cm}^{-1}$  corresponds to C-H stretching in aromatic compounds. In Figure 4.2b, the spectra of PPy, the strong peak observed at  $3447\text{ cm}^{-1}$  is related to N-H stretching. The peak at  $2915\text{ cm}^{-1}$  is related to  $\text{CH}_2$  and the peak observed at  $1536\text{ cm}^{-1}$  is due to C-C and C=C stretching in the ring. The peak of C-N stretching can be found at  $1483\text{ cm}^{-1}$ . The peak  $1169\text{ cm}^{-1}$  refers to C-C PPy ring, while the peaks of  $786\text{ cm}^{-1}$  and  $1036\text{ cm}^{-1}$  can be related to C-H out-of-plane bending and in-plane deformation, respectively. The FT-IR spectra for the PPy/PANI system in various compositions were shown in Figure 4.2c-f. The spectra of PPy: PANI = 70:30 and PPy: PANI = 90:10 on Figure 4.2f and e, respectively, indicated that there is a change of spectra due to the different compositions in the PPy/PANI system. The PPy: PANI= 50:50 and PPy: PANI= 80:20 spectra on Figure 4.2c and d, showed nearly very trivial change. Overall, the FT-IR spectra



showed that there is a change of intermolecular interactions between PPy and PANI with composition, resulting in the change of spectral shape. Specifically, we notice that the specific interactions between PPy and PANI macromolecule were confirmed not only by the change of intensity and shape observed in the range of spectra at  $1645\text{-}1130\text{ cm}^{-1}$  for the sample of PANI, PPy, and PPy: PANI= 50:50 but also by the peak shift observed around the spectra at  $980\text{-}786\text{ cm}^{-1}$ . Furthermore, the peak's broadening and the shift were observed around  $793\text{-}648\text{ cm}^{-1}$ . Therefore, we may expect that these intermolecular interactions might allow the PPy/PANI mixture to form blends.

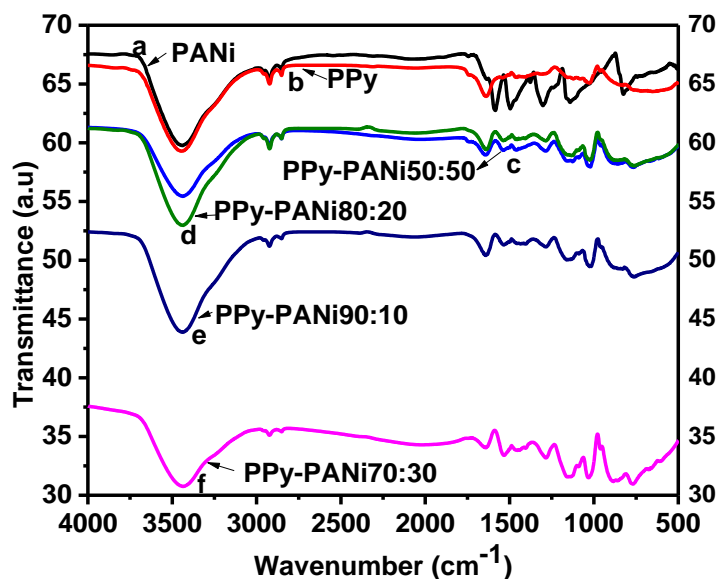


Figure 4.2: FT-IR spectra of PANI, PPy, the mixture of PPy:PANI = 50:50, PPy:PANI = 70:30, PPy:PANI = 80:20, and PPy:PANI= 90:10 (wt.%).

### 4.3.2 The XRD Characteristics

Figure 4.3a displays the PANI's XRD pattern, in which a broad peak was observed at about  $2\theta = 20^\circ$  and a sharp peak at about  $2\theta = 26^\circ$ . The peak at  $26^\circ$  is more intensive than the peak at  $20^\circ$ . The peak around the  $26^\circ$  indicates that PANI is a semicrystalline polymer, and the peak around  $20^\circ$  displays that PANI has an amorphous character, also. Figure 4.3b describes pure PPy spectra, in which the broad peaks at around  $2\theta = 24^\circ$  indicate that PPy has significant amorphous nature compared to PANI. The other two small peaks are observed at  $33^\circ$  and  $35^\circ$ , indicating chain

ordering in PPy macromolecules despite the major amorphous nature of PPy. Figure 4.3c to f shows the XRD spectra of the PPy/PANI system as a function of composition, in which we studied the miscibility and crystallinity of the PPy/PANI system. If phase separation occurs in the PPy/PANI system, x-ray diffraction peaks from both PPy and PANI are expected to be observed in the compound. However, if not, this absence of XRD peaks from pure polymer, PANI, or PPy indicates that the PPy/PANI system is in a single phase, confirming a blended system. Figure 4.3c to 4.3f showed that weight percent of PANI in the PPy/PANI system is 50, 30, 20, and 10, respectively. The result pointed out that the XRD spectra of PPy: PANI = 50:50 in Figure 4.3c is very distinguished from the other compositions, 70:30, 80:20, and 90:10 of the system in Figure 4.3d-f. In Figure 4.3d-f, the diffraction peaks of both pure PPy and PANI are observed, indicating they are composite rather than blend. This result showed that the PPy: PANI systems with 70:30, 80:20: 90:10 mixing ratio showed a phase separation, *i.e.*, they might be nanocomposites. In contrast, the spectrum of the PPy: PANI = 50:50 system in Figure 4.3c shows that the peaks at  $2\theta = 26^\circ$  (from PANI) and the peaks at  $2\theta = 26^\circ$  (from PPy) are disappeared. This XRD results indicated that in the PPy: PANI = 50:50 system, the crystallinity was disappeared through well miscibility (*i.e.*, no phase separation). This observation means that the interactions between PPy and PANI are very high to allow each polymer to mix at a molecular level. Therefore, we confirm that the PPy: PANI = 50:50 (wt. %) is a polymer blend instead of composite. Finally, we double-checked its blending/miscibility/single-phase possibility thorough thermal properties, *e.g.*, DSC results.

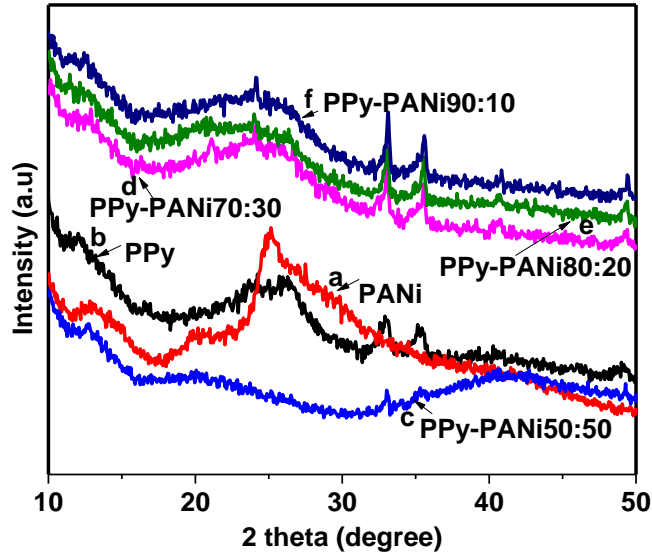


Figure 4.3: XRD of (a) PANI, (b) PPy, and (c-f) PPy/PANI Mixture

### 4.3.3 The DSC Characteristics

The DSC analysis was done to assess the thermal effect on phase behavior. In polymer science, the glass transition temperature is significantly important to determine whether a polymer-polymer mixture is miscible or immiscible or partly miscible. In the DSC thermogram, if a single T<sub>g</sub> was observed for a mixture, we would say that it is a blend with miscibility. However, if the two T<sub>g</sub> were observed in a mixture, we would decide that the components are an immiscible system, i.e., a composite. Figure 4.4a, b, and c show the glass transition temperatures of pure PANI, pure PPy, and the PPy:PANI=50:50 mixture, respectively. The DSC curve of PANI and PPy shows broad endothermic peaks at 359.95K and 384.85K, respectively. In literature, PANI's T<sub>g</sub> was observed at 385.15K (Ramesan and Sampreeth, 2018) and PPy's T<sub>g</sub> was displayed at 371.15K (Ramesan and Santhi, 2017) indicating our measured T<sub>g</sub> is close to the literature's reports within ~10-20 °C error. When evaluating the PPy: PANI = 50:50 system in Figure 4.4c, we observed that there is only a single glass transition temperature. This key result indicated that the two polymers, PPy and PANI, are a miscible system when we are blending them with 50:50 weight ratios. The glass transition temperatures of each pure polymers and their PPy:PANI= 50:50 mixture were

summarized in Table 4.1. Note that the  $T_g$  of the PPy:PANI= 50:50 system is falling between the pure component polymers.

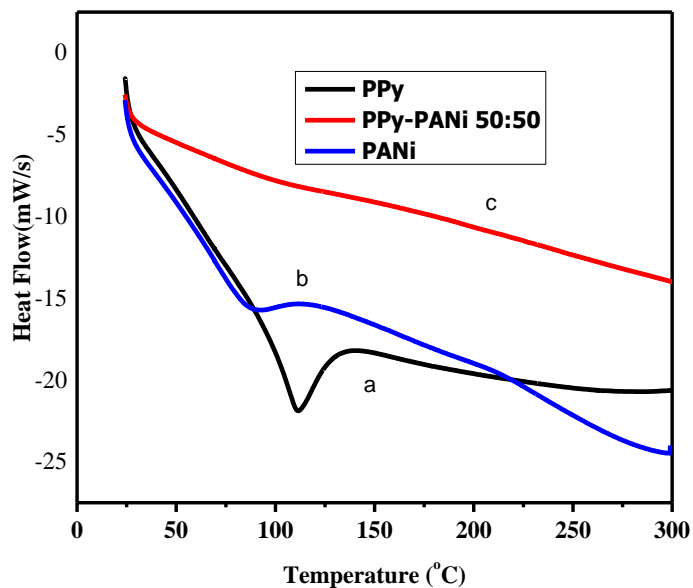


Figure 4.4: The DSC analysis to examine the miscibility of the PPy/PANI system

Table 4.1: Glass transition of PPy, PANI and PPy: PANI = 50:50

Polymer Mixture (wt.%)	$T_g$ (K)
PPy: PANI = 0:100	359.95
PPy: PANI = 100:0	384.85
PPy: PANI = 50:50	375.78

## 4.4 Conclusion

The PPy/PANI system was successfully obtained by the solution processing method using the DMSO solvent. In the XRD spectrum, the PPy: PANI= 50:50 system showed that the peaks originated from pure PPy or PANI disappeared, which indicates that the characteristic of crystallinity disappeared and resultantly the PPy: PANI= 50:50 system has amorphous nature. In the FT-IR analysis, the blending of PPy and PANI makes the FT-IR spectra's intensity and shape be changed. The broadening and shift of peaks were also observed. These phenomena confirm that there are specific interactions between PPy and PANI macromolecules when blended. Finally, the DSC thermogram indicated that there is only a single glass transition temperature for the PPy: PANI= 50:50 system. Therefore, we conclude that the PPy: PANI= 50:50 system is a miscible polymer blend.

## References

- AKUNDY, G. S., RAJAGOPALAN, R. & IROH, J. O. 2002. Electrochemical deposition of polyaniline–polypyrrole composite coatings on aluminum. 83, 1970-1977.
- BEHNIAFAR, H. & MALEKSHAHINEZHAD, K. 2014. A unique path to reach thermostable polypyrrole/Pd microfibers via chemical oxidative polymerization. *Colloid and Polymer Science*, 292, 2083-2088.
- CHAUDHARY, V. & KAUR, A. 2015. Enhanced and selective ammonia sensing behaviour of poly(aniline co-pyrrole) nanospheres chemically oxidative polymerized at low temperature. *Journal of Industrial and Engineering Chemistry*, 26, 143-148.
- FACCHETTI, A. 2011.  $\pi$ -Conjugated Polymers for Organic Electronics and Photovoltaic Cell Applications. *Chemistry of Materials*, 23, 733-758.
- FEKETE, E., FÖLDES, E., DAMSITS, F. & PUKÁNSZKY, B. 2000. Interaction-structure-property relationships in amorphous polymer blends. *Polymer Bulletin*, 44, 363-370.
- GUENTHNER, A. J., LAMISON, K. R., LUBIN, L. M., HADDAD, T. S. & MABRY, J. M. 2012. Hansen Solubility Parameters for Octahedral Oligomeric Silsesquioxanes. *Industrial & Engineering Chemistry Research*, 51, 12282-12293.

- HASEGAWA, N., KAWASUMI, M., KATO, M., USUKI, A. & OKADA, A. 1998. Preparation and mechanical properties of polypropylene-clay hybrids using a maleic anhydride-modified polypropylene oligomer. *Journal of Applied Polymer Science*, 67, 87-92.
- KANG, B., LEE, W. H. & CHO, K. 2013. Recent Advances in Organic Transistor Printing Processes. *ACS Applied Materials & Interfaces*, 5, 2302-2315.
- LE, T.-H., KIM, Y. & YOON, H. 2017. Electrical and Electrochemical Properties of Conducting Polymers. 9, 150.
- LI, J., ZHAO, Y., TAN, H. S., GUO, Y., DI, C.-A., YU, G., LIU, Y., LIN, M., LIM, S. H., ZHOU, Y., SU, H. & ONG, B. S. 2012. A stable solution-processed polymer semiconductor with record high-mobility for printed transistors. *Scientific Reports*, 2, 754.
- LI, M., LI, W., LIU, J. & YAO, J. 2013. Preparation and characterization of PPy doped with different anionic surfactants. 53, 2465-2469.
- OU, X. & XU, X. 2016. A simple method to fabricate poly(aniline-co-pyrrole) with highly improved electrical conductivity via pre-polymerization. *RSC Advances*, 6, 13780-13785.
- PUD, A., OGURTSOV, N., KORZHENKO, A. & SHAPOVAL, G. 2003. Some aspects of preparation methods and properties of polyaniline blends and composites with organic polymers. *Progress in Polymer Science*, 28, 1701-1753.
- RAMESAN, M. T. & SAMPREETH, T. 2018. In situ synthesis of polyaniline/Sm-doped TiO<sub>2</sub> nanocomposites: evaluation of structural, morphological, conductivity studies and gas sensing applications. *Journal of Materials Science: Materials in Electronics*, 29, 4301-4311.
- RAMESAN, M. T. & SANTHI, V. 2017. In situ synthesis, characterization, conductivity studies of polypyrrole/silver doped zinc oxide nanocomposites and their application for ammonia gas sensing. *Journal of Materials Science: Materials in Electronics*, 28, 18804-18814.
- SEONG, D.-W., YEO, J.-S. & HWANG, S.-H. 2016. Fabrication of polycarbonate blends with poly(methyl methacrylate-co-phenyl methacrylate) copolymer: Miscibility and scratch resistance properties. *Journal of Industrial and Engineering Chemistry*, 36, 251-254.
- SU, N. 2015. Improving Electrical Conductivity, Thermal Stability, and Solubility of Polyaniline-Polypyrrole Nanocomposite by Doping with Anionic Spherical Polyelectrolyte Brushes. *Nanoscale Research Letters*, 10, 301.

- TAHALYANI, J., RAHANGDALE, K. & KANDASUBRAMANIAN, B. 2016. The dielectric properties and charge transport mechanism of  $\pi$ -conjugated segments decorated with intrinsic conducting polymer. *RSC Adv.*, 6, 69733-69742.
- WANG, X., GROFF, L. C. & MCNEILL, J. D. 2014. Multiple Energy Transfer Dynamics in Blended Conjugated Polymer Nanoparticles. *The Journal of Physical Chemistry C*, 118, 25731-25739.
- XING, S., ZHAO, C., ZHOU, T., JING, S. & WANG, Z. 2007. Preparation and characterization of polyaniline–polypyrrole composite from polyaniline dispersions. *Journal of Applied Polymer Science*, 104, 3523-3529.

## Chapter Five

### 5.1 Optical Properties of Nanostructural Polyaniline Depending on Doping or Dedoping

#### Abstract

This work aims to present the optical and thermal study on doped and dedoped polyaniline (PANI) nanoparticles. Herein, PANI nanoparticles are successfully synthesized by chemical oxidative polymerization of aniline in the presence of hydrochloric acid and ammonium persulphate as oxidant. Then PANI power samples are characterized by Fourier-transform infrared spectroscopy (FT-IR), X-ray diffraction (XRD), thermogravimetric analysis (TGA), and UV-Vis spectroscopy (UV-Vis). The crystallinity of doped PANI is significantly decreased once it is dedoped. The average crystallite size of PANI is estimated to be ca. 24.27nm based on Scherrer's equation. The optical absorption peaks of transition are observed at 337nm and 320nm for doped and dedoped PANI, respectively.

**Keywords:** Absorption, Doping, Dedoping, Nanoparticle, Polyaniline.

#### 5.1.1 Introduction

Semiconducting and metallic polymers have been widely studied in the field of flexible and low-cost electronic devices. It is because these materials can be processed at low temperatures and deposited on plastic substrates for fabricating lightweight, flexible, and ultra-thin electronic devices (Dai et al., 2016). Conjugated polymers are currently used as semiconducting layers in organic field effect transistors (OFET), organic light-emitting diodes (OLED), organic solar cells (OSC), photodiodes and plastic lasers (Yao et al., 2016). Among them, polyaniline (PANI), a semi-flexible rod polymer, is one of the commercialize candidates due to its ease of synthesis with



environmental stability. Besides, when it is processed to have a nanostructure, it is believed to be promising due to its high surface area, controllable conductivity, and electrochromic behavior depending on doping or dedoping condition. Nanostructural PANIs are widely used in the area of electrochemical devices, light-emitting diodes, biosensors, biologic, chemical sensors, and battery electrodes (Alam et al., 2013). Their properties are known to be different depending on the oxidation states, crystallinity, and manufacturing process (Ikkala et al., 1995), (Masdarolomoor, 2007).

PANI normally exists in three major states, namely, leucoemeraldine, emeraldine, and pernigraniline. Among the aforementioned states, the fully reduced and oxidized states are leucoemeraldine and pernigraniline, respectively. The emeraldine form of polyaniline is emeraldine base (EB) with neutral characteristics (Nemade and Waghuley, 2013). In general, the doping process leads to a dramatic change in the electronic structure of materials, because the formation of charged species promotes a local distortion in the polymeric backbone (Dimitriev, 2004), (Sezen-Edmonds and Loo, 2017). Specifically, it causes the presence of local electronic states in the gap due to the shifting of molecular orbitals. For instance, PANI doped with strong hydrochloric acid with a pH less than 2 is known to be more conducting than that with other dopants. It is because chlorine is highly electronegative and hence delocalization of electrons is effective as compared to doping with weak organic acids like acetic acid, phytic acid (here, oxygen is lesser electronegative than chlorine).

Importantly, PANI has been synthesized in different dimensions and nanostructure such as nanotubes, nanofibers, nanowire, nanorod, nanoflake, nanoparticles, nanospheres even nanoflowers and so forth (Tran et al., 2011). When PANI is nanostructured, it is known to have improved material properties. Hence, these advanced physical, chemical, optoelectronic properties

of nanostructural PANI have attracted many research interests (Tran et al., 2011), (Ma et al., 2017). For example, several types of research have proved that nanostructural PANI can boost performance in applications needing a high surface contact area (Zhao et al., 2017). Recently, nanostructural PANIs were synthesized through various methods such as template synthesis, interfacial polymerization, self-assembly, and stepwise electrochemical deposition (Nguyen and Yoon, 2016).

PANI's electrical and optical properties are arising, of course, from the  $\pi$ -conjugation along the polymeric backbone. The fundamental understanding of its excited-state absorption is key for fabricating optical devices. The interest of this paper is to study the optical properties of PANI materials with doping or dedoping. Also, it is important to investigate the nanostructure of PANI materials in each redox state, which affords to fabricate high-performance plastic electronic devices. Herein the two different redox states of nanostructural PANI materials, i.e., doped and dedoped, were characterized. The doped PANI samples were prepared by doping them with HCl, and the dedoped ones were prepared by soaking them in  $\text{NH}_4\text{OH}$ . The resulting PANI samples were characterized by using various spectroscopic instruments.

### **5.1.2 Experimental**

PANI was synthesized by chemical oxidative polymerization of aniline in the presence of hydrochloric acid and ammonium persulphate (Awasthi et al., 2016). 1M of aniline was dissolved in a 1M hydrochloride solution. Then 0.15M ammonium persulfate (APS) was dissolved in 50ml of double-distilled water. After that, the APS solution was added with a dropwise manner to 1M hydrochloride solution to initiate the polymerization of aniline. The mixture was stirred with a magnetic stirrer for 9h under 50C. Then methanol was added to stop polymerization and leave the

mixture unagitated until precipitated. The resulting precipitate was collected by filtration. Then the product was washed successively by 0.2M of hydrochloride, double distilled water, and acetone, sequentially. By washing the products with hydrochloride, we can remove residuals, monomers, oxidants, and their decomposition. And this HCl treatment also gives uniform pronation to PANI. Then by washing them with acetone, we can additionally remove low molecular weight organic intermediates and oligomers. The products were obtained as fine powders, which were dried under vacuum at 50oC for 24 h. The above-synthesized powder (PANI-HCl) was washed with aqueous ammonia to remove the dopants by neutralization, which provides the dedoped emeraldine base (EB) form of the polymer. The EB powder was then obtained by the process of filtration, washing, drying, and crushing, successively. Then, finally, the dedoped PANI was prepared by soaking it in ammonium hydroxide (1.2 M) for 40 h. The filtered PANI samples were washed and dried, which were characterized by using various tools, e.g., FT-IR, XRD, TGA, and UV-Vis spectroscopy.

### **5.1.3 Results and Discussion**

#### **5.1.3.1 Functional-Group Identification by FT-IR spectroscopy**

Figure 5.1.1a shows the FT-IR spectra for the PANI samples doped with hydrochloric acid, in which the peak observed at  $3433.75\text{ cm}^{-1}$  is due to N-H stretching. Also, the absorption bands at  $2923.62$ , and  $2825.55\text{ cm}^{-1}$  are due to asymmetric C-H stretching and symmetric C-H stretching vibrations, respectively. The peaks at  $1639.54\text{ cm}^{-1}$  are attributed to C=C stretching in aromatic nuclei. The bands obtained at  $1600\text{-}1500\text{ cm}^{-1}$  corresponds to C-H stretching in aromatic compounds. For the doped sample, the peak at  $1240\text{ cm}^{-1}$  is associated with C-N<sup>+</sup> stretching vibration in polaron structure

The dedoped sample in Figure 5.1.1b is EB PANI, in which the peaks at 709 and 620  $\text{cm}^{-1}$  are related to the out-plane vibration in 1,4 distributed benzene rings having the para coupling structure. The vibration at 824  $\text{cm}^{-1}$  denotes N-H out of plane bending. The peaks at 1496.69 and 1585.27  $\text{cm}^{-1}$  ascribe to C=C, stretching vibration of quinoid and benzenoid rings, respectively. The band at 3443  $\text{cm}^{-1}$  is N-H stretching vibration, in which the reduction of intensity is observed due to the hydrogen bond. Hence, we can say that there is an overall change of microstructure of PANI samples depending on doping or dedoping, which bring for the shift of peaks and their intensities.

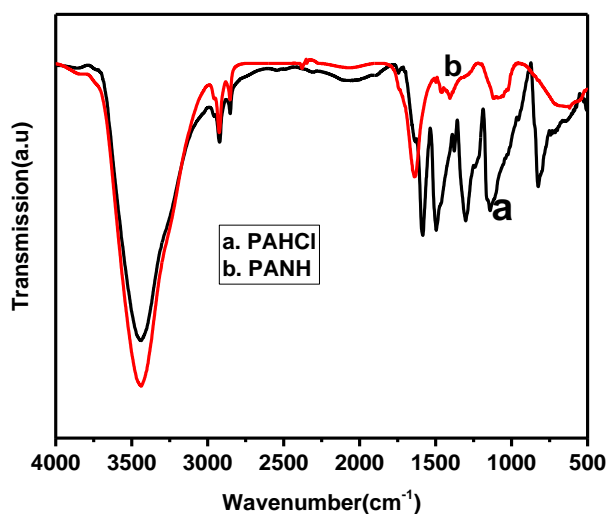


Figure 5.1.1: FT-IR Spectroscopy for HCl-doped PANI (PAHCl) and dedoped PANI (PANH) by  $\text{NH}_4\text{OH}$ .

### 5.1.3.2 Structure Analysis by X-ray Powder Diffraction

In Figure 5.1.2a for the PANI doped with HCl, the XRD peaks were observed at about  $2\theta = 20^\circ$  and  $2\theta = 26^\circ$ . The strong peaks at  $2\theta = 26^\circ$  indicate that the doped PANI is a semicrystalline polymer. In contrast, for the dedoped PANI shown in Figure 2b, the peak at  $26^\circ$  observed in Fig.

5.1.2a was a little shifted to the lower angle and, simultaneously, it was much broadened, indicating that the dedoped PANI has more amorphous nature than the doped PANI. Besides, the peak at  $2\theta=20^\circ$  in Fig. 2a disappears when dedoped as shown in Fig. 5.1.2b, similar to the report (Harb et al., 2015). The main x-ray peaks around  $2\theta=20^\circ$  and  $26^\circ$  describe the parallel and perpendicular periodicity of polycrystalline PANI material. Herein, the crystallite size ( $t$ ) of PANI sample can be calculated from the Scherrer's equation 5.1.1 (Gilja et al., 2018),

$$t = \frac{0.94\lambda}{B \cos \theta} \quad (\text{Eqn. 5.1.1})$$

where  $\lambda$  ( $= 0.15406 \text{ nm}$ ) is the wavelength of x-ray radiation,  $B$  ( $0.2854 \text{ rad}$ ) is the full width at half-maximum (FWHM) at angle  $\theta=23.837^\circ$ . In eq. 1, the estimated crystallite size is  $24.27 \text{ nm}$ .

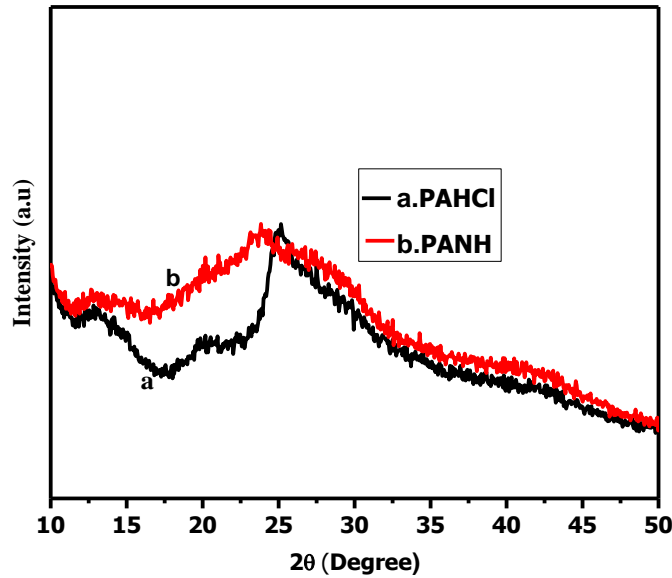


Figure 5.1.2: XRD Hydrochloric acid doped PANI (PAHCL) and Dedoped By Ammonia (PANH)

#### 5.1.3.4 Optical Absorption Study by UV-Vis Spectroscopy

UV-Vis spectra of PANI samples doped with HCl and dedoped with  $\text{NH}_4\text{OH}$  are shown in Figure 5.1.3. The black solid line (Fig. 5.1.3a) shows three absorption peaks. The first one at a wavelength of 337 nm ( $\pi \rightarrow \pi^*$  transition of the benzenoid ring) is considered as valence band to conduction band charge transfer, and it is also related to the quinonoid rings due to free nonbonding electrons absorbing relatively low energy radiation, which are well agreed with the results of literature (Karmakar et al., 2018). The peak at 418 nm is attributed to the transition from the valence band to the antibonding polaron state (i.e., *polaron*  $\rightarrow \pi^*$  transition), which is due to doping and/or defect in the PANI. The third peak appears at 690nm due to  $\pi \rightarrow \text{polaron}$  transition (i.e., bipolaron transition). In the contrast, the dedoped PANI shows a peak of 320 nm ( $\pi \rightarrow \pi^*$  transition) in Fig. 5.1.3b, in which the polaron peak disappears or decreases, and bipolaron also shifted to 600 nm. Thus, there is a clear difference in absorption depending on doping status. The valence band maximum (highest occupied molecular orbital: HOMO) and the conduction band minimum (lowest unoccupied molecular orbital: LUMO) are separated by an energy bandgap (Kahn, 2015).

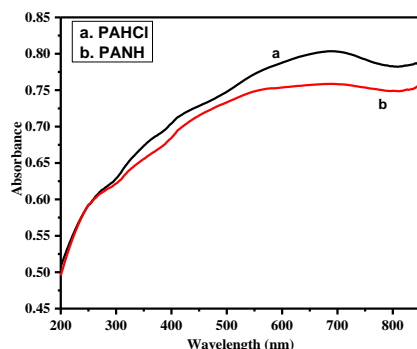


Figure 5.1.3: UV- Vis spectroscopy for HCl-doped PANI (PAHCl) and dedoped PANI (PANH) by  $\text{NH}_4\text{OH}$ .

The optical bandgap of sample is determined from the absorption spectra, the photon absorption in many amorphous materials is founded to obey the Tauc model, which is given by equation (Abdel Rafea and Roushdy, 2008):

$$\alpha hv = \beta (hv - E_g)^n \quad (\text{eq.5.1.2})$$

where  $\alpha$  is the absorption coefficient,  $hv$  is the photon energy,  $\beta$  is a factor depending on the transition probability ( $\beta$  is assumed to be constant within the optical frequency range), and  $E_g$  is energy bandgap. The index  $n$  is related to the transition of an electron, and its value is usually  $n=1/2$  or  $2$  depending on the transition direct or indirect, respectively (Böer and Pohl 2014). The optical bandgap is determined by extrapolation of  $(\alpha hv)^2$  versus  $hv$  plots to the x-axis. Figure 5.4 shows optical band gap  $E_g$  values of 1.72 eV (Fig. 5.1.4a) and 1.34eV (Fig. 5.1.4b). Hence, the optical band gap of dedoped PANH shows a decreased value by 0.38 eV ( $= 1.72 - 1.34$  eV).

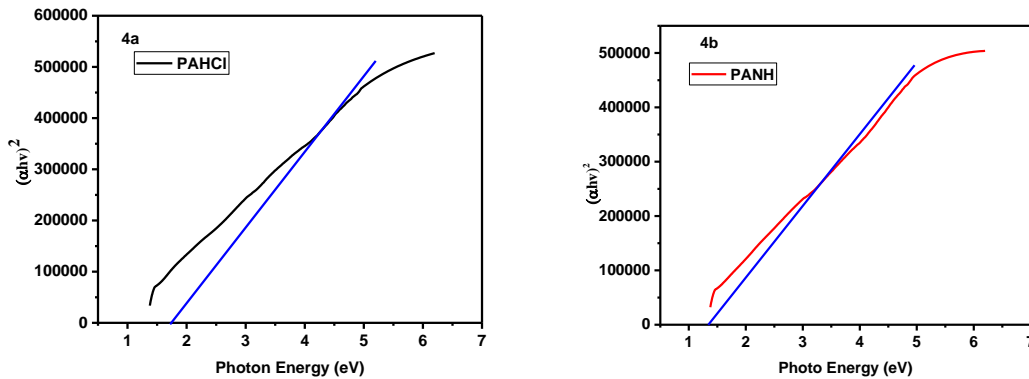


Figure 5.1.4: Plot of  $(\alpha hv)^2$  versus photon energy  $hv$  for (a) HCl-doped PANI (PAHCl) and (b) dedoped PANI (PANH) by  $\text{NH}_4\text{OH}$ .

### 5.1.3.5 Thermal Analysis by TGA

The TGA results for ES-PANI (emeraldine salt) and EB-PANI (emeraldine base) are shown in Figure 5.1.5a the thermogram of PAHCl (ES-PANI) shows the four steps of weight loss behavior. The first step indicates about 24% of weight loss at temperatures up to 135°C. This step can be attributed to the loss of water molecules from the PANI sample. In the second step, there is a small weight loss (2%) at a temperature from 135 to 226°C, which may be due to the impurities. The third stage occurs in the range of 226-294°C, which was assigned to the removal of HCl. The fourth step starts around 294°C, indicating the thermal degradation of the ES-PANI polymer. In contrast, in fig. 5.1.5 b the EB-PANI is more stable than the doped ES-PANI powders. There were three major stages of weight loss for the EB-PANI powder sample. The first weight loss (16%) is at around 106°C, resulted from the evaporation of moisture. The second small weight loss (4%) is in the range of 104-505°C. The third step begins around 505°C indicated chemical structure degradation of the PANH (EB-PANI).

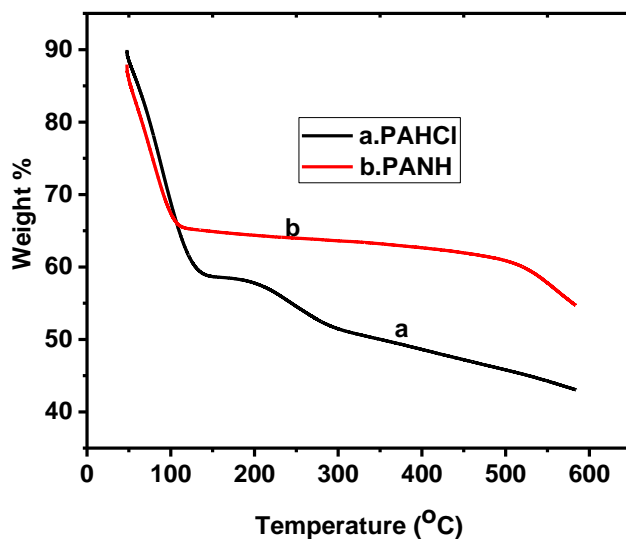


Figure 5.1.5: TGA data for HCl-doped PANI (PAHCl) and Dedoped PANI (PANH) by  $\text{NH}_4\text{OH}$ .



#### 5.1.4 Conclusions

Nanostructure PANIs were synthesized using chemical oxidative polymerization. When PANI is dedoped by  $\text{NH}_4\text{OH}$ , its crystallinity observed in the HCl-doped PANI samples was lost significantly, showing largely amorphous nature in the dedoped PANI. The crystallite size of PANI was estimated to be 24.27 nm. The optical absorption peaks of  $\pi \rightarrow \pi^*$  transition were observed at 337 nm and 320 nm for doped and dedoped PANI, respectively. Finally, when PANI is dedoped, its thermal stability was enhanced compared with HCl-doped PANI.

#### References

- ABDEL RAFEA, M. & ROUSHDY, N. 2008. Determination of the optical band gap for amorphous and nanocrystalline copper oxide thin films prepared by SILAR technique. *Journal of Physics D: Applied Physics*, 42, 015413.
- ALAM, M., ALANDIS, N., ANSARI, A. & SHAIK, M. 2013. Optical and Electrical Studies of Polyaniline/ZnO Nanocomposite. *Journal of Nanomaterials*, 2013, 5.
- AWASTHI, S. K., BAJPAI, S. K., UTIYE, A. S. & MISHRA, B. 2016. Gelatin/poly(aniline) composite films: Synthesis and characterization. *Journal of Macromolecular Science, Part A*, 53, 301-310.
- DAI, Y.-Z., AI, N., LU, Y., ZHENG, Y.-Q., DOU, J.-H., SHI, K., LEI, T., WANG, J.-Y. & PEI, J. 2016. Embedding electron-deficient nitrogen atoms in polymer backbone towards high performance n-type polymer field-effect transistors. *Chemical Science*, 7, 5753-5757.
- DIMITRIEV, O. P. 2004. Doping of Polyaniline by Transition-Metal Salts. *Macromolecules*, 37, 3388-3395.
- GILJA, V., VRBAN, I., MANDIĆ, V., ZIC, M. & HRNJAK-MURGIĆ, Z. 2018. Preparation of a PANI/ZnO Composite for Efficient Photocatalytic Degradation of Acid Blue. *Polymers*, 10, 940.
- HARB, M., SOLIMAN, M., TAYEL, M. & EBRAHIM, S. 2015. Preparation and characterization of pseudocapacitor electrode by spraying conducting polymer on a flexible substrate. *Journal of Taibah University for Science*, 10.

- IKKALA, O. T., PIETILÄ, L. O., AHJOPALO, L., ÖSTERHOLM, H., PASSINIEMI, P. J. & K., C. C. 1995. On the molecular recognition and associations between electrically conducting polyaniline and solvents. 103, 9855-9863.
- KAHN, A. 2015. Fermi level, work function and vacuum level. *Mater. Horiz.*, 3.
- KARMAKAR, H. S., ARUKULA, R., THOTA, A., NARAYAN, R. & RAO, C. R. K. 2018. Polyaniline-grafted polyurethane coatings for corrosion protection of mild steel surfaces. 135, 45806.
- MA, Y., HOU, C., ZHANG, H., QIAO, M., CHEN, Y., ZHANG, H., ZHANG, Q. & GUO, Z. 2017. Morphology-dependent electrochemical supercapacitors in multi-dimensional polyaniline nanostructures. *Journal of Materials Chemistry A*, 5, 14041-14052.
- MASDAROLOMOOR, F., 2007. Novel nanostructured conducting polymer systems based on sulfonated polyanilin. s.l., University of Wollongong.
- NEMADE, K. & WAGHULEY, D. S. 2013. Study of Cerium Doped Polyaniline Composites for Resistive Type CO<sub>2</sub> Gas Detection. *Walailak Journal of Science and Technology*, 11.
- NGUYEN, D. N. & YOON, H. 2016. Recent Advances in Nanostructured Conducting Polymers: from Synthesis to Practical Applications. 8, 118.
- SEZEN-EDMONDS, M. & LOO, Y.-L. 2017. Beyond Doping and Charge Balancing: How Polymer Acid Templates Impact the Properties of Conducting Polymer Complexes. *The Journal of Physical Chemistry Letters*, 8, 4530-4539.
- TRAN, H. D., D'ARCY, J. M., WANG, Y., BELTRAMO, P. J., STRONG, V. A. & KANER, R. B. 2011. The oxidation of aniline to produce “polyaniline”: a process yielding many different nanoscale structures. *Journal of Materials Chemistry*, 21, 3534-3550.
- YAO, J., YU, C., LIU, Z., LUO, H., YANG, Y., ZHANG, G. & ZHANG, D. 2016. Significant Improvement of Semiconducting Performance of the Diketopyrrolopyrrole–Quaterthiophene Conjugated Polymer through Side-Chain Engineering via Hydrogen-Bonding. *Journal of the American Chemical Society*, 138, 173-185.
- ZHAO, F., SHI, Y., PAN, L. & YU, G. 2017. Multifunctional Nanostructured Conductive Polymer Gels: Synthesis, Properties, and Applications. *Accounts of Chemical Research*, 50, 1734-1743.

## 5.2 Electrical and Optical Properties of Polypyrrole and Polyaniline Blends

### Abstract

This paper reported that PPy/PANI blend is successfully synthesized from the solution process. To high-performance optoelectronic devices, understanding the electrical and optical properties of materials should be significant. This work aims to study the polymer-blend morphologies as well as the electrical and optical properties of materials. The polymer blends were prepared as a function of composition. Scanning electron microscopy with energy dispersive X-ray analysis (SEM-EDX), ultraviolet-visible (UV-Vis) spectroscopy, photoluminescence (PL) and current-voltage (I-V) characteristics techniques were applied for characterizing the PPy/PANI blends. The PPy/PANI blend is a semiconductor by showing the conductivity in the range of  $10^{-6}$  to  $10^{-3}$  S/cm at room temperature. The result determines the optical band gap of each blend with different composition, providing the optical band gap of the blends at the range of 1.53-1.95 eV. Finally, the electrical transport and the chemical composition of the PPy/PANI blends were characterized.

**Keywords:** Blends, Electrical, optical, Tauc model, SCLC

### 5.2.1 Introduction

Conducting polymer blends or composites have been developed for various technical applications. Conducting polymer blends incorporating other materials such as inorganic particles, insulating polymers, and small molecules have been studied to improve various material properties such as insolubility, poor processability, and mechanical properties. Specifically, the optical and electrical properties of polymers can be tuned by several methods such as copolymerization, blending, plasticization, and addition of salt, ceramics, and nanoparticles. For example, in the mid-1980s, many polymer scientists have been devoted themselves to study the polymer blend issues to get a unique property as well as to develop new materials.

Herein, we will focus on the electrical and optical properties of polymer blends composed of polypyrrole (PPy) and polyaniline (PANI). Although some amounts of studies were carried out already to understand the nature of PPy, PANI, and PPy/PANI mixtures, still there is room to investigate the PPy/PANI blends or composite system for better understanding these material

systems (Xing et al., 2007). Among conducting polymers, PPy may be one of the most interesting semiconducting or metallic materials. It is because PPy has several strong points, such as easy synthesis, low cost, low toxicity, high electrical conductivity, good redox properties, and environmental stability (Wang et al., 2017). On the other hand, PANI is also the most extensively studied conducting polymers owing to easy synthesis, doping-dedoping chemistry, low cost, high conductivity, excellent environmental stability, and so forth. Specifically, PANI has wide potential applicability such as erasable optical information storage, shielding of electromagnetic interference, microwave and radar electrochemical capacitors, electrochromic devices, nonlinear optical, electromechanical actuators, antistatic and anticorrosion coatings, high specific capacitance and electroactivity (Zhang et al., 2013).

To date, various techniques or methodologies have been applied to PANI material for modifying the properties of materials using doping and/or blending. Especially, doping has been widely applied in conjugated polymers for improving their optoelectronic properties. Doping can be attained by either charge transfer or an applied external electric field. Doped materials usually display different electronic and optical properties (Kaloni et al., 2015). For example, PPy was doped with hydrochloric acid (HCl), sulfuric acid (H<sub>2</sub>SO<sub>4</sub>), and dodecylbenzene sulfonic acid (DBSO), indicating that alteration of donor groups is a successful methodology for enhancing conductivity as well as for decreasing the band gap of PPy. To date, conducting polymer samples have been usually synthesized by chemical oxidative polymerization technique with ammonium peroxydisulphate (APS) as an oxidant (Sadrolhosseini et al., 2016).

Besides, the effect of HCl concentration on the electrical conductivity of PANI-cellulose composites was studied, in which the sample with HCl concentration 3 M showed the highest electrical conductivity of 0.0816 S/cm (Yuningsih, et al., 2017). It was reported that the chemically synthesized PPy using dodecylbenzene sulfonic acid (DBSA) as a dopant yielded the conductivity of about 5 S/cm, whereas another study showed 18 S/cm when PPy was doped with camphor sulfonic acid (CSA). The nature of the solvent also is known to affect the conductivity of the prepared PPy (Rahaman et al., 2018). Blending is another engineering technique for adjusting the properties of conjugated polymers. One former research has been devoted to study the optical properties of PPy doped with polyvinyl chloride (PVC). The study compares the optical parameter

the PPy sample depending on PVC presence or not, indicating an increase of the reflective index when PPy was composited with PVC (Bhavsar and Tripathi, 2016). Similarly, another study reveals that the temperature, polarizing field, and concentration of PPy are factors for the electrical properties of PVC/polymethyl methacrylate (PMMA) blends. The order of D.C. electrical conductivity of unfilled PVC/PMMA was of the order of  $10^{-13} \text{ ohm}^{-1} \text{ cm}^{-1}$ . After doping of PPy in PVC/PMMA in sufficient quantity, it is increased to  $10^{-7} \text{ ohm}^{-1} \text{ cm}^{-1}$ . The optical band gap energy decreases with an increase in the percentage of polypyrrole in the PVC/PMMA system. The optical absorption shows that PPy-filled films have allowed direct transitions (Yussuf et al., 2018).

Furthermore, some research groups have studied PPy, PPy/silicon carbide (SiC), and DBSA doped PPy/SiC nanocomposite particles by direct oxidation of pyrrole with anhydrous ferric chloride through in-situ chemical polymerization. It was observed that the conductivity of PPy composite increases with increasing wt. % of SiC as well as the molar concentration of DBSA and I-V analysis gives a linear pitch curve (Shrikrushna and Kulkarni, 2015), (Mahmud Ekramul et al., 2005). Then, PPy-carboxymethyl cellulose (CMC) composite film was prepared by the electrochemical method, which showed electromagnetic interference (EMI) shielding applications. (Trivedi, 1999). In addition, it was reported that doping of counter ion creates a band structure and also stabilizes localized bound states to impart unusual optical and magnetic properties to the macromolecular system. This work also proved that the doping of counter ion influences the electrochemical properties of PANI and PPy (Mizobuchi et al., 1995), (Qin and Guo, 2012).

The electrical conductivity of PANI films is known to increase with increasing the dipping time in sulfuric acid solution and stabilize after 24 hours of dipping at a value equals to  $3.95 \times 10^{-3} \text{ S/cm}$ . This value increases significantly with the decrease of film thickness (Wang et al., 2017a). It is shown that electrically conductive PANI-polystyrene (PS) composite can be obtained by in-situ polymerization and blending in xylene solution with DBSA, oxidant aniline, and PS. The electrical conductivity of the prepared composite appears to be increased as the high value of  $10 \text{ S/cm}$  at only a small amount of conductive components as 12wt%. The PANI-PS composite was readily soluble in common organic solvents (Tahalyani et al., 2016). The blending of PANI with PPy has enhanced the performance of materials, based on improved mechanical, thermal,

electrical, and other processing properties (Tuncel and Demir, 2010). Conjugated polymer nanoparticles are highly versatile nanostructured materials that can potentially find applications in various areas such as optoelectronics, photonics, bio-imaging, bio-sensing, and nanomedicine (Su, 2015). In contrast, some researches showed that the large-scale application of PANI-PPy composite is sometimes limited by the difficulty of insolubility and infusibility of the material, leading to poor electronic conductivity and mechanical properties. The research stressed that further improvement of the PANI-PPy nanocomposite's properties is needed (Tikish et al., 2018). In our previous work, the PPy/PANI system was successfully obtained by the solution processing method using the DMSO solvent. PPy: PANI= 50: 50 system showed that a miscible polymer blend (Tikish et al., 2018). The present work will be focused on the optical band gap of the blend, the electrical properties of PPy/PANI blend as a function of blending composition. In this work, we used the SEM-EDX, UV-Vis, PL, and I-V curve for characterization purposes. In general, the optical properties provide information about the materials band structure, while electrical properties display the nature of charge transport prevalent in these materials.

### 5.2.2 Methods

Polyaniline was synthesized by chemical oxidative polymerization of aniline in the presence of hydrochloric acid and ammonium persulphate. Polypyrrole was synthesized by chemical oxidative polymerization of pyrrole. The 1 M of pyrrole was dissolved in double-distilled water (10ml). The PANI/PPy samples were prepared by the solution processing method. The polymer PPy was blended with PANI in various compositions, such as PPy: PANI = 50:50, 70:30, 80:20, and 90:10 in wt.%, for which the solvent DMSO was used. As a first step, the PPy and PANI solutions were prepared respectively, in which 20 mg of the polymer was dissolved in 10ml of DMSO and the mixture was ultrasonicated for 10 min. Then, the two individual solutions were mixed and again ultrasonicated for an additional 1hr. Finally, the solvent used was evaporated on the oven at 50°C for 12 h for obtaining our PANI/PPy samples.

## 5.2.3 Results and Discussion

### 5.2.3.1 The FT-IR Characteristics

In Figure 5.2.1a, the FT-IR spectra of PANI samples, the peak observed at  $3433.75\text{ cm}^{-1}$  is due to N-H stretching. The absorption bands at  $2923.21$  and  $2825.55\text{ cm}^{-1}$  are due to asymmetric C-H stretching and symmetric C-H stretching vibrations, respectively. The absorption peaks observed at  $1637.68\text{ cm}^{-1}$  were attributed to C=C stretching in aromatic nuclei. The band obtained at  $1600\text{-}1500\text{ cm}^{-1}$  corresponds to C-H stretching in aromatic compounds. In the study, PANI near result have been reported by (Al-Daghman, 2016). In Figure 5.2.1b, the spectra of PPy, the strong peak observed at  $3447\text{ cm}^{-1}$  is related to N-H stretching. The peak at  $2915\text{ cm}^{-1}$  is related to CH<sub>2</sub> and the peak observed at  $1536\text{ cm}^{-1}$  is due to C–C and C=C stretching in the ring. The peak of C–N stretching can be found at  $1483\text{ cm}^{-1}$ . The peak  $1169\text{ cm}^{-1}$  refers to C–C PPy ring, while the peaks of  $786\text{ cm}^{-1}$  and  $1036\text{ cm}^{-1}$  can be related to C–H out-of-plane bending and in-plane deformation, respectively. This also, observed in the research work by (Šetka et al., 2017).

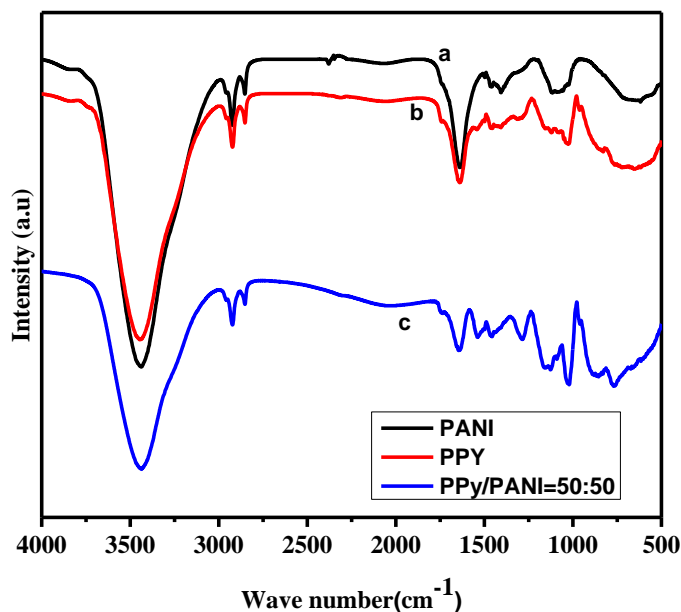


Figure 5.2.1 FT-IR spectra of PANI, PPy and PPy/PANI=50:50 Blend

Figure 4.2.1c. The spectra of PPy: PANI = 50:50, indicated that there is a change of spectra due to the different components in the PPy/PANI system. Overall, the FT-IR spectra showed that there is a change of intermolecular interactions between PPy and PANI with composition, resulting in the change of spectral shape. Specifically, researchers noticed that the specific interactions between PPy and PANI macromolecule were confirmed not only by the change of intensity and shape observed in the range of spectra at 1645-1130  $\text{cm}^{-1}$  for the sample of PANI, PPy, and PPy: PANI= 50:50 but also by the peak shift observed around the spectra at 980-786  $\text{cm}^{-1}$ . Furthermore, the peak's broadening and a shift were observed around 793-648  $\text{cm}^{-1}$ . Therefore, we may expect that these intermolecular interactions might allow the PPy/PANI mixture to form blends. In the study of (Velhal et al., 2014) have been reported that the peak shift was observed as the result of the change of chemical environment and the formation of composite made an effective change in the molecular structure. The FT-IR assignment is given in the Table 5.2.1.

Table 5.2.1: The FT-IR assignment of PANI, PPY and PPy/PANI=50:50 Blend

Polyaniline (PANI)		Polypyrrole (PPy)		Polypyrrole-Polyaniline (PPy/PANI=50:50)	
Wave number ( $\text{cm}^{-1}$ )	Assignment	Wave number ( $\text{cm}^{-1}$ )	Assignment	Wave number ( $\text{cm}^{-1}$ )	Assignment
644.7	out of plane deformation of C-H	819.7 and 653	C-H out of plane bending and in-plane deformation	767	C-H out of the plane Bending vibration
1110.6	vibration mode of N=Q=N	1036	C-C ring	1021	Plane deformation
1459	C=N stretching in aromatic compounds	1459	stretching of C-N	1124	C-C stretching
1635	C=C stretching in aromatic nuclei			1460	C-N stretching
2908	C-H stretching and symmetric C-H stretching vibrations	2923	stretching of CH	1458	C=C stretching vibration
3440.5	N-H stretching	3447	stretching of N-H	1541	Benzene Ring stretching
				1644	Quinine ring stretching
				2925	C-H stretching
				3440	N-H stretching



### 5.2.3.2 Morphological analysis

The morphology of polymer blend is a determinant factor for the optical and electrical properties. Figure 5.2.2 shows the comparison of SEM images of PANI, PPy, and PPy/PANI=50:50 blends. The SEM image (fig. 5.2.2a) shows that the PANI is both amorphous and highly porous, The SEM images (fig. 5.2.2b) PPy displays a closely stacked granular structure, while PPy/PANI=50:50 blend (fig. 5.2.2c) shows a spherical like structure. The SEM image of the PPy/PANI=50:50 blend also shows that distinct changes in the morphology from that of the pure PANI and PPy polymers. This miscible blend shows interconnected crystallites in addition to porous morphology.

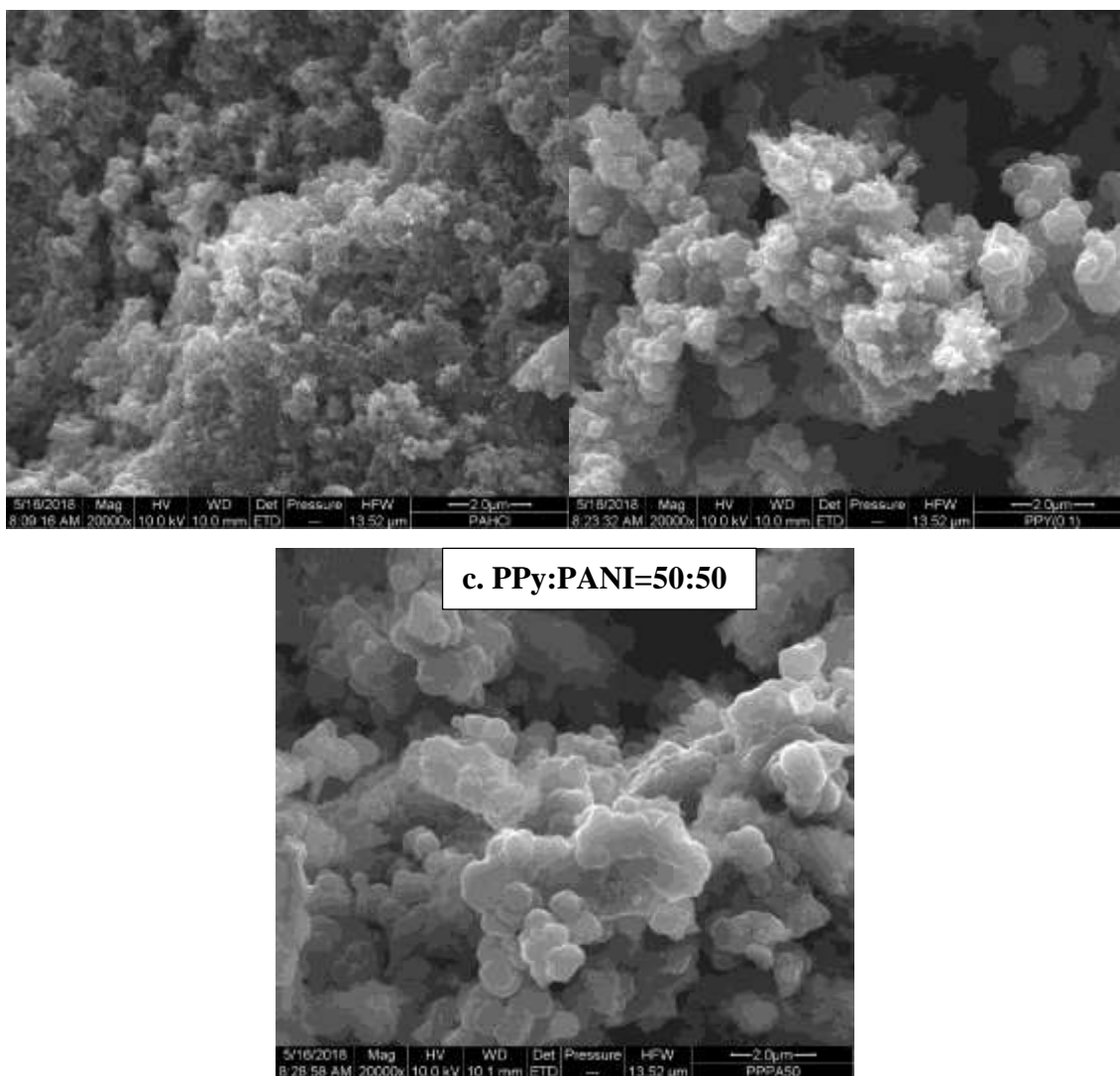


Figure 5.2.2: SEM images of the a. PANI, b. PPy and c. PPy:PANI=50:50 blend

### 5.2.3.2 The chemical composition analysis

The EDX spectra in figure 5.2.3a were confirmed that the pure PANI contains C, N, O, S, and Cl. This also confirmed by research work (Hafeez et al., 2017). The figure 5.2.3 b the spectra of pure PPy showed that the presence of elements C, N, O, Cl, and Fe. This also confirmed by (Šetka et al., 2017). The EDX spectra in figure 5.2.3 c were confirmed that the presence of elements C, N, O, S, Cl, and Fe in the blends contain. Besides, the EDX profiles indicate that the elemental compositions throughout the sample are relatively uniform. The EDX analysis shows that the signal corresponding to Sulfur appeared on the spectrum, suggested that the doping of SDS in the PPy:PANI blend. Based on the result the PPy:PANI blend has been successfully obtained.

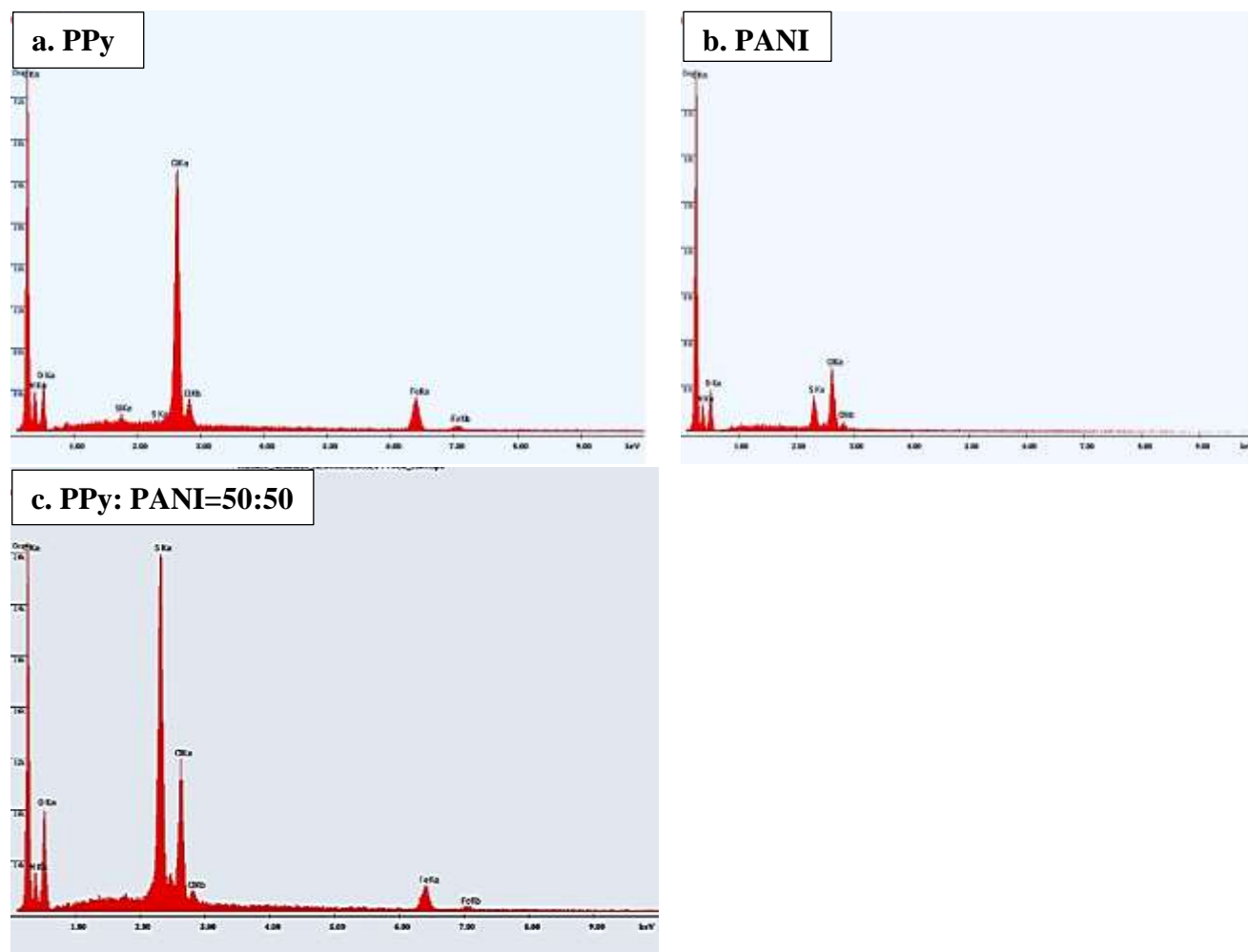


Figure 5.2.3: EDX Spectra of the a. PPy, b. PANI, and c. PPy:PANI=50:50 blend

### 5.2.3.3 UV-Vis spectrum

The optical properties of the blends are determined as usual by the UV-Vis spectroscopy. The characteristic absorption of a polymer blend should be important in the utilization of the materials in optoelectronic applications. It explained also the transition of electrons between energy levels indicating the electronic structure of materials.

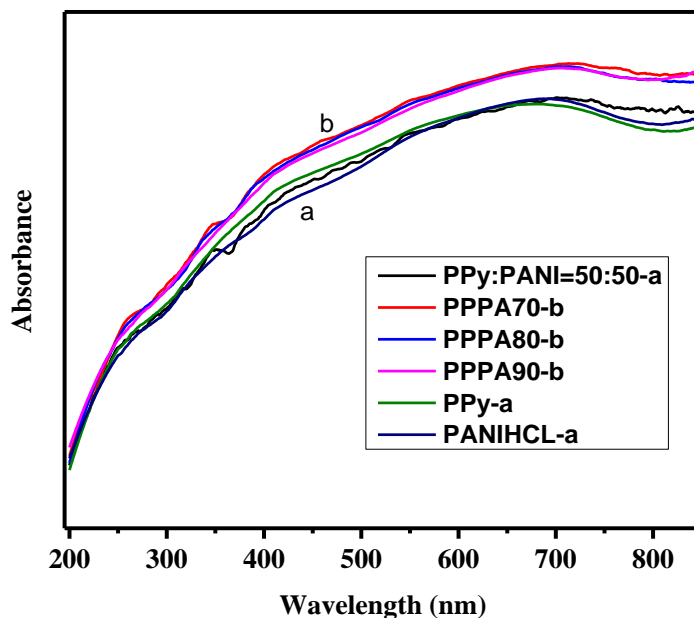


Figure 5.2.4: UV-Vis spectra of the blends PPy:PANI=50:50, PPy:PANI=70:30, PPy:PANI=80:20, PPy:PANI=90:10, PPy and PANI-HCl

Figure 5.2.4 has two parts, a and b. Figure 5.2.4a includes PPy, PANI-HCL, and PPy:PANI=50:50. Figure 5.2.4b shows each blends of PPy:PANI=70:30, PPy:PANI=80:20, PPy:PANI=90:10. The evaluation of wt. % of PANI in the blends and the assessment of the absorption result indicate that absorption decreases with increasing wt.% PANI. However, there is no significant difference at less than 30 % of PANI in the polymers blend as shown in Fig. 5.2.4b. Furthermore, the miscibility of the polymers enhances the absorption. Optical properties are observed to fall between PPy and PANI when they are blended. On the other hand, the immiscible or semi-immiscible blend with the phase separation has shown enhanced absorption. The optical properties of PPy-PANI=50:50 may change due to the presence of sulfur in a polymer. Some

researchers have been reported that the optical properties of sulfur-containing polymer (Lee et al., 2019). From the EDX analysis high contain was observed. This also modified the optical properties of the blends. In the study of (Cruz et al., 2018) have been reported that the PPy composite absorption in the visible region from 340-880 nm.

#### 5.2.3.4 Optical Band Gap

The optical bandgap of the blend polymer is determined from the absorption spectra. The photon absorption in many amorphous materials is founded to obey the Tauc model, which is given by Eq. 5.2.1 (Ghobadi, 2013):

$$\alpha hv = \beta (hv - E_g)^n \quad \text{Eq. 5.2.1}$$

where  $\alpha$  is the absorption coefficient,  $hv$  is the photon energy,  $\beta$  is a factor depending on the transition probability ( $\beta$  is assumed to be constant within the optical frequency range), and  $E_g$  is energy bandgap. The index  $n$  is related to the transition of an electron, and its value is usually  $n=1/2$  or  $2$  depending on the transition direct or indirect, respectively (Campos et al., 2014). The optical bandgap is determined by extrapolation of  $(\alpha hv)^2$  versus  $hv$  plots to the x-axis. Figure 5.2.5a and b shows the optical band gap ( $E_g$ ) values of PANI-HCl is 1.72 eV (Fig. 5.2.5a) and PPy is 1.25eV (Fig. 5.2.5b). The band gap result is closer to those reported in previous works (Veluru et al., 2013) PANI doped with Camphor Sulfonic acid (CSA) and HCl (1.57 and 1.81 eV) respectively. The optical band gap decreased from 2.32 to 1.3 eV due to  $\pi-\pi^*$  transition polarons and bipolarons states (Patel et al., 2017), (Padmapriya and Harinipriya, 2019).

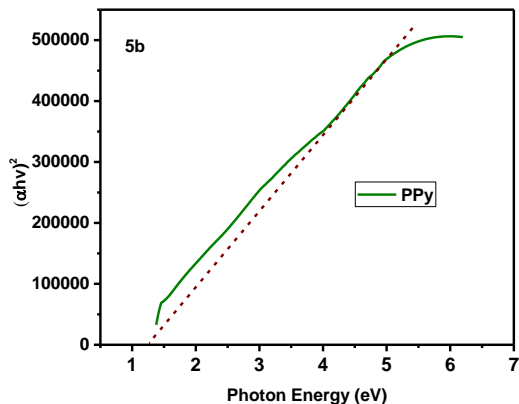
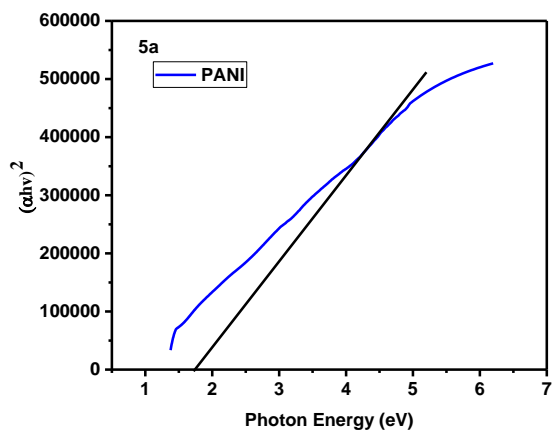
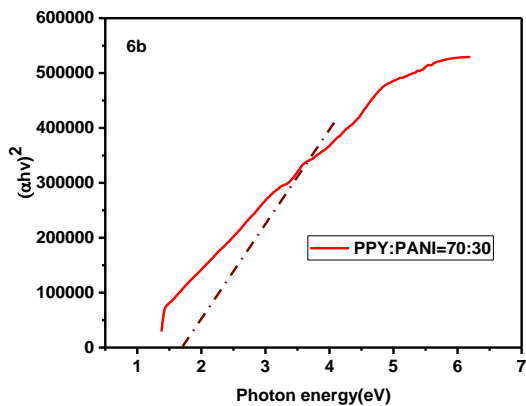
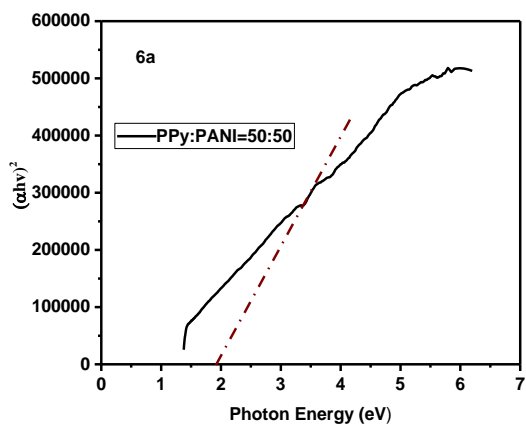


Figure 5.2.5: Plot of  $(\alpha h\nu)^2$  versus photon energy  $h\nu$  for (a) PANI and (b) PPy

Determine the optical band gap of blends polymer of different composition in figure 5.2.6 (a)PPy:PANI=50:50, (b)PPy:PANI=70:30, (c)PPy:PANI=80:20 and (d)PPy:PANI=90:10 using Tauc Model.



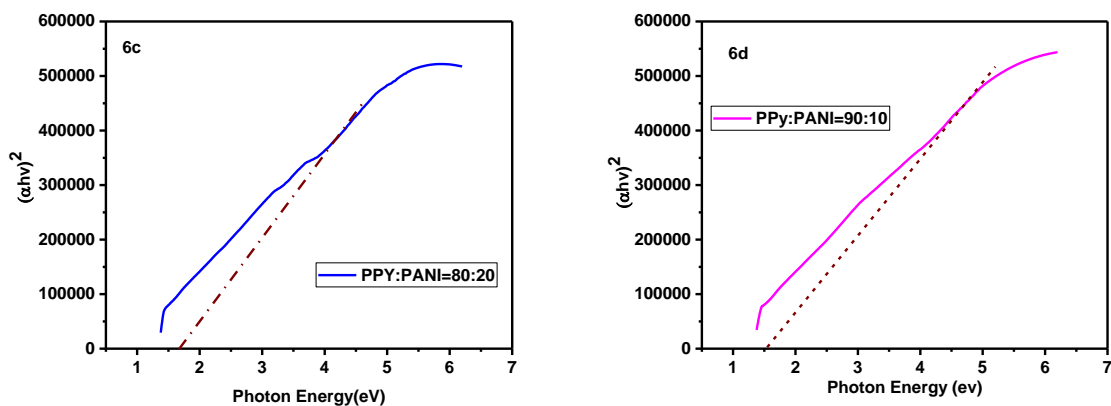


Figure 5.2.6: the band gap of blends using Tauc's models (a) PPy:PANI=50:50, (b) PPy:PANI=70:30, (c) PPy:PANI=80:20 and (d) PPy:PANI=90:10

Table 5.2.2 shows the band gap of conjugated polymers and their band gap of the blend (PPy: PANI) that is determined from Tauc models.

Table 5.2.2: The band gap of conjugated polymers and their blends using Tauc models

<b>Polymers and blends</b>	<b>Cal. Band gap (eV)</b>
<b>PANI</b>	1.72
<b>PPy</b>	1.25
<b>PPy:PANI=50:50</b>	1.95
<b>PPy:PANI=70:30</b>	1.67
<b>PPy:PANI=80:20</b>	1.68
<b>PPy:PANI=90:10</b>	1.53

### 5.2.3.5 Photoluminescence

Another interesting characterization is to study the basic excitation of organic blend materials. The photoluminescence describes the photoexcitation or light generation of the polymer blends. The broadband indicates the energy distribution corresponding to  $\pi^* \rightarrow \pi$ . In figure 5.2.7, the PL curves for the four different compositions were studied at the excitation wavelength of 320 nm.

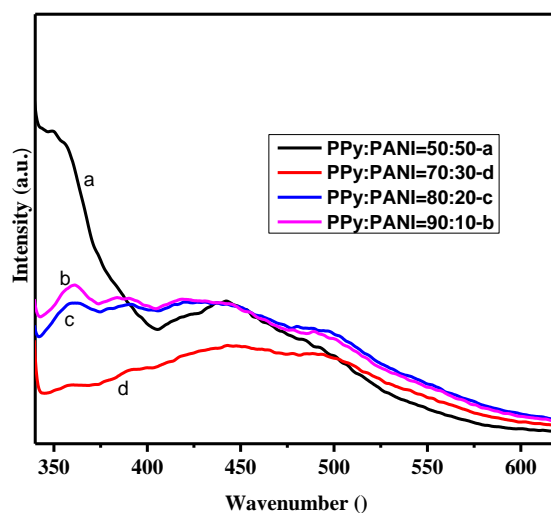


Figure 5.2.7: PL curve of blends, PPy:PANI=50:50, PPy:PANI=70:30, PPy:PANI=80:20 and PPy:PANI=90:10

The graph shows two clear intensity at 360 nm and 442 nm. The PPy:PANI=50:50 has the highest intensity peak. Also, it was observed that the polymer blends, PPy:PANI=50:50 emits light in the range of 350 -400 nm (maximum emission at about 360 nm and again emission at 442nm) and the polymer blend, PPy:PANI=70:30 at 350 nm–375 nm (maximum emission at about 360 nm). The excited electron loses its energy by collision or falls to the lowest vibrational level. From the observation of the graph in figure 5.2.7, the variation of PANI wt. % in the blend is related to the effect of miscible and immiscible polymer blends. Figure 5.2.7a shows the miscible PPy:PANI=50:50 blends, indicating stronger PL results than the other blend compositions, PPy:PANI=70:30b, PPy:PANI=90:10c and PPy:PANI=70:30d of PPY: PANI. This PL difference is considered to be resulting from the phase separation effects, which affects the luminous process and efficiency. In this study, miscibility is observed to enhance the PL process.

### 5.2.3.6 Current and Voltage (I-V) Characterization

The generated carriers during the doping process are known to be self-trapped in the conjugated polymeric chains in the form of polarons or bipolarons. Hence, the electrical conduction mechanism is a complex one and has been explained using different mechanisms such

as Mott's variable range hopping, Schottky, Poole-Frenkel, Fowler-Nordheim, space charge limited current (SCLC), and tunneling conduction (Lim and Ismail, 2015). Considering the purpose of this work, the researcher explains the behavior of the I-V-T characteristics of the blend PANI-DBSA/poly(acrylonitrile-butadiene-styrene) (ABS), using the existing electrical conduction models to determine the predominant charge transport mechanism (Kipnusu et al., 2009), (Cristovan et al., 2009). The electrical conductivity of PPy is the most important property for practical applications. Schottky diodes in organic electronics are expected to have a non-linear J-V curve. The J-V characteristics are described by different processes, according to the values of the electrical currents. The electrical measurements as a function of temperature were recorded using Keithley-2400 source meter with a probe station by applying a DC voltage ranging from -10V to 10V. Various models are applied to explain different transport mechanisms in organic semiconductors at different modes of the supplied voltage. Among them, two models are used most frequently to explain the J-V characteristics: (a) the trapping model with space-charge-limited current (SCLC) and (b) the field-dependent mobility model (Röhr et al., 2018), (Liu et al., 2017). The J-V curve important to describe traps, kind of rectification, and models of transport.

The PANI doped with HCl is showed non-linear and slight asymmetric characteristics as shown in figure 5.2.8. This behavior is common in organic semiconductors. The applied voltage is changed from -7 to +7 V. In both forward and reverse bias region, the current is directly proportional to the applied voltage. The spectrum reveals that the current increases with an increase in the voltage. The current increases rapidly up to the saturation point and then increases slowly. The current-voltage relationship is  $I-V^n$ .



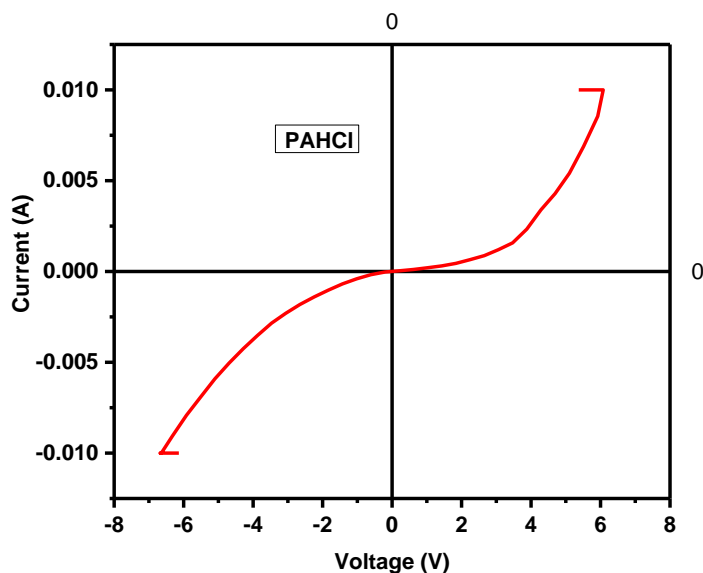


Figure 5.2.8: J-V curve PANI

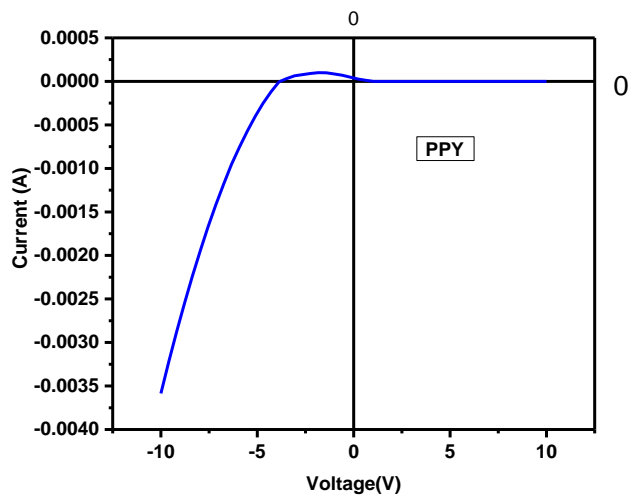


Figure 5.2.9: J-V curve PPY

Figure 5.2.9 shows relatively linear I-V at the range of -10V to -3V and saturation reached (switched off) occur above -3V. Besides, it also displays that the I-V characteristics between -10V to -3V is linear and the corresponding exponent 'n' for this region is around 1. Traps at locations is considered to be originated from disorders, dangling bonds, impurities, etc., which is called localized states, often capturing free charge carriers.

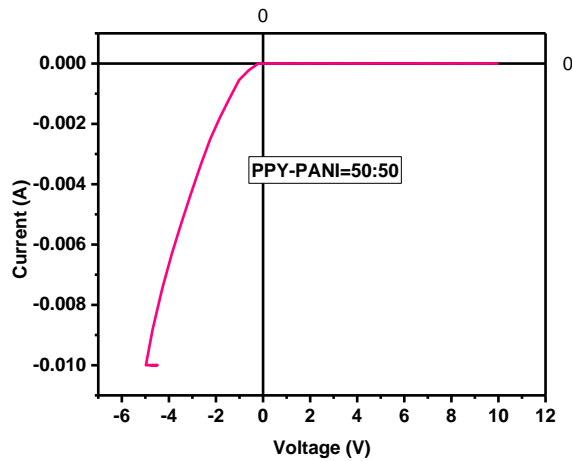


Figure 5.2.10: The J-V characteristics of Blends PPY: PANI= 50:50

The blend PPY-PANI=50:50 in Fig. 5.2.10 shows relatively linear I-V at the range of -5V to -1V and then saturation (switched off) occurs above -1V. Fig. 5.2.10 reveals that the I-V characteristics between -5V to -1V are linear and the corresponding exponent ‘n’ for this region is around 1. The analysis was done by log scale,  $\ln J - \ln V$ , and the curve was described by  $J - V^n$ , in which the value of n was determined from the slope of the double logarithmic and the value is  $n=0.83$ . Most frequently, an exponential distribution of traps in the energy band is assumed.

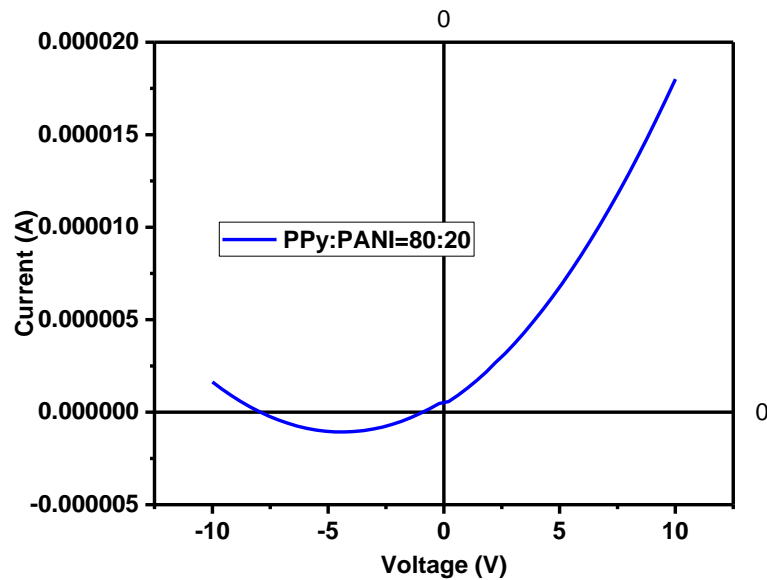


Figure 5.2.11: The J-V characteristics of Blend PPy:PANI=80:20

Figure 5.2.11 shows that non-ohmic region, I-V curve of PPy:PANI=80:20 blend, which confirms that there is a non-ohmic junction in the device. This non-ohmic behavior of conduction is reported to be governed by such processes as space charge limited current (SCLC) mechanism. Hence, the J-V curve could be characterized by  $J-V^n$ , in which the value of n is determined from the slope of the double logarithmic, and the value is  $n=6/5$ .

#### 5.2.4 Electrical conductivity

Electrical conductivity is an important property to understand the mechanism of electrical conductivity of conducting polymer and to design their application. Because conducting polymer exhibits insulator to conductor during acid treatment. Nonetheless, for many applications higher conductivity is not significant.

The conductivity of the polymer sample was calculated from the slope of the current-voltage curves. The conductivity of conductive pressed polymer is measured according to the following equations 5.2.2 and 5.2.3(Çolak and Sökmen, 2000), (Bose et al., 2011):

$$\rho = \frac{\pi t}{\ln 2} R \text{-----} 5.2.2$$

Where  $\rho$  is the resistivity, t is the thickness of the sample, and R is the resistance.

$$\delta = \frac{1}{\rho} \text{-----} \text{eq 5.2.3}$$

Where  $\delta$  is electrical conductivity in ( $\text{S.cm}^{-1}$ ),  $\rho$  is the resistivity sample.

The conductivity computed by using equation 5.2.3 and the corresponding value is given in Table 5.2.3. The blend samples PPy-PANI=50:50 has the highest conductivity value observed  $3.67 \times 10^{-3} \text{ S.cm}^{-1}$  at room temperature. This may happen due to the blending, the interchain interaction was formed between PPy and PANI. The result was showed higher conductivity than both the pure PPy and PANI ( $7.73 \times 10^{-4}$  and  $3.48 \times 10^{-3} \text{ S.cm}^{-1}$ ) respectively. Here the PPy may be due to relatively soluble polypyrrole (Hammed et al., 2017). In the previous work (Jangid, 2019) have been reported undoped and doped polyaniline in the order of magnitude  $10^{-10}$  and  $10^1 \text{ S.cm}^{-1}$ . The PPy-PANI=50:50 higher conductivity compared to the research work reported by (Jangid,

2019) that the conductivity of doped PANI with H<sub>2</sub>SO<sub>4</sub> and Dodecylbenzene sulfonic acid both in the order of magnitude 10<sup>-8</sup> S.cm<sup>-1</sup>. In the study (Shaktawat et al., 2008) have reported the conductivity of PPy doped with Phosphoric acid and sulfuric acid (1.96\*10<sup>-2</sup> and 3.26\*10<sup>-6</sup> S.cm<sup>-1</sup>) respectively. Also, (Hernández de la Cruz et al., 2018) have been reported that PPy doped by sodium dodecyl sulfate (SDS). In early work (Rahaman et al., 2018) have been reported that the nature of the solvent also affects the conductivity of the prepared PPy. It has been shown that electrochemically synthesized PPy doped with di(2-Ethylhexyl) sulfosuccinate (DEHS) displays conductivity from 1.0×10<sup>-4</sup> S/cm, using methyl alcohol as a solvent, and 6.6×10<sup>-2</sup> S/cm, using oleyl alcohol. The blend materials PPy-PANI=50:50 higher conductivity compared to sulfuric acid doped PPy. Furthermore, it was closer to the report indicated in (Velhal et al., 2014), that have been reported the conductivity of PPy/PANI composite in the order of 10<sup>-3</sup> S.cm<sup>-1</sup>.

Table 5.2.3: Conductivity of Pure PPy, PANI and Blend

<b>Sample</b>	<b>Conductivity (S.cm<sup>-1</sup>)</b>
<b>PPy</b>	7.73*10 <sup>-4</sup>
<b>PANI</b>	3.48*10 <sup>-3</sup>
<b>PPy-PANI=50:50</b>	3.67*10 <sup>-3</sup>
<b>PPy-PANI=70:30</b>	4.61*10 <sup>-5</sup>
<b>PPy-PANI=80:20</b>	2.20*10 <sup>-6</sup>
<b>PPy-PANI=90:10</b>	4.20*10 <sup>-5</sup>

### 5.2.5 Conclusion

Polymer semiconductor materials (PPy/PANI blends) were successfully developed from the solution process. Then, through the electrical characterization, we observed that the PPy/PANI blend is a semiconductor by showing the conductivity in the range of 10<sup>-6</sup> to 10<sup>-3</sup> S/cm at room temperature. The UV-vis absorption spectra showed broad absorption as expected from their bandgap. Using the Tauc model, the optical bandgap of each blend material was determined, which was 1.53-1.95 eV. The composition of PANI was observed to do an important role in the bandgap of the PPy/PANI blend. Increasing the wt. % of PANI in the blend system increases the band gap of the materials. Finally, based on the value of the optical bandgaps, the electrical conductivities,

and the processibility of the PPy/PANI blend, we expect that our blends could be applied to a semiconductor device as a component in polymer electronics.

## References:

- AL-DAGHMAN, A. 2016. *EFFECT OF DOPING BY STRONGER IONS SALT ON THE MICROSTRUCTURE OF CONDUCTIVE POLYANILINE-ES: STRUCTURE AND PROPERTIES*.
- BHAVSAR, V. & TRIPATHI, D. 2016. Study of refractive index dispersion and optical conductivity of PPy doped PVC films. *Indian Journal of Pure and Applied Physics*, Vol. 54.
- BOSE, S., KIM, N. H., KUILA, T., LAU, K. T. & LEE, J. 2011. Electrochemical performance of a graphene-polypyrrole nanocomposite as a supercapacitor electrode. *Nanotechnology*, 22, 295202.
- CAMPOS, M., MIZIARA, T. A. S., CRISTOVAN, F. H. & PEREIRA, E. C. 2014. Investigations of the electrical conduction mechanisms of polyaniline-DBSA/poly(acrylonitrile-butadiene styrene) blends. 131.
- ÇOLAK, N. & SÖKMEN, B. 2000. Doping of chemically synthesized polyaniline. *Designed Monomers and Polymers*, 3, 181-189.
- CRISTOVAN, F., LEMOS, S. & PEREIRA, E. 2009. Systematic Evaluation of the Preparation of Conducting PANI/ABS Blends. *Journal of Applied Polymer Science*, 116, 825-831.
- CRUZ, T., TENORIO, C., CASTAÑEDA, M., SAAVEDRA, H. & SÁNCHEZ, J. 2018. Effects produced by sodium dodecyl sulfate (SDS) surfactant on polypyrrole film electrochemically synthesized and doped with glow discharge plasma. *MRS Advances*, 3, 1-8.
- GHOBADI, N. 2013. Band gap determination using absorption spectrum fitting procedure. *International Nano Letters*, 3, 2.

- HAFEEZ, M., FAHEEM, M., ABDIN, Z., AHMAD, K., FAZIL, S. & KHAN, B. 2017. Synthesis and characterization of polyaniline-based conducting polymer and its anti-corrosion application. *Digest Journal of Nanomaterials and Biostructures*, 12, 707-717.
- HAMMED, W. A., RAHMAN, M. S., MAHMUD, H. N. M. E., YAHYA, R. & SULAIMAN, K. 2017. Processable dodecylbenzene sulfonic acid (DBSA) doped poly(N-vinyl carbazole)-poly(pyrrole) for optoelectronic applications. *Designed Monomers and Polymers*, 20, 368-377.
- HERNÁNDEZ DE LA CRUZ, T., HERNÁNDEZ TENORIO, C., VILLANUEVA CASTAÑEDA, M., MORENO SAAVEDRA, H. & PACHECO SÁNCHEZ, J. H. 2018. Effects produced by sodium dodecyl sulfate (SDS) surfactant on polypyrrole film electrochemically synthesized and doped with glow discharge plasma. *MRS Advances*, 3, 3839-3846.
- JANGID, N. 2019. Recent advancement in synthesis and properties of Polyaniline. *International Journal of Innovative Research in Computer and Communication Engineering*, 8, 3751-3772.
- KALONI, T. P., SCHRECKENBACH, G. & FREUND, M. S. 2015. Structural and Electronic Properties of Pristine and Doped Polythiophene: Periodic versus Molecular Calculations. *The Journal of Physical Chemistry C*, 119, 3979-3989.
- KIPNUSU, W., KATANA, G., MIGWI, C., RATHORE, I. V. & SANGORO, J. 2009. Charge Transport Mechanism in Thin Cuticles Holding Nandi Flame Seeds. *International journal of biomaterials*, 2009, 548406.
- LEE, J. M., NOH, G. Y., KIM, B. G., YOO, Y., CHOI, W. J., KIM, D.-G., YOON, H. G. & KIM, Y. S. 2019. Synthesis of Poly(phenylene polysulfide) Networks from Elemental Sulfur and p-Diiodobenzene for Stretchable, Healable, and Reprocessable Infrared Optical Applications. *ACS Macro Letters*, 8, 912-916.
- LIM, E. W. & ISMAIL, R. 2015. Conduction Mechanism of Valence Change Resistive Switching Memory: A Survey. *Electronics*, 4, 586-613.
- LIU, C., HUANG, K., PARK, W.-T., LI, M., YANG, T., LIU, X., LIANG, L., MINARI, T. & NOH, Y.-Y. 2017. A unified understanding of charge transport in organic semiconductors: the importance of attenuated delocalization for the carriers. *Materials Horizons*, 4, 608-618.

- MAHMUD EKRAMUL, ANUAR KASSIM, ZAINALA, Z. & YUNUS, W. M. M. 2005. Electronic conducting polymer composite films with enhanced mechanical properties. *ScienceAsia*, 31, 313-317.
- MIZOBUCHI, H., KAWAI, T., ARAKI, H., YAMASAKI, N., YOSHIMO, K. & SAKAMOTO, A. 1995. Unique pH dependent optical and magnetic properties of self-doping type copolymers of aniline and aminonaphthalene derivatives with sulfonic groups. *Synthetic Metals*, 69, 239-240.
- PADMAPRIYA, S. & HARINIPRIYA, S. 2019. Hydrogen storage capacity of polypyrrole in alkaline medium: effect of oxidants and counter anions. *Journal of Materials Research and Technology*, 8.
- PATEL, A., PATANIYA, P., PATEL, K. D., SOLANKI, G. K., PATHAK, V. M., S., P. H., R., R. J., D., P. K., M., P. V. & R., S. 2017. Preparation of H<sub>2</sub>SO<sub>4</sub> doped Polyaniline thin film solar cells by spin coating technique MoSe<sub>2</sub> / POLYANILINE SOLAR CELLS. 1837, 040047.
- QIN, Q. & GUO, Y. 2012. Preparation and Characterization of Nano-Polyaniline Film on ITO Conductive Glass by Electrochemical Polymerization. *Journal of Nanomaterials*, 2012.
- RAHAMAN, M., ALDALBAHI, A., ALMOIQLI, M. & ALZAHLY, S. 2018. Chemical and Electrochemical Synthesis of Polypyrrole Using Carrageenan as a Dopant: Polypyrrole/Multi-Walled Carbon Nanotube Nanocomposites. *Polymers*, 10, 632.
- RÖHR, J. A., SHI, X., HAQUE, S. A., KIRCHARTZ, T. & NELSON, J. 2018. Charge Transport in Spiro-OMeTAD Investigated through Space-Charge-Limited Current Measurements. *Physical Review Applied*, 9, 044017.
- SADROLHOSSEINI, A., ABDUL RASHID, S., MUHAMMAD NOOR, A. S., KHARAZMI, A., LIM, H. & MAHDI, M. A. 2016. Optical Band Gap and Thermal Diffusivity of Polypyrrole-Nanoparticles Decorated Reduced Graphene Oxide Nanocomposite Layer. *Journal of Nanomaterials*, 2016, 1-8.
- ŠETKA, M., DRBOHLAVOVÁ, J. & HUBÁLEK, J. 2017. Nanostructured Polypyrrole-Based Ammonia and Volatile Organic Compound Sensors. 17, 562.
- SHAKTAWAT, V., SAXENA, N., SHARMA, K. & SHARMA, T. 2008. Structural and Electrical Characterization of Protonic Acid Doped Polyaniline. *AIP Conference Proceedings*, 1004, 241-246.

- SHRIKRUSHNA, S. & KULKARNI, J. 2015. Influence of Dodecylbenzene Sulfonic Acid Doping on Structural, Morphological, Electrical and Optical Properties on Polypyrrole/3C-SiC Nanocomposites. *Journal of Nanomedicine & Nanotechnology*, 06.
- SU, N. 2015. Improving Electrical Conductivity, Thermal Stability, and Solubility of Polyaniline-Polypyrrole Nanocomposite by Doping with Anionic Spherical Polyelectrolyte Brushes. *Nanoscale Research Letters*, 10, 301.
- TAHALYANI, J., RAHANGDALE, K. & KANDASUBRAMANIAN, B. 2016. The dielectric properties and charge transport mechanism of  $\pi$ -conjugated segments decorated with intrinsic conducting polymer. *RSC Adv.*, 6, 69733-69742.
- TIKISH, T. A., KUMAR, A. & KIM, J. Y. 2018. Study on the Miscibility of Polypyrrole and Polyaniline Polymer Blends %J *Advances in Materials Science and Engineering*. 2018, 5.
- TRIVEDI, D. C. 1999. Influence of counter ion on polyaniline and polypyrrole. *Bulletin of Materials Science*, 22, 447-455.
- TUNCEL, D. & DEMIR, H. V. 2010. Conjugated polymer nanoparticles. *Nanoscale*, 2, 484-494.
- VELHAL, N., PATIL, N., JAMDADE, S. & PURI, V. 2014. Studies on galvanostatically electropolymerised polypyrrole/polyaniline composite thin films on stainless steel. *Applied Surface Science*, 307, 129-135.
- VELURU, J. B., VEMPATI, S. & RAMAKRISHNA, S. 2013. Conducting Polyaniline-Electrical Charge Transportation. *Materials Sciences and Applications*, 04, 1-10.
- WANG, J., LI, X., DU, X., WANG, J., MA, H. & JING, X. J. C. P. 2017a. Polypyrrole composites with carbon materials for supercapacitors. 71, 293-316.
- WANG, Q., WANG, Y., MENG, Q., WANG, T., GUO, W., WU, G. & YOU, L. 2017b. Preparation of high antistatic HDPE/polyaniline encapsulated graphene nanoplatelet composites by solution blending. *RSC Adv.*, 7, 2796-2803.
- XING, S., ZHAO, C., ZHOU, T., JING, S. & WANG, Z. 2007. Preparation and characterization of polyaniline-polypyrrole composite from polyaniline dispersions. *Journal of Applied Polymer Science*, 104, 3523-3529.
- YUNINGSIH, L. M., MULYADI, D. & ARIPANDI, I., 2017. Effect of Various Dopant HCL Concentration on Electrical Conductivity of Pani-Cellulose Composite with Cellulose Isolated from Reed Plant (*Imperatacy lindrica* (L.)). *American Journal of Materials Science*, 7(3), 59-63.



- YUSSUF, A., AL-SALEH, M., AL-ENEZI, S. & ABRAHAM, G. 2018. Synthesis and Characterization of Conductive Polypyrrole: The Influence of the Oxidants and Monomer on the Electrical, Thermal, and Morphological Properties. *International Journal of Polymer Science*, 2018, 1-8.
- ZHANG, D.-Q., YANG, X., CHENG, J., LU, M., ZHAO, B. & CAO, M. 2013. Facile Preparation, Characterization, and Highly Effective Microwave Absorption Performance of CNTs/Fe<sub>3</sub>O<sub>4</sub>/PANI Nanocomposites. *Journal of Nanomaterials*, 2013, 1-7.

## Chapter Six

### The Polypyrrole-Polyaniline (PPy-PANI) Blend Electrode Material for Energy Storage

#### Abstract

This chapter described the deposition of polypyrrole (PPy), polyaniline (PANI), and PPy/PANI blend thin film on indium tin oxide (ITO) substrate through the drop-casting method, and then the conducting polymer electrodes were tested for the electrochemical supercapacitor electrodes. Cyclic voltammetry (CV) showed that the PPy/PANI blend has an ideal capacitive behavior. Electrochemical impedance spectroscopy (EIS) proved that the PPy/PANI=50:50 blend electrode with 0.01 M sodium dodecyl sulfate (SDS) has a low equivalent series resistance (ESR) without any semicircle in Nyquist plot. Importantly, the galvanostatic charge-discharge (GCD) measurements exhibited that the blend electrode has a high specific capacitance of 134.36 F/cm at 0.1 mA/cm<sup>2</sup>. Therefore, the PPy/PANI blend electrode should be promising as a component for the electrochemical supercapacitor.

#### 6.1 Introduction

Conducting polymers such as polyaniline (PANI) and polypyrrole (PPy) have been studied extensively for the pseudocapacitor application owing to their low cost, fast redox rate, ease of synthesis, and high theoretical capacitance (Lin et al., 2013), (Shen et al., 2015), (Liu et al., 2014). Specifically, during the last two decades, there has been considerable expansion of studies in the field of  $\pi$ -conjugated polymers. The reason is that they could be used as active materials in light-emitting diodes (LED), organic photovoltaics (OPV), field-effect transistor (FET) and electrochromic devices. Extensive and systematic investigations revealed that the chemical structure of polymers plays an important role in the properties of these materials based on structure-property relationship (Camurlu et al., 2013). Another researcher (Haihua et al., 2013) reported that PANI could be promising as a component for an electrochemical supercapacitor based on its excellent properties such as high power density and energy density. In the case of PPy,

it has been also one of the most extensively studied materials with PANI because it is easy to synthesize PPY and simultaneously it has a good redox property. Therefore, PPY could be applied to batteries, artificial muscles, supercapacitors, sensors, microwave shielding, etc. (Sardar et al., 2018). PPY is also known to have a high capacitance (Wang et al., 2019).

However, PPY and PANI have some fatal drawbacks such as low conductivity, limited transport rate of anions, and poor stability due to the structural degradation through electrode redox processes. Therefore, it was proposed that the composite electrode based on carbon and conducting polymer should be advantageous for enhanced performance in terms of capacitance (Shen et al., 2015) In a similar vein, several research groups have developed the composite electrode by mixing conducting polymer with metal oxide or graphene. These versatile composite approaches based on organic-inorganic nanocomposite were investigated to improve the performance of these homopolymers for their applications in energy storage devices such as batteries and supercapacitors (Reddy et al., 2018; Maiti, 2014). Furthermore, some researchers (Myasoedova et al., 2016) have studied the properties of PANI when it was blended with saturated polymers such as polyvinyl alcohol (PVA), polyethylene oxide (PEO), and poly(methyl methacrylate) (PMMA). Others (Kulandaivalu et al., 2019) demonstrated that the PPY/graphene oxide(GO)/PPy:MnO<sub>2</sub>-based supercapacitor have a high specific capacitance of 786.6 F/g as well as a good cyclic stability. In the report of (Ma et al., 2018), they fabricated a flexible supercapacitor based on a three-dimensional Co<sub>3</sub>O<sub>4</sub>/PPy nanorods bundle arrays on carbon fiber cloths (CFCs). The Co<sub>3</sub>O<sub>4</sub>/PPy electrode exhibited a high capacitance of 6.67 F/cm at a current density of 2 mA/cm<sup>2</sup> and 2.47 F/cm<sup>2</sup> at 4 mA/cm<sup>2</sup>, respectively. Interestingly, some researchers (Yin et al., 2019) reported the nanostructural PPY nanowires with ordered large mesopores through a simple chemical polymerization method. Herein, they utilized some templates incorporating self-assembled silica nanospheres in porous anodic aluminum oxide (AAO) membrane channels, which showed a large surface area (231.5 m<sup>2</sup>/g), high aspect ratio, and interconnected large mesopores (~23 nm). Furthermore, some research groups (Wang, 2016) synthesized poly(aniline-co-pyrrole) (PANPY) copolymer in a mixed acid solution using an electrochemical method, and pointed out the importance of the molar ratio between aniline and pyrrole monomers from the viewpoint of the electrochemical performances. For examples, when the molar concentration ratio is aniline: pyrrole = 1:1, the specific capacity was 227.88 F/g at a current density of 4 mA/cm. Hence,

PANPY copolymer materials could be used as a component for electrochemical supercapacitors. Interestingly, some reserachers (Zhang et al., 2011) fabricated a PPy/PANI composite through the two-step electrochemical polymerization, indicating that this PPy/PANI composite showed better electrochemical capacitance than a single PPy or PANI. The specific capacitance of this composite electrode was 523 F/g at a current of 6 mA/cm<sup>2</sup> in 0.5 M H<sub>2</sub>SO<sub>4</sub> electrolyte.

In this study, the homopolymers (PPy and PANI) and their PPy/PANI blends were dissolved in a solvent, dimethyl sulfoxide (DMSO). And then, each polymer solution or dispersion was poured on the top of indium tin oxide (ITO) glass for fabricating a drop-cast film. Then, the prepared film samples were characterized through electrochemical methods.

## 6.2 Methods

The PPy, PANI, and their blend (PPy/PANI) were each deposited on the ITO/glass substrate by using a drop-casting method. For this process, the ITO substrates were consecutively cleaned in deionized (DI) water, detergent, and acetone. Then, they were sonicated (Branson 2500) for 15 min, and additionally cleansed with isopropanol alcohol (IPA) for additional 15 min and then finally dried by air. For the electrochemical measurements such as cyclic voltammetry, three electrodes (i.e., working, counter, and reference) were used as usual. Then drop-cast films were characterized at different scan rates in an electrolyte solution of 0.5 M H<sub>2</sub>SO<sub>4</sub>.

## 6.3 Result and Discussion

Table 6.1: The blend composition

<b>Polymer Mixture (wt.%)</b>
PPy: PANI = 0:100
PPy: PANI = 100:0
PPy: PANI = 50:50
PPy: PANI = 70:30
PPy: PANI = 80:20
PPy: PANI = 90:10
PPy: PANI = 50:50 + 0.01 SDS
<b>PPy: PANI = 50:50 + 0.05 SDS</b>

### 6.3.1 Electrochemical Characterization

The cyclic voltammetry (CV) measurement was carried out to evaluate the electrochemical behavior of PPy, PANI and PPy/PANI blend. Fig 6.1 shows the electrochemical behavior of pure PANI, pure PPy, and PPy/PANI blends as a function of composition. Here, the scan rates were 10, 50, 100, and 200 mV/sec. The potential range for this experiment was maintained between  $-0.4$  and  $+0.7$ V (or  $+0.8$  V or  $+1.0$  V) depending on electrochemical behavior.

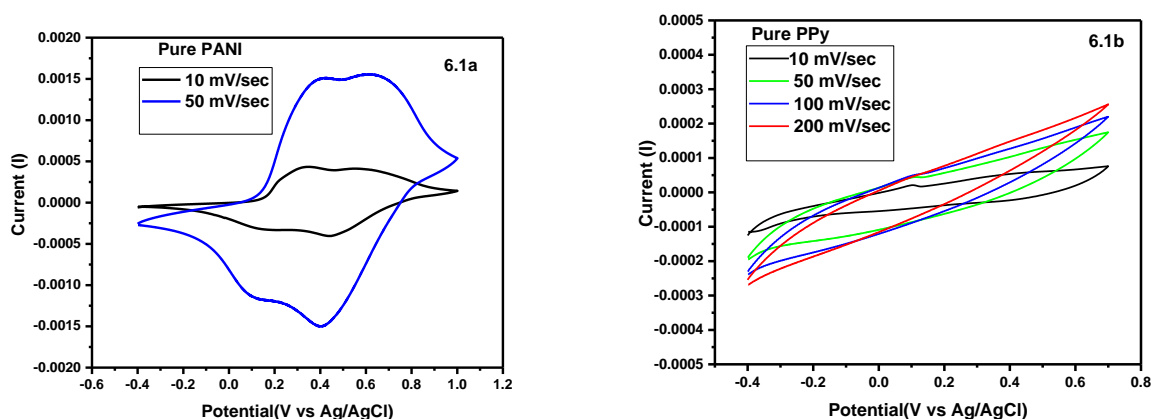


Figure 6.1: Cyclic voltammograms of (a) pure PANI and (b) pure PPy.

The shape of the CV curve in Fig 6.1a shows a partial reversibility of ‘Pure PANI’ sample. Specifically, the two broad anodic peaks were observed at 0.4 and 0.7 V, whereas the cathodic peaks were at around 0.1 and 0.4 V, respectively, indicating the presence of two main redox couples. In literature reports, the oxidation peaks of PANI were observed at 0.31V and 0.72V in the forward scan, and the corresponding reduction peaks were at 0.09 V and 0.48V, respectively, (Haihua et al., 2013), indicating that the author’s report and theirs are in good agreement. Furthermore, it is noteworthy that the aforementioned two peaks are related to the transition of leucoemeraldine/emeraldine and emeraldine/pernigraniline of PANI (Zhang et al., 2018). In Fig. 6.1b shows the CV curves of ‘Pure PPy’ samples, which displayed that PPy has only electric double layer capacitance (EDLC) in this potential range, i.e., without any pseudocapitance. This result is correspondent the literature report, in which PPy showed a rectangular shape only without obvious redox peaks (Wang et al., 2016).

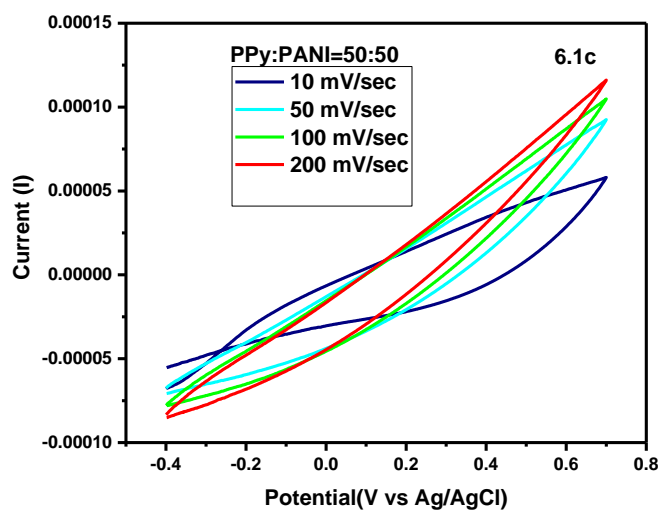


Figure 6.1c: Cyclic voltammograms of the PPY:PANI = 50:50 blend samples

Fig. 6.1c shows the CV curves of the ‘PPy:PANI = 50:50’ blend sample. As shown in Fig. 6.1c, although the blend sample contains PANI, the CV curve is very similar to that of pure PPy sample in Fig. 6.1b. This observation indicates that PPy:PANI = 50:50 blend sample can be used as an electrode materials for EDLC supercapacitor instead of pseudo-supercapacitor because there is no observation of redox behavior. Note that the carbon bundle fiber(CBF)/PPy or CBF/PPy/reduced graphite oxide (GO) also showed pseudo-rectangular-shaped cyclic voltammogram without any observable redox peaks at a scan rate of 100 mV/sec, indicating a good capacitive behavior for the EDLC supercapacitors (Abdul Bashid et al., 2017).

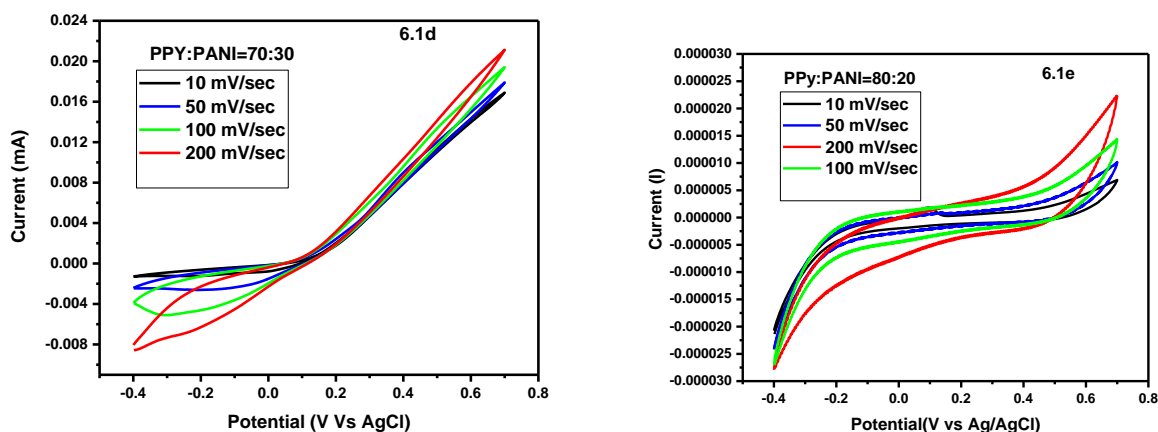


Figure 6.1: Cyclic voltammograms of (d) PPY:PANI = 70:30 and (e) PPY:PANI= 80:20 blend samples

Figure 6.1d shows the electrochemical behavior of the ‘PPy:PANI= 70:30’ blend sample, whereas Fig. 6.1e displays that of the ‘PPy: PANI = 80:20’ blend sample. Here, although two blends have the same materials, PPy and PANI, they showed the different shapes of CV curves, indicating that the internal 3-dimensional morphologies (i.e., not simply composition only) of each blend film may give effects on the electrochemical behavior of a film. Specifically, Fig. 6.1e is a typical behavior of EDLC supercapacitor observed in supercapacitors with carbon-based electrodes (Mousa et al., 2017). Finally, Fig 6.1f shows the electrochemical behavior of the ‘PPy:PANI = 90:10’ blend sample. Herein, a long narrow spiky shape was observed, which is relatively similar to Fig. 6.1d. Although, based on 90% PPy in the ‘PPy:PANI = 90:10’ blend sample, the CV curve for this blend was expected to be similar to that of ‘Pure PPy’ sample (Fig. 6.1b), the results were not like that, indicating that the internal morphologies of drop-cast films might give a significant effect on the electrochemical behavior as mentioned before in Fig. 6.1d.

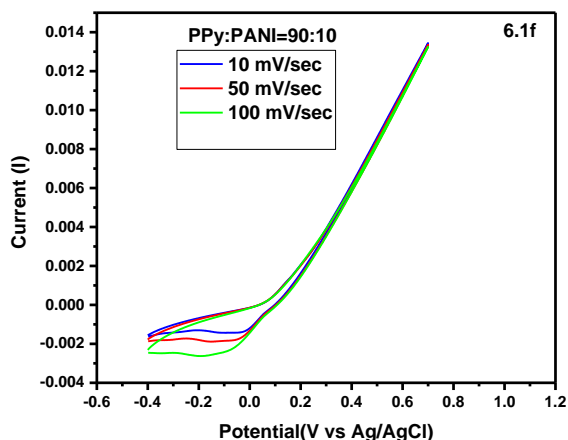


Figure 6.1f: Cyclic voltammograms of PPy:PANI = 90:10 blend sample.

Importantly, the effect of anionic surfactant sodium dodecyl sulfate (SDS) on the electrochemical behavior for the ‘PPy:PANI = 50:50’ blend sample was investigated. Figure 6.2 shows the CV curve of the ‘PPy:PANI = 50:50’ blend sample when SDS (0.01 or 0.05 M) was incorporated in the blend sample. As shown in Fig. 6.2a and b, the both blend films displayed the redox behavior, which is very different from the CV curves in Fig. 6.1c (i.e., the PPy:PANI = 50:50’ blend sample without SDS). Hence, the author conclude that, if there is a surfactant, SDS

in a blend film, PANI polymeric chains are 3-dimensionally well distributed in a blend film, which allows redox behavior to be observed, leading to additional pseudocapacitance in addition to EDLS observed in Fig. 6.1c. In details, the CV curve of ‘PPy:PANI= 50:50 + 0.05 SDS’ blend sample showed a similar redox behavior with ‘PPy:PANI = 50:50 + 0.01 SDS’. However, the former exhibited a larger area compared with the latter, indicating that a sufficient amount of SDS should be helpful for the distribution of PANI in a PPy:PANI blend film. Note that PANI-Fe<sub>2</sub>O<sub>3</sub> composite also showed a similar redox behavior observed in Fig. 6.2 (Letti et al., 2017). In general, both the non-rectangular nature and the observed redox peaks in the CV curves indicate that there is a significant deviation from the ideal EDLC behavior, i.e., the presence of additional pseudocapacitance (Mousa et al., 2017).

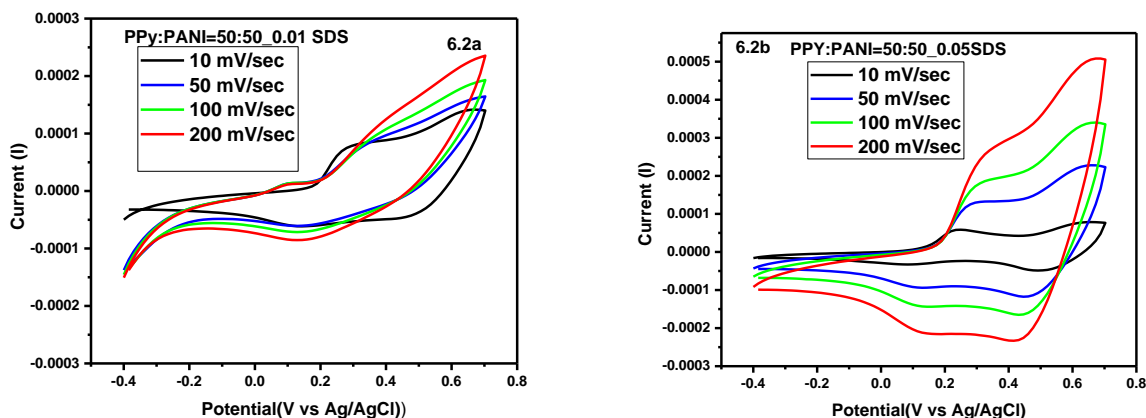


Figure 6.2: Cyclic voltammograms of (a) PPy:PANI = 50:50 with 0.01 M SDS and (b) PPy:PANI = 50:50 with 0.05 M SDS.

### 6.3.2 Galvanostatic Charge-Discharge (GCD)

The charge-discharge behavior for the supercapacitor device was characterized at a constant current. Here, the area of working electrode was 0.35 cm<sup>2</sup>. The current (i) applied to working electrode was calculated to be 0.35 cm<sup>2</sup> × 0.1 mA/cm<sup>2</sup> when the constant current was 0.1 mA/cm<sup>2</sup>. Here, the constant current could be 0.1, 0.2, 0.4 and 0.8 mA/cm<sup>2</sup>, respectively.

$$i = 0.35 \text{ cm}^2 \times 0.1 \text{ mA/cm}^2$$



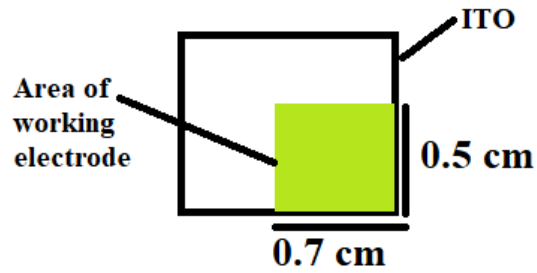
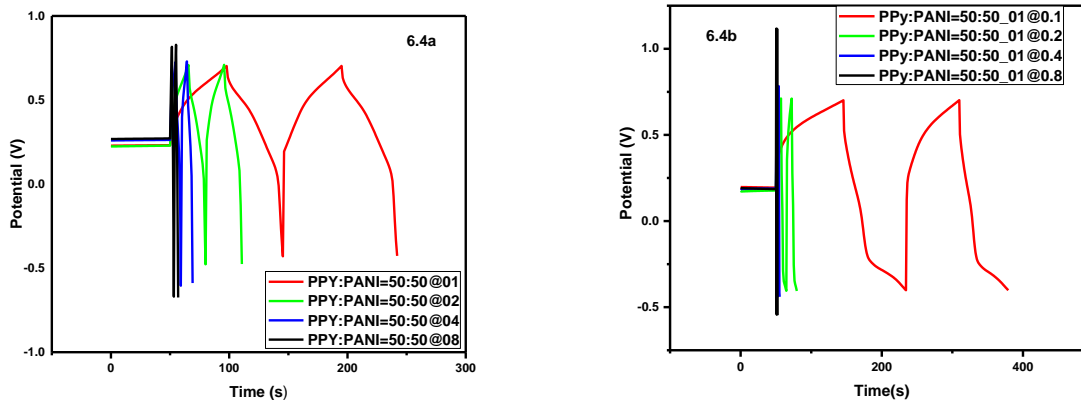


Figure 6.3: The area of the working electrode

Figure 6.4 shows the galvanostatic charge-discharge (GCD) curves at various current densities, indicating that charging/discharging time decreases with increasing the current density. The GCD curves showed  $iR$  drops in the decay section. It seems that this ‘ $iR$  drop’ is more relevant to the internal resistance of the electrode material. The ‘ $iR$  drop’ in Fig. 6.4c shows smaller compared to those in Fig. 6.4a and b, indicating that the charge transport in the blend film (Fig. 6.4c) is more effective than that in other samples. This  $iR$  drop is known to increase with the equivalent series resistance ( $R_s$ ) of electrode materials (Liu et al., 2014; Ashok et al., 2017).



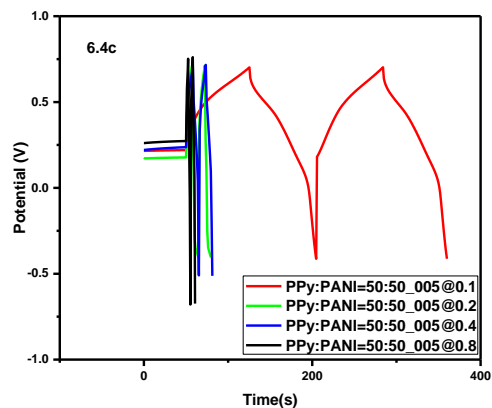


Figure 6.4: GCD curves for (a) PPy:PANI = 50:50, (b) PPy:PANI= 50:50 with 0.01 SDS, and (c) PPy:PANI= 50:50 with 0.05 SDS at different current density.

As shown in Fig. 6.4a-c, all charge/discharge curves displayed an internal resistance drop, in which the equivalent series resistance is known to comprise of both electrode and electrolyte resistances (Mousa et al., 2017). In contrast, the charge/discharge curves in Fig. 6.4d-e display only a triangular curve with a low charge/discharge time, indicating that these blend systems are not much effective compared to those in Fig. 6.4a-c.

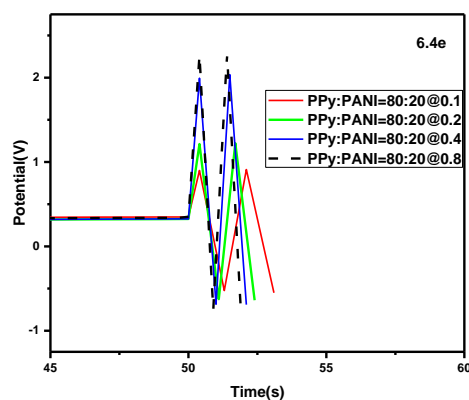
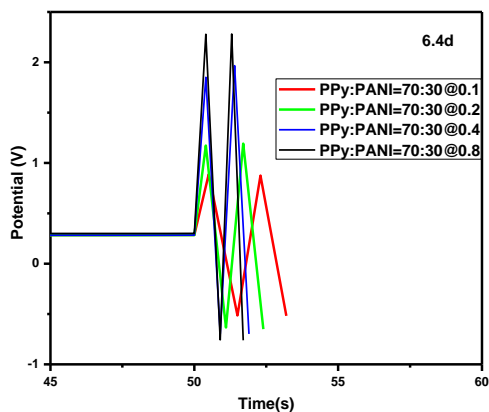


Figure 6.4: GCD curves for (d) PPy:PANI= 70:30 and (e) PPy:PANI= 80:20 at different current densities.

### 6.3.3 The Specific Capacitance

Specific capacitance (F/cm<sup>2</sup>) was measured via GCD methods, which could be calculated based on the following equation:

$$C_a = \frac{2It}{A\Delta V}$$

where  $C_a$  is specific capacitance,  $I$  is the discharge current (mA),  $t$  is charging/discharging time (sec),  $A$  is the electrode area (cm<sup>2</sup>), and  $\Delta V$  is the potential window (V). In this study, the specific capacitance of 'PPy:PANI = 50:50 with 0.01 SDS' was estimated to be 134.36 F/cm<sup>2</sup> at 0.1 mA/cm<sup>2</sup>, and the charging/discharging time was significantly large like 164.6 sec. Note that this capacitance value is much higher than that from the 'PPy: PANI = 50:50' blend sample without SDS (where  $C_a = 81.62$  F/cm<sup>2</sup>, and the charging/discharging time = 100 sec), and it is better than that from 'PPy: PANI = 50:50 with 0.05 SDS' ( $C_a = 127.1$  F.cm<sup>-2</sup>, and the charging/discharging time = 155.7 sec).

In literature reports, the specific capacitance for the PPy/PANI samples was reported (Shiri et al., 2019). When PPy thin film was deposited on the surface of yttrium aluminum garnet (YAG, Y<sub>3</sub>Al<sub>5</sub>O<sub>12</sub>), the specific capacitance of the PPy was 109 F/g at the current density of 1 mA/cm<sup>2</sup>. In another case (Mi et al., 2008), when a PPy/PANI core-shell nanocomposite was prepared for supercapacitor electrodes, the specific capacitance was 416 F/g. Furthermore, one research group reported the specific capacitance of PPy in the range of 90-480 F/g (Jiang et al., 2009). And another group (Meng et al., 2013) reported that PPy/MnO<sub>2</sub>/cigarette filter (CF) system showed the capacitance of 69.3 F/cm<sup>3</sup> at 0.1 A/cm<sup>3</sup>. Then a research group (Wang et al., 2013) reported that carbon nanotube (CNT)/PANI electrode showed the specific capacitance of 38 mF/cm<sup>2</sup> at 800 cycle with 9% capacity loss. Furthermore, another group (Liu et al., 2014) reported the total capacitances of bare PANI nanowires (NWs) (724.63 mF/cm<sup>2</sup> or 190.69 F/g) and PPy NWs (99.01 mF/cm<sup>2</sup> or 110.01 F/g). Then other research groups (Tripathi et al., 2013) showed that the overall capacitance of PPy was 128 mF/cm<sup>2</sup> or 514F/g. Furthermore, another group (Fusalba and Bélanger, 1999) reported that PANIPY copolymer had the low-frequency capacitance of about 100 mF/cm<sup>2</sup> or 60 F/g, which is superior to the values in this work. The CF or PANI electrode showed a lower specific capacitance ( $C_{sp}$ ) than the CF/PANI composite electrodes:  $C_{sp}$  for CF = 4.77 F/g;  $C_{sp}$  for PANI = 20.14 F/g; and  $C_{sp}$  for CF/PANI is 180 F/g (Fonseca et al., 2015).

Fig. 6.5 shows the specific capacitance ( $C_{sp}$ ) for all samples as a function of current density, indicating that  $C_{sp}$  decreases with increasing the charge/discharge current density. This observation is attributed to the fact that both the redox reaction and the charge diffusion could not match the rapid increase of the current densities. In literature report (Wang, 2016), the capacitance was observed to decrease owing to the poor transport of electrolyte ions within the electrode material. Furthermore, the faradaic reactions of PANI could not occur completely because of the fast change in potential, which causes the disappearance of the redox peaks leading to a lower capacitance value. A research group (Ramirez et al., 2017) reported that the highest capacitance values were obtained at 5 mV/s from the PANI/CNT/pineapple-polyester blended woven fabric (PPWF) ( $340 \text{ mF cm}^{-2}$ ) and the PANI/CNT/polyester woven fabric (PWF) ( $235 \text{ mF cm}^{-2}$ ).

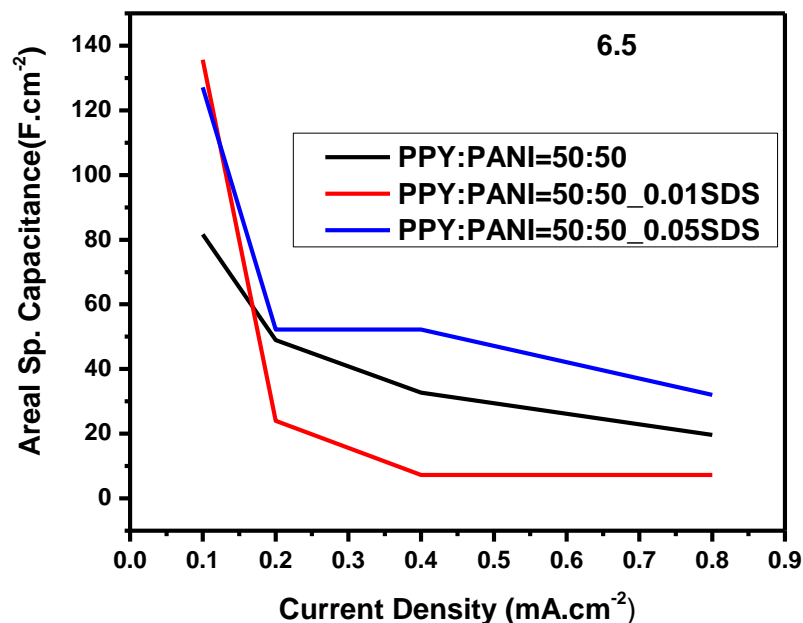


Figure 6.5: Comparison of specific capacitance of blend with current density

### 6.3.4 The Electrochemical Impedance Spectroscopy (EIS)

Nyquist plots were obtained using 0.5 M  $\text{H}_2\text{SO}_4$  electrolyte solution at a frequency range from 100 kHz to 0.1 Hz at the voltage 0.2 V. The plots in Fig. 6.6a-c displayed a low ESR and no

semicircle in the high frequency region. These observations indicated that charge transfer was high between electrode and electrolyte. In addition, in the low-frequency region, the slop towards to the imaginary impedance axis exhibits low Warburg impedance. As explained in the literature reports (Mousa et al., 2016), the straight lines become more vertical for a binary system, representing somewhat ideal EDLC behavior (Vellacheri et al., 2014). Interestingly, the Nyquist plot did not show any semicircle portion at the high-frequency region, indicating that there was a complete interfacial contact between the electrode surface and electrolyte (Lee et al., 2013). As shown in the literature reports (Ramirez et al., 2017), a higher resistance is due to the poor ionic charge transport within the electrode materials, and that the internal resistance increases with increasing the electrode thickness (Xu et al., 2011). Fig. 6.6d displays the equivalent circuit for the PPy/PANI-based electrode materials.

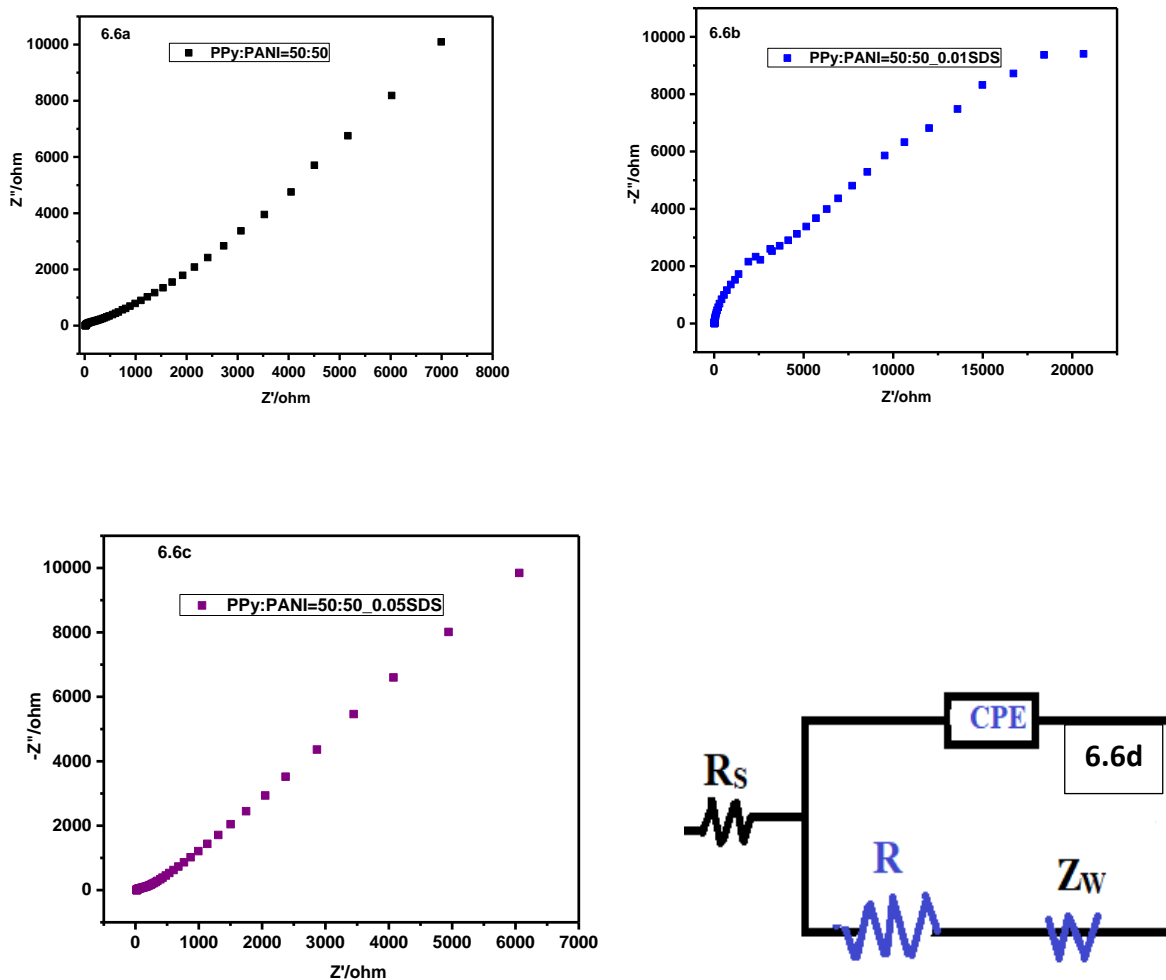


Figure 6.6: Nyquist plots of (a) PPy:PANI = 50:50, (b) PPy:PANI = 50:50 with 0.01 SDS, and (c) PPy:PANI = 50:50 with 0.05 SDS. (d) The equivalent circuit for the electrode materials.

## 6.4 Conclusion

Drop-cast PPy/PANI blend films were electrochemically characterized as a function of composition. Furthermore, the effects of anionic surfactant, sodium dodecyl sulfate (SDS), on the electrochemical behavior of the PPy/PANI blend samples were studied. Resultantly, the PPy:PANI = 50:50 with 0.01 or 0.05 SDS surfactant exhibited both a high specific capacitance and a

low equivalent series resistance. Therefore, the PPy:PANI = 50:50 blend sample with some amounts of SDS surfactants should be promising as electrode materials for electrochemical pseudo-supercapacitor applications. Here, SDS may contribute for the 3-dimensional distribution of PANI and PPy polymeric chain molecules in a blend sample, leading to a good morphology for charge transport, about which more studies should be needed in future from the viewpoint of structure (morphology)-property (electrochemical behavior including charge transport) relationship.

## References

- ABDUL BASHID, H. A., LIM, H. N., KAMARUZAMAN, S., ABDUL RASHID, S., YUNUS, R., HUANG, N. M., YIN, C. Y., RAHMAN, M. M., ALTARAWNEH, M., JIANG, Z. T. & ALAGARSAMY, P. 2017. Electrodeposition of Polypyrrole and Reduced Graphene Oxide onto Carbon Bundle Fibre as Electrode for Supercapacitor. *Nanoscale Research Letters*, 12, 246.
- ASHOK, K. S., GUNJANA, C., PREETAM, B., INDU, K. & SURENDER, D. 2017. Studies on Metal Doped Polyaniline-Carbon Nanotubes Composites for High Performance Supercapacitor. *Current Analytical Chemistry*, 13, 277-284.
- CAI, Y.-M., QIN, Z.-Y. & CHEN, L. 2011. Effect of electrolytes on electrochemical properties of graphene sheet covered with polypyrrole thin layer. *Progress in Natural Science: Materials International*, 21, 460-466.
- CAMURLU, P., GÜLTEKIN, C. & GÜRBULAK, V. 2013. Optoelectronic Properties and Electrochromic Device Application of Novel Pyrazole Based Conducting Polymers. *Journal of Macromolecular Science Part A Pure and Applied Chemistry*, 50.
- FONSECA, C. P., ALMEIDA, D. A. D. L., OLIVEIRA, M. C. D. D., BALDAN, M. R. & FERREIRA, N. G. 2015. Influence of the polymeric coating thickness on the electrochemical performance of Carbon Fiber/PAni composites %J Polímeros. 25, 425-432.

- FUSALBA, F. & BÉLANGER, D. 1999. Electropolymerization of Polypyrrole and Polyaniline–Polypyrrole from Organic Acidic Medium. *The Journal of Physical Chemistry B*, 103, 9044-9054.
- HAIHUA, Z., PENG, S. & JIANG, W. 2013. Electrochemical Properties of PANI as Single Electrode of Electrochemical Capacitors in Acid Electrolytes. *TheScientificWorldJournal*, 2013, 940153.
- JIANG, F., ZHOU, T., TAN, S., ZHU, Y., LIU, Y. & YUAN, D. 2009. Porous Polypyrrole Prepared by Using Nanoscale Calcium Carbonate as a Core for Supercapacitance Materials. *International Journal of Electrochemical Science*, 4.
- KULANDAIVALU, S., SUHAIMI, N. & SULAIMAN, Y. 2019. Unveiling high specific energy supercapacitor from layer-by-layer assembled polypyrrole/graphene oxide|polypyrrole/manganese oxide electrode material. *Scientific Reports*, 9, 4884.
- LEE, K. Y. T., NAGUIB, H. & LIAN, K. 2013. Flexible Multiwall Carbon Nano-Tubes/Polyaniline Composite for Supercapacitor Application.
- LETTI, C. J., COSTA, K. A. G., GROSS, M. A., PATERNO, L. G., SILVA, M. D. A. P. D., MORAIS, P. C. & SOLER, M. A. G. 2017. Synthesis, morphology and electrochemical applications of iron oxide based nanocomposites. *Advances in Nano Research*, 5, 215-230.
- LIN, H., LI, L., REN, J., CAI, Z., QIU, L., YANG, Z. & PENG, H. 2013. Conducting polymer composite film incorporated with aligned carbon nanotubes for transparent, flexible and efficient supercapacitor. *Scientific Reports*, 3, 1353.
- LIU, T., FINN, L., YU, M., WANG, H., ZHAI, T., LU, X., TONG, Y. & LI, Y. 2014. Polyaniline and Polypyrrole Pseudocapacitor Electrodes with Excellent Cycling Stability. *Nano Letters*, 14, 2522-2527.
- MA, L., FAN, H., WEI, X., CHEN, S., HU, Q., LIU, Y., ZHI, C., LU, W., ZAPIEN, J. A. & HUANG, H. 2018. Towards high areal capacitance, rate capability, and tailorable supercapacitors: Co<sub>3</sub>O<sub>4</sub>@polypyrrole core–shell nanorod bundle array electrodes. *Journal of Materials Chemistry A*, 6, 19058-19065.
- MAITI, S. 2014. Polyaniline integrated carbon nanohorn: A superior electrode materials for advanced energy storage. *Express Polymer Letters*, 8, 895-907.
- MELLO, H. J. N. P. D. & MULATO, M. 2018. PANI/PPY blend thin films electrodeposited for use in EGFET sensors. *Journal of Applied Polymer Science*, 135.



- MENG, Y., WANG, K., ZHANG, Y. & WEI, Z. 2013. Hierarchical Porous Graphene/Polyaniline Composite Film with Superior Rate Performance for Flexible Supercapacitors. *Advanced materials (Deerfield Beach, Fla.)*, 25.
- MI, H., ZHANG, X., YE, X. & YANG, S. 2008. Preparation and enhanced capacitance of core-shell polypyrrole/polyaniline composite electrode for supercapacitors. *Journal of Power Sources - J POWER SOURCES*, 176, 403-409.
- MOUSA, M., KHAIRY, M. & SHEHAB, M. 2016. Nanostructured ferrite/graphene/polyaniline using for supercapacitor to enhance the capacitive behavior. *Journal of Solid State Electrochemistry*, 21, 1-11.
- MYASOEDOVA, T., SHISHLYANIKOVA, E., MOISEEVA, T. & BRZHEZINSKAYA, M. 2016. Preparation And Electrochemical Characterization Of PANI/PVA And PANI/Zr/PVA Composites For Supercapacitor Application. *Advanced Materials Letters*, 7, 441-444.
- RAMIREZ, F. C. R., RAMAKRISHNAN, P., FLORES-PAYAG, Z. P., SHANMUGAM, S. & BINAG, C. A. 2017. Polyaniline and carbon nanotube coated pineapple-polyester blended fabric composites as electrodes for supercapacitors. *Synthetic Metals*, 230, 65-72.
- REDDY, C., BOBBA, R., KUMARI, K., KALLURU, R. & HOLZE, R. 2018. SnO<sub>2</sub>/PANI nanocomposite electrodes for supercapacitors and lithium ion batteries. *Electrochemical Energy Technology*, 4, 32-38.
- SARDAR, A., GUPTA, P. S., M., W. & J., B. R. 2018. Polypyrrole based nanocomposites for supercapacitor applications: A review. 1953, 030020.
- SHEN, K., RAN, F., ZHANG, X., LIU, C., WANG, N., NIU, X., LIU, Y., ZHANG, D., KONG, L., KANG, L. & CHEN, S. 2015. Supercapacitor electrodes based on nano-polyaniline deposited on hollow carbon spheres derived from cross-linked co-polymers. *Synthetic Metals*, 209, 369-376.
- SHIRI, H., EHSANI, A., BEHJATMANESH-ARDAKANI, R. & HAJGHANI, S. 2019. Electrosynthesis of Y<sub>2</sub>O<sub>3</sub> nanoparticles and its nanocomposite with POAP as high efficient electrode materials in energy storage device: Surface, density of state and electrochemical investigation. *Solid State Ionics*, 338, 87-95.
- THAKUR, A. V. & LOKHANDE, B. J. 2018. Morphological Modification for Optimum Electrochemical Performance of Highly Pristine Polypyrrole Flexible Electrodes, via

- SILAR Immersion Time and Fabrication of Solid State Symmetric Device %J Portugaliae Electrochimica Acta. 36, 377-392.
- TRIPATHI, S. K., JAIN, A. & GUPTA, A. 2013. Studies on redox supercapacitor using electrochemically synthesized polypyrrole as electrode material using blend polymer gel electrolyte. *Indian Journal of Pure and Applied Physics*, 51, 315-319.
- VELLACHERI, R., AL-HADDAD, A., ZHAO, H., WANG, W., WANG, C. & LEI, Y. 2014. High performance supercapacitor for efficient energy storage under extreme environmental temperatures. *Nano Energy*, 8.
- WANG, K., MENG, Q., ZHANG, Y., WEI, Z. & MIAO, M. 2013. High-Performance Two-Ply Yarn Supercapacitors Based on Carbon Nanotubes and Polyaniline Nanowire Arrays. 25, 1494-1498.
- WANG, K., LI, L., LIU, Y., ZHANG, C. & LIU, T. 2016. Constructing a “Pizza-Like” MoS<sub>2</sub>/Polypyrrole/Polyaniline Ternary Architecture with High Energy Density and Superior Cycling Stability for Supercapacitors. 3, 1600665.
- WANG, L., ZHANG, C., JIAO, X. & YUAN, Z. 2019. Polypyrrole-based hybrid nanostructures grown on textile for wearable supercapacitors. *Nano Research*, 12, 1129-1137.
- WANG, W. 2016. Electrosynthesis and Performance of Poly(aniline/pyrrole) Copolymer. *International Journal of Electrochemical Science*, 4000-4006.
- XU, Y., ZHUANG, S., FANG, Y.-Z., HE, P. & FANG, Y. 2011. Configuration and capacitance properties of polypyrrole/aligned carbon nanotubes synthesized by electropolymerization. *Chinese Science Bulletin*, 56.
- YIN, F., REN, J., WU, G., ZHANG, C. & ZHANG, Y. 2019. Polypyrrole Nanowires with Ordered Large Mesopores: Synthesis, Characterization and Applications in Supercapacitor and Lithium/Sulfur Batteries. 11, 277.
- ZHANG, A.-Q., ZHANG, Y., WANG, L.-Z. & LI, X.-F. 2011. Electrosynthesis and capacitive performance of polyaniline–polypyrrole composite. 32, 1-5.
- ZHANG, R., LIAO, Y., YE, S., ZHU, Z. & QIAN, J. 2018. Novel ternary nanocomposites of MWCNTs/PANI/MoS<sub>2</sub>: Preparation, characterization and enhanced electrochemical capacitance. *Royal Society Open Science*, 5, 171365.

## Chapter Seven

### General Conclusion and Recommendations (Future Perspective)

#### 7.1 General Conclusion

The recent approaches for preparing polymer semiconductors are through solution processing methods. This method is advantageous from various points of view, such as cost minimization, scale-up, and roll-to-roll processing. The variety of functional chain molecules can be blended with other materials for fine-tuning a device performance. Specifically, this blended approach is extremely common in OPVs, OLED, and OFETs when they prepare the active layer and the semiconducting channel layer. The first part of this work, chapter 4, is on the miscibility and phase behavior of polypyrrole-polyaniline (PPy-PANI) blend as a function of composition. The PPy-PANI blends were prepared by solution processing method, using dimethyl sulfoxide (DMSO) solvent. Characterization of the polymer blends was carried out based on the data analysis from FT-IR, XRD, and DSC. The PPy-PANI system was successful to form blends when the DMSO solvent was used. The polymer blends showed almost amorphous nature in XRD spectra because of intermolecular interaction between PPy and PANI macromolecules, which was confirmed by FT-IR data. Specifically, the DSC result for the PPy: PANI= 50:50 wt.% blend showed only one glass transition temperature ( $T_g$ ), which indicates that the two polymers are well miscible without undergoing phase separation. In the second part of this work, contains two sub-sections. In the first chapter 5.1, I examined the nanostructural PANIs materials, which was synthesized using chemical oxidative polymerization. When PANI is dedoped by  $\text{NH}_4\text{OH}$ , its crystallinity observed in the HCl-doped PANI samples was lost significantly, showing largely amorphous nature in the dedoped PANI. The crystallite size of PANI was estimated to be 24.27 nm. The optical absorption peaks of  $\pi \rightarrow \pi^*$  transition were observed at 337 nm and 320 nm for doped and dedoped PANI, respectively. Finally, when PANI is dedoped, its thermal stability was enhanced compared with HCl-doped PANI. The second section chapter 5.2, which study the optical and electrical properties of the PPy/PANI blend materials. The optical property of the blends is determined by both the UV-Vis and photoluminescence (PL) spectra. The assessment of the optical results points out that the miscibility of the polymer may enhance the absorption, which usually falls between the absorption of PPy and PANI polymers. The developed polymer blends of the PPy/PANI system were prepared

from solution processing as usual for organic polymer materials. Based on the electric properties of materials, I conclude that the blend is a semiconductor with the conductivity in the range of  $10^{-6}$  to  $10^{-3}$  S/cm at room temperature. The UV-vis absorption spectra for the blends shows a broad absorption. Using the Tauc model, the optical bandgap determined is ca. 1.53-1.95 eV. The fraction of PANI in a blend was observed to play an important role in the bandgap of the PPy/PANI blend. Increasing the wt. % of PANI in the blends also increases the bandgap of the of PPy/PANI. Finally, based on the optical bandgaps, the electrical conductivities, and the processibility of blend materials, the researcher suggest that it can be used as a component in polymer electronic devices. The last work chapter 6, the PPy-PANI thin film with different weight percentage PPy: PANI have been successfully prepared via a drop-casting method. The PPy: PANI = 50:50+0.01SDS materials showed the highest areal specific capacitance and the lowest lower value of ESR. The PPy: PANI = 50:50+0.01SDS exhibited the promising materials consider as a potential candidates for the electrode of the supercapacitor.

## 7.2 Recommendations (Future Perspective)

In the future, organic polymer semiconductors may play a leading role in emerging technologies. Miscible polymer semiconductors could be easily synthesized using a solution process. Preparing a device with this solution-processing approach affords some advantages from various points of view, such as cost minimization, scale-up, and roll-to-roll processing. In my research work, I used a common organic solvent, DMSO. In the future, I recommend that the water-soluble polymer blend should be more significant, which is good for the environment, i.e., eco-friendly, by evaporating solvent at room temperature in open-air condition. The PPy/PANI blends may be further compounded with various materials, such as nanomaterials, nanoparticles, and other organic materials for fine-tuning a device based on improved materials' properties. As future work, I also recommend that PANI/PPy could be used as semiconducting.

This material is a sulfur-containing polymer. It will need further studies for the application of lithium-sulfur battery as an electrode material. It may also consider as in medicine, drug delivery, self-healing. And it will be promising for the application of electrochromic and display applications. Of course, this research may have other variety of applications such as OLED, RFID,

printed electronics, etc. Future application of organic semiconductor is in the area of smart textiles, lab on a chip, portable compact screens, and skin cancer treatment in the area of biotechnology.

## Declaration Form

**I, the undersigned, declared that this is my bona fide original work, has never been presented in this or any other University, and that all the resources and materials used for the thesis, have been fully acknowledged.**

**Name:** \_\_\_\_\_

**Signature:** \_\_\_\_\_

**Date:** \_\_\_\_\_

**Place:** \_\_\_\_\_

**Date of submission:** \_\_\_\_\_

**This dissertation has been submitted for examination with my approval as the Candidate's Promoter (supervisor).**

**Name:** \_\_\_\_\_

**Signature:** \_\_\_\_\_

**Date:** \_\_\_\_\_

**Name:** \_\_\_\_\_

**Signature:** \_\_\_\_\_

**Date:** \_\_\_\_\_